Curriculum Vitae

Leon P. McLean, M.D., M.P.H.
Gastroenterology Fellow, Department of Medicine
University of Maryland School of Medicine

Date June 30, 2014

Contact Information

Business Address:	Department of Medicine 22 S. Greene St., Room N3W62 Baltimore, MD 21201
Business Phone Number:	(410) 328-5780
Fax:	(410) 328-8315
Email:	lmclean@medicine.umaryland.edu

Education

2001	B.S., Biology, Tufts University (Cum Laude)
2006	M.D., Tufts University School of Medicine
2006	M.P.H., Tufts University School of Medicine
2014	Ph.D. (expected), Molecular Medicine, University of Maryland, Baltimore Thesis Advisors: Terez Shea-Donohue, Ph.D. and Jean-Pierre Raufman, M.D. "Type 3 Muscarinic Receptors Contribute to Homeostasis and Host Defense within the Gastrointestinal Tract"

Post Graduate Education and Training

2006 - 2007	Internship, University of Maryland Medical Center
2007 - 2009	Residency, Internal Medicine, University of Maryland Medical Center
2009 - 2010	Fellowship, Gastroenterology, John. H. Stroger Jr. Hospital of Cook County
2010 - 2014	Fellowship, Gastroenterology, University of Maryland Medical Center

Certifications

2009	Diplomate, American Board of Internal Medicine

Medical Licensures

Inactive	Illinois
Active	Maryland

Employment History

Academic Appointments

2010-2014	Graduate Research Assistant, Department of Medicine, University of Maryland School of Medicine

Professional Society Membership

2002 - 2006	Student Member, Massachusetts Medical Society
2006 - present	Member, Massachusetts Medical Society
2006 - present	Associate, American College of Physicians
2006 - present	Member, American Medical Association
2007 - present	Member, American Gastroenterological Association
2009 - present	Member, American College of Gastroenterology
2009 - present	Member, American Society for Gastrointestinal Endoscopy

Honors And Awards

2006	Bernard A. Berman Travel Fund Award, Tufts University School of Medicine, awarded to medical students offered the opportunity to present at a conference
2008	Poster of Distinction, Digestive Disease Week, awarded to presenters whose abstracts were judged to be in the top 10% of abstracts selected for poster presentation
2011	Poster of Distinction, Digestive Disease Week, awarded to presenters whose abstracts were judged to be in the top 10% of abstracts selected for poster presentation
2013	Travel Grant, Fellowship2Leadership Salix Fellows Program, awarded to the 50 “best and brightest” gastroenterology/hepatology fellows for travel to a national gastroenterology/hepatology meeting
2014	AGA-AASLD Academic Skills Workshop Travel Grant, awarded to junior faculty or fellows based on quality of training, research experience, and plans for an academic career
2014	Poster of Distinction, Digestive Disease Week, awarded to presenters whose abstracts were judged to be in the top 10% of abstracts selected for poster presentation

Clinical Activities

Clinical Expertise

Board certified in internal medicine
Clinical and research focus in inflammatory bowel disease, host defense, and mucosal homeostasis

Administrative Service

Institutional Service

2002 - 2007	Tufts Alumni Admissions Program
2007 - 2009	Resident Member, Post-Graduate Education Committee
2012 - present	Tufts Alumni Admissions Program

Teaching Service

Medical Student Teaching

2013 - 2014	Small Group Leader, Introduction to Clinical Medicine II (ICME 520) Taught physical diagnosis to four 2nd year medical students, 3-4 contact hours approximately every 2-3 weeks

Grant Support

Active Grants

7/1/2014 – 6/30/2015	Leon McLean (PI, 10%) *Polycystins in Intestinal Mucosal Homeostasis and Development of Murine Colitis* Pilot & Feasibility Award from P30 DK090868 Annual Direct Costs: $50,000 Total Direct Costs: $50,000

Publications

Peer-reviewed journal articles

1. Packer AI, Jane-Wit D, **McLean L**, Panteleyev AA, Christiano AM and Wolgemuth DJ. *Hoxa4* expression in developing mouse hair follicles and skin. Mech Dev. 2000;99(1-2):153-157.
2. Makhzoumi ZH, **McLean LP**, Lee JL, Ibe AI. Diabetic ketoacidosis associated with aripiprazole. Pharmacotherapy. 2008;28(9):1198-1202.
3. **McLean LP**, Shea-Donohue T, Cross RK. Vedolizumab for the treatment of ulcerative colitis and Crohn's disease. Immunotherapy. 2012;4(9):883-898.
4. Yang Z, Sun R, Grinchuk V, Notari L, Stiltz J, **McLean LP**, Ramalingam TR, Wynn TA, Urban JF, Vogel SM, Shea-Donohue T, Zhao A. Dependence of IL-33-induced alterations in intestinal function and cytokine response on MyD88, STAT6, and IL-13 in mice. Am J Physiol Gastrointest Liver Physiol. 2013;304(4):G381-9.
5. **McLean LP**, Cross RK, Shea-Donohue T. Combined blockade of IL-17A and IL-17F may prevent the development of experimental colitis. Immunotherapy. 2013 Sep;5(9);923-5.
6. Notari L, Riera DC, Sun R, Bohl JA, **McLean LP**, Madden K, van Rooijen N, Vanuytsel T, Urban JF, Zhao A, Shea-Donohue T. Role of Macrophages in the Altered Epithelial Function during a Type 2 Immune Response Induced by Enteric Nematode Infection. PLoS One. 2014;9(1):e84763
7. Cheng FF, **McLean LP**, Cross RK. What is the Role of Vedolizumab in the Era of Anti-TNF Agents? Ann Transl Med 2014;2(1):4.
8. **McLean LP**, Cross RK. Adverse Events in IBD: To Stop or Continue Immune Suppressant and Biologic Therapy. Expert Rev Gastroenterol Hepatol. 2014 Mar;8(3):223-40.
9. **McLean LP**, Chun JS, Cross RK. Right Lower Quadrant Pain in a Patient with IBD of Undetermined Type. Clin Gastroenterol Hepatol. 2014 Apr;12(4):A29-30.

Book Chapters

1. **McLean LP** and Greenwald BD. Diarrhea and Constipation. Gastroenterology Pocket. Edited by Nichita D and Ghugari R, Börm Bruckmeier Publishing, El Segundo, CA, 2014.
2. **McLean LP** and Patil SA. Gastrointestinal Bleeding. Gastroenterology Pocket. Edited by Nichita D and Ghugari R, Börm Bruckmeier Publishing, El Segundo, CA, 2014.

Abstracts

1. **McLean LP**, Salas FL, Lazar JD, McCarthy TA, Hamer DH. Attitudes of Healthcare Workers Towards Smallpox Vaccination. Poster Presentation, 42nd Annual Meeting of the Infectious Diseases Society of America, Boston, MA, October, 2004.
2. **McLean LP** and Fairchild DG. Compliance with Dyspepsia Guidelines: Experience

in a Primary Care General Medicine Setting. Poster Presentation, American College of Gastroenterology Annual Scientific Meeting and Postgraduate Course, Las Vegas, NV, October, 2006. Am J Gastroenterol 101:S83, 2006.

3. **McLean LP**, Sun R, Stiltz J, Zhao A, Raufman JP, Shea-Donohue T. Muscarinic Type 3 Receptors (M_3R) Contribute to Ileal Mucosal Barrier Function. Digestive Disease Week 2007, Washington, DC, May, 2007. Gastroenterology 132:A405, 2007.
4. **McLean LP**, Zhao A, Sun R, Stiltz JA, Riera DC, Urban JF, Raufman JP, Shea-Donohue T. Role of Muscarinic 3 Receptors in the Immune, Epithelial, and Smooth Muscle Responses to Enteric Nematode Infection. Digestive Disease Week 2008, San Diego, CA, May, 2008. Gastroenterology 134:A393, 2008.
5. **McLean LP**, Notari L, Sun R, Stiltz JA, Grinchuk V, Yan S, Zhao A, Raufman JP, Shea-Donohue T. Type 1 and Type 3 Muscarinic Receptors Modulate Intestinal Barrier Function. Digestive Disease Week 2011, Chicago, IL, May, 2011. Gastroenterology 140:S474-5, 2011.
6. **McLean L**, Grinchuk V, Zhao A, Sun R, Raufman JP, Shea-Donohue T. Type 3 Muscarinic Receptors Modulate Macrophage Phenotype in the Presence of Th1 Cytokines. Digestive Disease Week 2012, San Diego, CA, May, 2012. Gastroenterology 142:S140, 2012.
7. Vanuytsel T, Notari L, Yan S, Zhao A, Bohl J, **McLean L**, Sun R, Urban J, Smith A, Tack J, Shea-Donohue T. Immune Regulation of the Intestinal Progenitor Cell Microenvironment. Digestive Disease Week 2012, San Diego, CA, May, 2012. Gastroenterology 142:S597, 2012.
8. Bohl J, Urban J, Notari L, Sun R, Zhao A, Yan S, Grinchuk V, Vanuytsel T, **McLean L**, Yang Z, Shea-Donohue T. Nematode Generated Protease Activation of PAR2 Plays a Key Role in the Th2 Protective Immune Response. Digestive Disease Week 2012, San Diego, CA, May, 2012. Gastroenterology 142:S596, 2012.
9. **McLean L**, Grinchuk V, Zhao A, Sun R, Raufman JP, Shea-Donohue T. Type 3 Muscarinic Receptors Modulate Macrophage Phenotype in the Presence of Th2 Cytokines. American College of Gastroenterology Annual Scientific Meeting, Las Vegas, NV, October 2012. Am J Gastroenterol 107:S682, 2012.
10. Rachakonda V, Urrunaga N, Ahmad D, Twadell W, Saxena N, Cheng K, **McLean L**, Raufman JP, Khurana S. Genetic Ablation of M1 Subtype Muscarinic Receptor (M1R) Attenuates Azoxymethane (AOM)-Induced Liver Injury by Altering Expression of Fibrogenic Mediators and Inflammatory Cytokines. The 63rd Annual Meeting of the American Association for the Study of Liver Diseases, Boston, MA, November, 2012. Hepatology 56(4):143A, 2012.
11. Urrunaga N, Rachakonda V, Ahmad D, **McLean L**, Twadell W, Saxena N, Cheng K, Raufman JP, Khurana S. In Mice, Genetic Ablation of M1 Subtype Muscarinic Receptors ($Chrm1^{-/-}$) Attenuates Acetaminophen (APAP)-Induced Liver Injury. The 63rd Annual Meeting of the American Association for the Study of Liver Diseases, Boston, MA, November, 2012. Hepatology 56(4):187A, 2012.
12. **McLean LP**, Notari L, Sun R, Bohl J, Yan S, Grinchuk V, Zhao A, Raufman JP, Shea-Donohue T. Type 3 Muscarinic Receptor Deficiency is Associated with Impaired Paracellular Permeability and Activation of Myosin Light Chain (MLC) 2. Digestive Disease Week 2013, Orlando, FL, May, 2013. Gastroenterology

144:S123-4, 2013.

13. **McLean LP**, Chun J, Cross RK. Crohn's Disease: An Uncommon Cause of Appendicitis. American College of Gastroenterology Annual Scientific Meeting, San Diego, CA, October 2013. Am J Gastroenterol 108:S426, 2013.
14. Rachakonda V, Urrunaga NH, Jadeja R, Ahmad D, **McLean L**, Cheng K, Saxena NK, Raufman J, Khurana S. Genetic Ablation of M1 Muscarinic Receptors (M1R) Attenuates Azoxymethane (AOM)-Induced Murine Liver Injury by TRAIL-R2-Mediated Hepatic Stellate Cell (HSC) Apoptosis. The 64th Annual Meeting of the American Association for the Study of Liver Diseases, Washington, DC, October, 2013. Hepatology 58(4):577A, 2013.
15. Urrunaga NH, Jadeja R, Rachakonda V, Ahmad D, **McLean L**, Saxena NK, Cheng K, Raufman J, Khurana S. Mechanisms Underlying Attenuated Acetaminophen (APAP)-Induced Liver Injury in M1R-Deficient (M1R$^{-/-}$) Mice. The 64th Annual Meeting of the American Association for the Study of Liver Diseases, Washington, DC, October, 2013. Hepatology 58(4):947A, 2013.
16. **McLean LP**, Smith A, Cheung L, Sun R, Grinchuk V, Zhao A, Raufman JP, Shea-Donohue T. Type 3 Muscarinic Receptor Activity Facilitates Clearance of *Citrobacter rodentium*. Digestive Disease Week 2014, Chicago, IL, May, 2014. Gastroenterology 146:S286, 2014.

Major Invited Speeches

Local

1. **McLean LP**. Evaluation of the Patient with Dysphagia. Union Memorial Hospital, Baltimore, MD, 2012.
2. **McLean LP**. Type 3 Muscarinic Receptors Contribute to Host Defense within the GI Tract. The Johns Hopkins Hospital, Baltimore, MD, 2014.

National

3. **McLean L**, Grinchuk V, Zhao A, Sun R, Raufman JP, Shea-Donohue T. Type 3 Muscarinic Receptors Modulate Macrophage Phenotype in the Presence of Th1 Cytokines. Digestive Disease Week 2012, San Diego, CA, 2012.
4. **McLean LP**, Notari L, Sun R, Bohl J, Yan S, Grinchuk V, Zhao A, Raufman JP, Shea-Donohue T. Type 3 Muscarinic Receptor Deficiency is Associated with Impaired Paracellular Permeability and Activation of Myosin Light Chain (MLC) 2. Digestive Disease Week 2013, Orlando, FL, 2013.

Proffered Communications

Local

1. **McLean LP**, Sun R, Stiltz J, Zhao A, Raufman JP, Shea-Donohue T. Muscarinic Type 3 Receptors and Ileal Mucosal Barrier Function. Poster Presentation, Associates Day, Maryland Chapter of the American College of Physicians, Baltimore, MD, May 2007.
2. Erickson C, **McLean LP**. The Aberrant Right Subclavian Artery. Poster Presentation, Associates Day, Maryland Chapter of the American College of Physicians, Baltimore, MD, May 2008.
3. Bagi P, **McLean LP**. Advanced Lupus Nephritis as an Uncommon Initial Presentation of Systemic Lupus Erythematosus. Poster Presentation, Associates Day, Maryland Chapter of the American College of Physicians, Baltimore, MD, May 2008.
4. Faust RR, Frayha N, **McLean L**, Lee JH. Comparing the Automated and Non-Automated Sign-Out Systems Used by Medicine Interns in Transfers of Patient Care. Poster Presentation, Associates Day, Maryland Chapter of the American College of Physicians, Baltimore, MD, May 2008.

ABSTRACT

Title of Dissertation: Type 3 Muscarinic Receptors Contribute to Homeostasis and Host Defense within the Gastrointestinal Tract

Leon McLean, Doctor of Philosophy, 2014

Dissertation Directed by:
Terez Shea-Donohue, PhD; Professor; Department of Radiation Oncology
Jean-Pierre Raufman, MD; Professor; Department of Medicine

Although activation of the alpha 7 nicotinic receptor exerts anti-inflammatory effects on immune cells, the contribution of muscarinic receptors to mucosal homeostasis, response to enteric pathogens, and modulation of immune cell function is undefined. WT and type 3 muscarinic receptor (M3R)-deficient (*Chrm3*$^{-/-}$) mice were infected with *Citrobacter rodentium*, an attaching/effacing gram-negative bacterium that infects murine colon and evokes a highly polarized T_H1/T_H17 response, or *Nippostrongylus brasiliensis*, an enteric nematode that infects murine small intestine and induces a stereotypic T_H2 response. Permeability and expression of T_H1/T_H17 cytokines is increased in *Chrm3*$^{-/-}$ small intestine; however, no changes in permeability or cytokine expression occur in *Chrm3*$^{-/-}$ colon. Clearance of both *C. rodentium* and *N. brasiliensis* was delayed from *Chrm3*$^{-/-}$ mice; however, *Chrm3*$^{-/-}$ mice infected with *C. rodentium* retained their ability to mount a T_H1/T_H17 response whereas upregulation of T_H2 cytokines in response to *N. brasiliensis* was abrogated. Delayed clearance of *C. rodentium* from *Chrm3*$^{-/-}$ mice is associated with decreased goblet cell number and mucin 2 expression. Within *Chrm3*$^{-/-}$ small intestine, T_H2-dependent changes in gut function (smooth muscle hypercontractility, increased permeability, decreased secretion and absorption, and goblet cell expansion) did not occur despite infection with *N. brasiliensis*. Furthermore, treatment of bone-marrow derived macrophages (BMDM) with

bethanechol, a muscarinic-specific agonist, induces a classically activated macrophage phenotype, an effect dependent on M3R. *Chrm3*$^{-/-}$ BMDM retain their ability to attain a classically activated phenotype when exposed to the T_H1 cytokine IFN-γ. Our data establish a role for M3R in host defense against enteric pathogens. Interestingly, in *Chrm3*$^{-/-}$ mice cytokine generation is intact in the setting of a T_H1/T_H17 inducing stimulus, but abrogated in the setting of a T_H2 inducing stimulus. In addition, M3R exerts pro-inflammatory effects on macrophage phenotype and function and contributes to barrier function and mucosal homeostasis in uninfected small intestine. These findings support an expanding role for cholinergic receptors not only in mucosal homeostasis and the response to inflammatory stimuli, but also in clearance of enteric pathogens.

Type 3 Muscarinic Receptors Contribute to Homeostasis
and Host Defense within the Gastrointestinal Tract

by

Leon P. McLean

Dissertation submitted to the Faculty of the Graduate School of the
University of Maryland, Baltimore in partial fulfillment
of the requirements for the degree of
Doctor of Philosophy
2014

ACKNOWLEDGEMENTS

Innumerable people deserve thanks and gratitude for their assistance in completing this work. I owe much to my mentor, Dr. Terez Shea-Donohue. This would not have been possible without her guidance and support. I met Terez during my first year of medical residency. She graciously offered me the opportunity to join her lab despite my very limited laboratory experience. She and Dr. Aiping Zhao have guided my development over the past eight years, from teaching me how to use a pipette to helping me develop my ability to design experiments, analyze data, and effectively communicate my findings. They have both given countless hours to this project for which I am extremely grateful.

I would also like to thank my thesis committee -- Dr. Alessio Fasano, Dr. Bret Hassel, Dr. Jean-Pierre Raufman, Dr. Joseph Urban, and Dr. Li Zhang. They offered many thoughtful comments that improved the quality of this work. Dr. Fasano deserves an extra word of thanks as he transitioned to Massachusetts General Hospital part way through my studies, yet he remained accessible throughout, going as far as traveling to Baltimore for my dissertation defense.

Past and current member of the Shea-Donohue lab deserve a special thank you. In addition to Terez and Aiping, Rex Sun, Shu Yan, Luigi Notari, Tim Vanuytsel, Viktoriya Grinchuk, Neemesh Desai, and Zhonghan Yang all helped me learn basic laboratory techniques, run experiments, and provide words of encouragement when data did not turn out as expected.

The clinical faculty and my co-fellows in gastroenterology also deserve a word of thanks. There were many occasions where I needed to spend a little extra time in the lab;

the gastroenterology faculty and my co-fellows were very accommodating and willing to help me with last minute schedule adjustments, despite the fact that these requests resulted in personal inconvenience on their part. Dr. Raufman deserves a special thanks as he took a personal interest in my development as a scientist very early in my career. I would also like to thank the IBD faculty, particularly Dr. Ray Cross and Dr. Mark Flasar, for guiding my clinical development and making it possible for me to join the faculty at University of Maryland upon the completion of my training.

Finally, I would like to thank my family and friends for their love and support. From an early age my mother provided encouragement while stressing the importance of hard work and how those habits could make anything possible. In addition, my friends have always been there to provide words of support, even when I seemed to disappear into the lab. Leyla, in particular, has stood by my side and supported me through what seems like countless weekends and evenings spent with my macrophages and/or computer. I would not have been able to do this without her.

TABLE OF CONTENTS

ACKNOWLEDGEMENTS i

TABLE OF CONTENTS v

LIST OF FIGURES vi

LIST OF ABBREVIATIONS xi

Chapter 1: Introduction 1

Acetylcholine 1

Cholinergic Receptors 3

Cholinergic Regulation of Inflammation 4

Functions of the Gastrointestinal Tract 8

Chapter 2: Type 3 Muscarinic Receptors Contribute to Host Defense Against *Citrobacter rodentium* and Exert Pro-Inflammatory Effects on Macrophages 13

Introduction 13

Methods 17

Results 25

Discussion 47

Chapter 3: Type 3 Muscarinic Receptors Contribute to Mucosal Homeostasis, Clearance of *Nippostrongylus brasiliensis*, and Expression of Th2 Cytokines 51

Introduction 51

Methods 53

Results 59

Discussion 69

Chapter 4: Discussion 73

REFERENCES 76

LIST OF FIGURES

Figure 1: Neuronal acetylcholine production, release, degradation, and interaction with cholinergic receptors 2

Figure 2: Efferent and afferent arcs of the cholinergic anti-inflammatory reflex......5

Figure 3: Branches of the cholinergic anti-inflammatory pathway 6

Figure 4: Gene expression of T_H1/T_H17 and T_H2 cytokines in WT C57BL/6 and *Chrm3*$^{-/-}$ C57BL/6 colon......25

Figure 5: TEER of muscle-free WT and *Chrm3*$^{-/-}$ colon in C57BL/6 mice and SvEv x CF1 (50%:50%) mice 26

Figure 6: Representative image of colon from WT mouse. Representative image of colon from *Chrm3*$^{-/-}$ mouse......26

Figure 7: Vehicle treated *Chrm3*$^{-/-}$ mice weigh less than sex and age-matched vehicle-treated WT mice. WT and *Chrm3*$^{-/-}$ mice experience a significant decrease in body mass at 13 DPI. Both WT and *Chrm3*$^{-/-}$ mice experience a similar loss of body mass when normalized to vehicle-treated WT or *Chrm3*$^{-/-}$ mass 27

Figure 8: Fecal bacterial content of *C. rodentium* infected WT and *Chrm3*$^{-/-}$ mice at 6, 9, 12, 14, 16, and 19 DPI. Immunoblot of *C. rodentium* extract probed with rabbit polyclonal anti-*C. rodentium* antibody 28

Figure 9: Immunofluorescent staining demonstrating persistent adherence of *C. rodentium* in *Chrm3*$^{-/-}$ colon mucosa 13 DPI......29

Figure 10: Spleen weight per body weight in *C. rodentium* infected *Chrm3*$^{-/-}$ mice 13 DPI is significantly increased compared to spleen weight per body weight in WT mice 13 DPI and uninfected *Chrm3*$^{-/-}$ mice......30

Figure 11: *C. rodentium* was detected in spleen of 1 of 4 WT mice and 3 of 4 *Chrm3*$^{-/-}$ mice 13 DPI 31

Figure 12: Gene expression of IFN-γ in WT and *Chrm3*$^{-/-}$ uninfected and *C. rodentium*-infected colon. Gene expression of TNF-α in WT and *Chrm3*$^{-/-}$ uninfected and *C. rodentium*-infected colon. Gene expression of IL-17A in WT and *Chrm3*$^{-/-}$ uninfected and *C. rodentium*-infected colon 32

Figure 13: Gene expression of *Nos-2* in WT and *Chrm3*$^{-/-}$ uninfected and *C. rodentium*-infected colon..33

Figure 14: Gene expression of *CD3* in WT and *Chrm3*$^{-/-}$ uninfected and *C. rodentium*-infected colon..33

Figure 15: BrdU-labeled cells in uninfected and *C. rodentium*-infected WT and *Chrm3*$^{-/-}$ colon...35

Figure 16: Mean ± SEM of BrdU-positive cells per crypt in uninfected and *C. rodentium*-infected WT and *Chrm3*$^{-/-}$ colon mucosa 36

Figure 17: Goblet cells per crypt in uninfected and *C. rodentium*-infected WT and *Chrm3*$^{-/-}$ mice. Gene expression of CLCA3 in muscle-free WT and *Chrm3*$^{-/-}$ uninfected and *C. rodentium*-infected colon..37

Figure 18: Gene expression of *Muc2* in WT and *Chrm3*$^{-/-}$ uninfected and *C. rodentium*-infected colon. Gene expression of *Muc5AC* in WT and *Chrm3*$^{-/-}$ uninfected and *C. rodentium*-infected colon 38

Figure 19: H&E stained sections of uninfected and *C. rodentium*-infected WT and *Chrm3*$^{-/-}$ colon 39

Figure 20: Relative serum levels of IgM in WT and *Chrm3*$^{-/-}$ uninfected and *C. rodentium*-infected mice 40

Figure 21: Bone marrow cells differentiated in M-CSF for 7 days that express CD11b and F4/80 41

Figure 22: WT BMDM gene expression of *Chrm1*, *2*, *3*, *4* and *α7* nicotinic receptor 41

Figure 23: Gene expression of *Chrm3* in WT BMDM treated with vehicle or bethanechol 1-100 nM...42

Figure 24: Gene expression of *Chrm3* in vehicle, IFN-γ, and IL-4 treated WT BMDM. Gene expression of *Chrm1*, *Chrm2*, *Chrm4*, and *α7* in vehicle and IFN-γ treated WT BMDM...42

Figure 25: Immunoblot demonstrating expression of M3R in vehicle, IFN-γ, and IL-4 treated BMDM..43

Figure 26: Gene expression of *Nos-2* in WT BMDM treated with vehicle or bethanechol 100 nM. Gene expression of *Nos-2* in *Chrm3*$^{-/-}$ BMDM treated with vehicle or bethanechol 100 nM..43

Figure 27: Gene expression of *Nos-2* in WT BMDM treated with vehicle or atropine 50 nM. Gene expression of *Nos-2* in *Chrm3*$^{-/-}$ BMDM treated with vehicle or atropine 50 nM 44

Figure 28: Gene expression of *Nos-2* in WT BMDM treated with vehicle or IFN-γ. Gene expression of *Nos-2* in *Chrm3*$^{-/-}$ BMDM treated with vehicle or IFN-γ...........................45

Figure 29: Gene expression of *Nos-2* in WT BMDM treated with IFN-γ 10 ng/mL, IFN-γ 10 ng/mL and bethanechol 100 nM, and IFN-γ 10 ng/mL, bethanechol 10 nM, and atropine 50 nM. Gene expression of *Nos-2* in *Chrm3*$^{-/-}$ BMDM treated with IFN-γ 10

ng/mL, IFN-γ 10 ng/mL and bethanechol 100 nM, and IFN-γ 10 ng/mL, bethanechol 10 nM, and atropine 50 nM....46

Figure 30: Proposed model of effects of M3R on macrophage phenotype 50

Figure 31: TEER of muscle-free small intestine from WT and *Chrm3*$^{-/-}$ 129S6/SvEv:CF1 (50%:50%) mice. TEER of muscle-free small intestine from WT and *Chrm3*$^{-/-}$ C57BL/6 mice....59

Figure 32: Flux of 4 kDa FITC-dextran across WT and *Chrm3*$^{-/-}$ muscle-free smooth intestine at various time points 60

Figure 33: Gene expression of *IFN-γ*, *IL-17A* and *TNF-α* in WT and *Chrm3*$^{-/-}$ 129S6/SvEv:CF1 (50%:50%) mice, *IFN-γ*, *IL-17A* and *TNF-α* in WT and *Chrm3*$^{-/-}$ C57BL/6 mice, and *IL-4* and *IL-13* in WT and *Chrm3*$^{-/-}$ 129S6/SvEv:CF1 (50%:50%) mice....61

Figure 34: Representative sections of H&E stained small intestine from WT C57BL/6 mice and *Chrm3*$^{-/-}$ C57BL/6 mice....61

Figure 35: Fecal egg content at 9 DPI from WT and *Chrm3*$^{-/-}$ mice. Nematode count within the proximal small intestine at 9 DPI 62

Figure 36: Gene expression of IL-13 and IL-4 in uninfected and *N. brasiliensis*-infected WT and *Chrm3*$^{-/-}$ intestine. Gene expression of T_H1/T_H17 cytokines in infected WT and *Chrm3*$^{-/-}$ intestine 63

Figure 37: Gene expression of *Arg-1* in uninfected and *N. brasiliensis*-infected WT and *Chrm3*$^{-/-}$ small intestine....64

Figure 38: Gene expression of *Chrm3* in vehicle, IFN-γ, and IL-4 treated WT BMDM .64

Figure 39: Gene expression of *Arg-1* in WT BMDM treated with vehicle or bethanechol65

Figure 40: Gene expression of *Arg-1* in WT or *Chrm3*$^{-/-}$ BMDM treated with vehicle or IL4...65

Figure 41: Percent change in TEER in uninfected and *N. brasiliensis*-infected WT and *Chrm3*$^{-/-}$ mice. Percent change in smooth muscle contraction in response to acetylcholine 100 μM in uninfected and *N. brasiliensis*-infected WT and *Chrm3*$^{-/-}$ mice. Percent change in epithelial secretion in response to acetylcholine 100 μM in uninfected and *N. brasiliensis*-infected WT and *Chrm3*$^{-/-}$ mice. Percent change in epithelial absorption in response to glucose 40 μM in uninfected and *N. brasiliensis*-infected WT and *Chrm3*$^{-/-}$ mice...67

Figure 42: Representative H&E-stained sections of ileum from uninfected and *N. brasiliensis*-infected WT and *Chrm3*$^{-/-}$ mice demonstrating goblet cell expansion in WT small intestine 9 DPI, but not in *Chrm3*$^{-/-}$ small intestine 9 DPI 68

Figure 43: Proposed model of delayed nematode clearance in *Chrm3*$^{-/-}$ mice.................72

LIST OF ABBREVIATIONS

$\alpha 7$	alpha 7
AAM	alternatively activated macrophage
AChE	acetylcholinesterase
AChR	acetylcholine receptor
AMP	antimicrobial peptide
ANOVA	analysis of variance
A/E	attaching/effacing
BCA	bicinchoninic acid
BChE	butyrylcholinesterase
BMDM	bone-marrow derived macrophages
BrdU	bromodeoxyuridine
BSA	bovine serum albumin
C57BL/6	C57 black 6
CAM	classically activated macrophage
CD	Crohn’s disease
CD11b	cluster of differentiation molecule 11b
CD3	cluster of differentiation 3
CD4	cluster of differentiation 4
CD8	cluster of differentiation 8
cDNA	complementary DNA
CFU	colony forming units

ChAT	choline acetyltransferase
ChT1	choline transporter 1
CLCA3	chloride channel, calcium activated, family member 3
cm	centimeter
CNS	central nervous system
Chrm3	cholinergic receptor muscarinic, type 3
COPD	chronic obstructive pulmonary disease
C. rodentium	*Citrobacter rodentium*
d	days
D9	day 9
D13	day 13
D21	day 21
DAPI	4',6-diamidino-2-phenylindole
DC	dendritic cell
DMEM	Dulbecco's Modified Eagle Medium
DPI	days post infection
DSS	dextran sulfate sodium
EDTA	ethylenediaminetetraacetic acid
FBS	fetal bovine serum
FITC	fluorescein isothiocyanate
g	grams
GALT	gut-associated lymphoid tissue
GI	gastrointestinal

GLUT5	glucose/fructose transporter member 5
GPCR	G-protein coupled receptor
h	hours
H&E	hematoxylin and eosin
IBD	inflammatory bowel disease
IBS	irritable bowel syndrome
IF	immunofluorescence
IFN-γ	interferon-gamma
Ig	immunoglobulin
ILC	innate lymphoid cell
IL-x	interleukin-x
I_{SC}	short-circuit current
L	liter
L3	third-stage larvae
LB	Luria-Bertani broth
LPS	lipopolysaccharide
m	meter
M	molar
MEM	Minimum Essential Medium
min	minute
MR	muscarinic receptor
MxR	Type x (1-5) Muscarinic Receptor
MLN	mesenteric lymph node

Muc	mucin
M-cell	microfold cell
M-CSF	macrophage colony stimulating factor
NR	nicotinic receptor
N. brasiliensis	*Nippostrongylus brasiliensis*
PAGE	polyacrylamide gel electrophoresis
PBS	phosphate buffered saline
pH	potential of hydrogen
PMN	polymorphonuclear leukocyte
PNS	peripheral nervous system
RegIIIγ	regenerating islet-derived protein 3 gamma
RNA	ribonucleic acid
rRNA	ribosomol ribonucleic acid
RT-PCR	real time polymerase chain reaction
s	seconds
SDS	sodium dodecyl sulfate
SEM	standard error of the mean
SGLT1	sodium/glucose cotransporter 1
TBS-T	tris buffered saline with tween-20
TEER	transepithelial electrical resistance
Th1	type 1 helper T cell
Th17	type 17 helper T cell
Th2	type 2 helper T cell

TJP	tight junction protein
TLR	toll-like receptor
TNF-α	tumor necrosis factor alpha
T-PER	tissue-protein extract reagent
UC	ulcerative colitis
US	United States
V	volt
VAChT	vesicular acetylcholine transporter
WT	wild-type
ZO	zonula occludens

Chapter 1: Introduction

Acetylcholine

Acetylcholine is a major signaling molecule classically discussed in the context of neurotransmission in the central (CNS) and peripheral nervous systems (PNS). Acetylcholine was discovered in 1914, but its function as a neurotransmitter was not established until 1926 [1]. In 1936, Otto Loewi and Sir Henry Dale received the Nobel Prize for contributions related to the discovery of acetylcholine [2]. More recently there has been an emerging role for “non-neuronal” acetylcholine and it is now recognized that in addition to neurons, acetylcholine is synthesized and released by epithelial cells [3], endothelial cells [3], immune cells [4], and subcutaneous fat [3]. Receptors for acetylcholine are expressed widely, suggesting that multiple cell types have the potential to respond to cholinergic input and act as effector cells. Recently, the contribution of acetylcholine to modulation of pathologic inflammatory states has been recognized [5-11].

Acetylcholine is an ester of choline and acetyl coenzyme A with chemical formula $CH_3COO(CH_2)_2N^+(CH_3)_3$. Multiple enzymes act in concert to synthesize, store, and release acetylcholine. Key enzymes that participate in the synthesis of acetylcholine include plasma membrane choline transporter (ChT1), which transports choline into cells, and choline acetyltransferase (ChAT), which links choline and acetyl coenzyme A to form acetylcholine. In neurons, vesicular transporters (e.g. vesicular acetylcholine transporter [VAChT] and ChT1) store acetylcholine in vesicles prior to release. Release of acetylcholine occurs upon neuron depolarization, which causes vesicle fusion with the plasma membrane releasing acetylcholine at the synaptic cleft, neuromuscular junction, or other adjacent effector cell. Neurons and a subset of non-neuronal cells produce and release cholinesterases such as acetylcholinesterase (AChE) or butyrylcholinesterase (BChE), which rapidly hydrolyze acetylcholine to acetate and choline, contributing to its relatively short half-life (Figure 1) [1]. A variety of pathologic conditions involving different organ systems are associated with disorders in acetylcholine synthesis, release, recognition, or hydrolysis including atopic dermatitis, psoriasis, asthma, atherosclerosis, colon cancer, inflammatory bowel disease (IBD), overactive bladder, urinary retention, and rheumatoid arthritis [2].

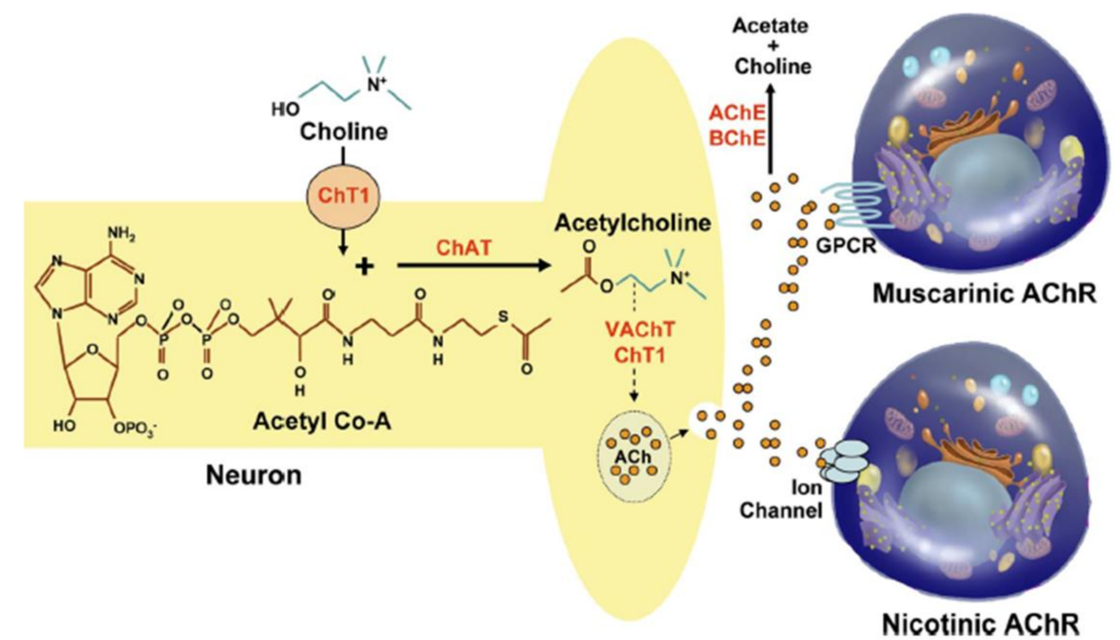

Figure 1: Neuronal acetylcholine production, release, degradation, and interaction with cholinergic receptors. From [1].
ChAT: choline acetyltransferase. ChT1: choline transporter 1. VAChT: vesicular acetylcholine transporter. ChAT: choline acetyltransferase. AChE: acetylcholinesterase. BChE: butyryl cholinesterase. GPCR: G-protein coupled receptor. AChR: acetylcholine receptor.

Cholinergic Receptors

Acetylcholine binds to either nicotinic receptors (NR) or one of five subtypes of muscarinic receptor (MR) (Figure 1), designated M1R – M5R. MR are G-protein coupled receptors (GPCR) that mediate cholinergic neurotransmission at effector cells. Structurally, MR are composed of three intracellular and three extracellular loops with intracellular signaling determined primarily by the amino acid sequence of the second intracellular loop as well as a portion of the third intracellular loop [12]. M1R, M3R, and M5R share a common signaling pathway that activates phospholipase C-β via G_q/11 G-proteins ultimately increasing intracellular calcium concentration through the phosphatidylinositol triphosphate system. M2R and M4R inhibit adenylyl cyclase activity via $G_i/_o$ G-proteins [1].

MR are expressed in a variety of organ systems and on numerous cell types, suggesting a broad role for muscarinic signaling in the regulation of multiple organ systems. In fact, MR activity affects ocular (ciliary muscle contraction, pupillary constriction), cardiac (chronotropy, inotropy), vascular (vasodilation, vasoconstriction), pulmonary (bronchoconstriction), and genitourinary (micturition) function [1]. In addition, it has been suggested that MR activity may augment inflammation, particularly in the lung [13]. Even so, the contribution of MR to immune homeostasis and response to inflammatory stimuli remains undefined.

In addition to MR, acetylcholine acts at NR, which are ligand-gated ion channels. NR are pentamers that consist of varying combinations of at least 17 identified subunits (α1-α10, β1-β4, γ, δ, ε), although they may also exist as homomers (e.g. α7) [14]. NR have several conformational states that vary depending on ligand binding. In the setting of a cholinergic stimulus NR move from a resting state in which ion channels are effectively closed to an activated state where they are open, permitting ion flux to occur [15]. If a sufficient number of channels open membrane conductance is altered, leading to depolarization and the generation of an action potential.

Like MR, NR are also expressed in a variety of organ systems and on numerous cell types including neurons, myocytes, epithelial cells, immune cells and in organs such as pancreas, lung, and brain [16]. Deficiencies in NR have been implicated in the pathogenesis of Alzheimer's disease [17]. Additionally, patients who are smokers tend to develop less severe forms of Parkinson's disease [16]. Similarly, nicotine is protective in patients with ulcerative colitis (UC); however, nicotine exposure worsens disease activity in patients with Crohn's disease (CD). As with MR, the contribution of NR to non-neuronal functions is increasingly recognized.

Cholinergic Regulation of Inflammation

One of the most interesting and potentially paradigm-shifting discoveries in the realm of cholinergic signaling is the relatively recent realization that cholinergic tone can modulate inflammatory conditions through the α7 NR. The cholinergic anti-inflammatory reflex, transduced by the vagus nerve, is implicated in amelioration of a variety of inflammatory conditions including septic shock, post-operative ileus, experimental arthritis, pancreatitis, and dextran sulfate sodium (DSS)-induced colitis [18].

The anti-inflammatory reflex consists of two arcs – one an afferent sensory arc and the other an efferent motor arc. The ability of neurons to respond to inflammatory cytokines is established as neurons within the brain are capable of responding to intracerebral cytokines, effecting physiologic and behavioral changes such as fever, anorexia, decreased social activity, and somnolence [19-21]. Watkins *et al.* described the ability of peripheral nerves to respond to local inflammation [22] and demonstrated that the vagus nerve transduces signals from the periphery to the CNS ultimately inducing downstream effects such as pyrexia. The ability of peripheral nerves to respond to local inflammatory stimuli is significantly inhibited in mice that have undergone vagotomy [23]. The efferent arc of the anti-inflammatory reflex exerts its effects through the release of acetylcholine, which acts on immune cells via α7 (Figure 2). The key role of α7 in mediating these effects was demonstrated by studying α7-deficient mice, which have significantly higher levels of circulating TNF-α than wild-type (WT) controls [10]. Furthermore, electrical stimulation of the vagus nerve decreases production of inflammatory cytokines including TNF-α, IL-1, IL-6, and IL-8 without affecting levels of IL-10 or TGF-β [24].

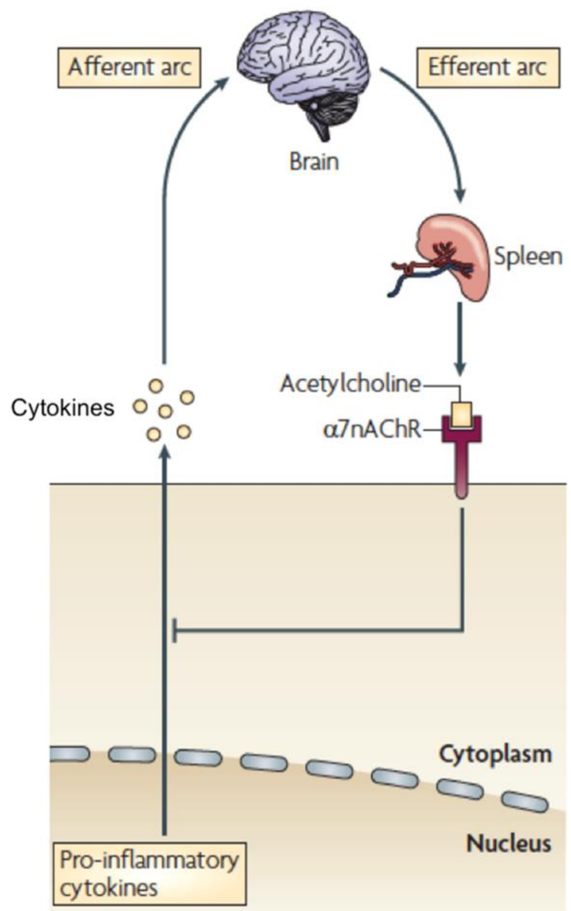

Figure 2: Efferent and afferent arcs of the cholinergic anti-inflammatory reflex. Modified from [24].
α7nAChR: α7 nicotinic acetylcholine receptor.

Considerable investigation has focused on elucidating the mechanisms underlying the ability of α7 to modulate inflammatory conditions. Early experiments suggested that the anti-inflammatory reflex, in a sepsis model, may act via the splenic nerve releasing norepinephrine at splenic T cells. It was suggested that adrenergic stimulation of these T cells triggers acetylcholine release, which then exerts anti-inflammatory effects on splenic macrophages in turn dampening systemic or circulating levels of TNF-α [25,26] (Figure 3). More recently, it has been suggested that in a post-operative ileus model modulation of GI inflammation occurs via a neural circuit involving the release of acetylcholine by cholinergic enteric neurons independent of T cells or the spleen. Acetylcholine released by enteric nerves is thought to modulate the phenotype and activity of intestinal muscularis resident macrophages [26,27], promoting the

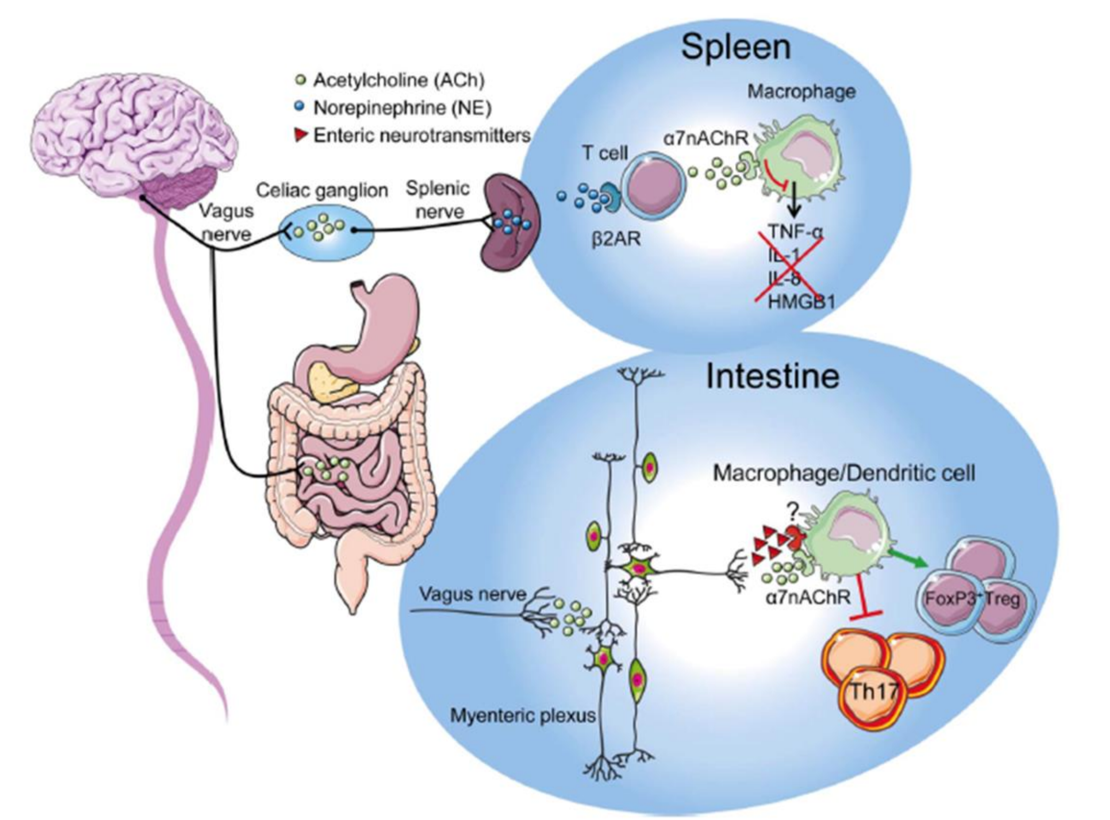

Figure 3: Branches of the cholinergic anti-inflammatory pathway. In systemic inflammation, afferent signaling is transduced via the vagus and splenic nerves. Adrenergic stimulation triggers splenic T cells to release acetylcholine, which then exerts anti-inflammatory effects on macrophages via α7 NR. In intestinal inflammation, cholinergic tone is transduced via the vagus nerve to enteric nerves, which release acetylcholine at resident macrophages, also exerting anti-inflammatory effects via α7 NR. From [26].
α7nAChR: α7 nicotinic acetylcholine receptor.

development of a more tolerogenic phenotype (Figure 3**)**.

The anti-inflammatory effects of cholinergic signaling and its effects on resident macrophages have been studied in a variety of animal models. Transection of the vagus nerve causes WT mice to become more susceptible to DSS-colitis [28] as well as experimental models of pancreatitis [9]. Similarly, a mouse model of depression was more susceptible to DSS [29,30] and when macrophages were transferred from depressed mice to WT mice they too became more susceptible to DSS [31]. In addition, the phenotype and function of resident macrophages have been implicated in the development of diabetic gastroparesis [32], post-operative ileus [33], and ileus related to sepsis [34] suggesting a role for vagal modulation of GI function through actions at macrophages.

Although the effect of cholinergic tone acting at α7 is well described, relatively little is known about the ability of muscarinic signaling to modulate inflammatory conditions or the function of immune cells. A link between MR and pro-inflammatory signaling has been proposed as pulmonary fibroblasts release pro-inflammatory cytokines in the presence of cholinergic stimulation, an effect that is blocked by tiotropium, a MR antagonist [35]. The contribution of MR subtype to cigarette smoke-induced inflammation also has been examined. Neutrophil infiltration in bronchoalveolar lavage fluid from M3R-deficient (*Chrm3*$^{-/-}$) mice is decreased, whereas neutrophil infiltration was increased in *Chrm1*$^{-/-}$ and *Chrm2*$^{-/-}$ mice. Similarly, levels of immune cell chemoattractants and pro-inflammatory cytokines were decreased in *Chrm3*$^{-/-}$ mice, but increased in *Chrm1*$^{-/-}$ and *Chrm2*$^{-/-}$ mice. Pharmacologic blockade of M3R also attenuates release of inflammatory cytokines and immune cell chemoattractants, demonstrating a role for M1R, M2R, and M3R in modulation of cigarette smoke-induced inflammation [13]. In addition, M3R may promote lipopolysaccharide (LPS)-induced TNF-α release from alveolar macrophages [36].

Functions of the Gastrointestinal Tract

The GI tract is responsible for a variety of homeostatic functions including separation of the internal and external milieu, nutrient uptake and fluid secretion, immune surveillance of luminal contents, and host defense. The small intestine and colon participate in these functions to varying degrees and regional variations within these structures also exist.

The intestinal epithelium comprises approximately 400 m^2 and is the largest mucosal surface in humans [37]. This surface represents one of the interfaces between the internal milieu and the exterior world. The epithelium is comprised of a variety of cell types, the most numerous of which is the absorptive enterocyte; however, specialized cells such as enteroendocrine cells, goblet cells, and Paneth cells (small intestine only) are also found in varying proportions along the GI tract. Stability of the intestinal barrier is dependent upon proper functioning and regulation of intercellular tight junction proteins (TJP). Multiple TJP have been identified including occludin, claudins, zonula occludens (ZO), and junctional adhesion molecule. ZO proteins link the TJP complex to the actin cytoskeleton [38]. The conformation and interaction of these proteins is determined, in part, by the cytokine microenvironment and activation (phosphorylation) of myosin light chain by myosin light chain kinase, causing contraction of the actin cytoskeleton. Cytoskeletal contraction has a “purse-string” effect pulling adjacent epithelial cells away from each other thereby promoting increased flux between epithelial cells [39]. TNF-α and IFN-γ expression, which are increased in inflammatory conditions such as IBD, affect permeability through this mechanism [40,41]. Derangements in enteric barrier function are associated with a variety of pathologic conditions including celiac disease, IBD, and irritable bowel syndrome (IBS) as well as multiple extraintestinal diseases such as ankylosing spondylitis, type 1 diabetes, IgA nephropathy, nonalcoholic steatohepatitis, and multiple sclerosis [42,43]. Although a number of receptors, cytokines, and neurotransmitters have been studied with respect to their impact on barrier function [44,45], the contribution of MR to barrier stability remains undefined. Even so, a role for M3R, which is expressed on GI epithelial cells, in modulation of epithelial permeability is suggested as *Chrm3*$^{-/-}$ mice are more susceptible to DSS-colitis [46].

Although one of the primary functions of GI epithelium is to prevent uptake of non-nutrient and pathogenic enteral contents, it must do so while facilitating absorption of nutrients and water. The proportion of water and electrolytes absorbed from the GI tract varies from segment to segment (i.e. jejunum vs. distal colon), and along the crypt-villus axis, and is determined by the transporters present in the apical and/or basolateral membranes as well as the regional composition of TJP. The basolateral membrane of epithelial cells contains a Na^+ pump (Na^+/K^+ ATPase) that establishes cell polarity by expelling 3 Na^+ ions in exchange for 2 K^+ ions, thereby contributing to the establishment of a resting potential across the cell. Transport of ions and small molecules across the epithelium is bidirectional and occurs across the cell (transcellular) and between cells (paracellular). Paracellular flux is driven by a combination of concentration, electrical, osmotic, and hydrostatic gradients whereas transcellular flux occurs via active or passive transport mechanisms. Water absorption or secretion is largely determined by osmotic gradients although it has been suggested that aquaporins [47] and the apical Na^+-glucose transporter may also contribute [48]. A variety of channels, carriers, and transporters contribute to electrolyte flux across the membrane. Nutrient transporters in the small intestine permit uptake of carbohydrates such as glucose, galactose, and fructose. Carbohydrates are digested by salivary and pancreatic amylases as well as brush border hydrolases, ultimately permitting their uptake by transporters such as SGLT1 (glucose, galactose) and GLUT5 (fructose). Lipids are predominantly absorbed in the proximal small intestine after emulsification, lipolysis, and micelle formation. Finally, proteins are digested by pepsins, proteases, and peptidases and are transported across the epithelium as di- or tripeptides by peptide transporters or as amino acids by the protein-coupled amino acid transporter [49].

In addition to permitting uptake of nutrients and establishing a physical barrier between the internal and external milieu, the GI tract plays a key role in immunity and host defense. Not only do epithelial cells establish a physical barrier separating the internal and external environment, the release of mucins and antimicrobial peptides (AMP) as well as secretory immunoglobulin (Ig) establishes a biochemical barrier that complements the physical barrier established by the epithelium. Mucins, which are secreted by goblet cells, form the intestinal mucus layer on the mucosal surface [50]. This layer limits apposition of bacterial cells with the mucosal surface. Mucin-2 (Muc2), the primary mucin produced by goblet cells in the small intestine and colon [51], plays a key role in host defense as Muc2-deficient (*Muc2*$^{-/-}$) mice spontaneously develop colitis [52].

Additionally, over 90% of *Muc2*$^{-/-}$ mice succumb to infection with *Citrobacter rodentium* (*C. rodentium*), an attaching/effacing (A/E) gram-negative bacterium [53]. In addition to mucins, a variety of AMP such as regenerating islet-derived protein IIIγ (RegIIIγ), defensins, cathelicidins, and lysozyme are produced by enterocytes, also contributing to host defense. AMP play an important role in innate host defense by targeting common bacterial antigens leading to destruction of bacterial cells without damage to nearby host cells. In the small intestine RegIIIγ also limits direct contact of bacteria with the mucosal surface [52]. By limiting contact of luminal bacteria with the mucosal surface the host limits interaction of these microorganisms with immune cells and, consequently, activation of the mucosal immune system.

Finally, the GI tract has an important role in immune surveillance and mucosal homeostasis. Lymphocytes as well as macrophages and dendritic cells (DC) are found throughout the GI tract in gut-associated lymphoid tissue (GALT) such as Peyer's patches and isolated lymphoid follicles as well as in non-immune structures including the lamina propria, which contains CD4^{+} and CD8^{+} T cells, plasma cells, macrophages, DC, eosinophils, and mast cells as well as intestinal mucosa, which contains primarily lymphocytes. Peyer's patches are adjacent to microfold (M) cells, which are interspersed among enterocytes, permitting sampling of microorganisms and luminal antigens. These microorganisms and other antigens are taken up by DC for presentation to T lymphocytes. DC also reside in the lamina propria and extend processes through the epithelium to sample luminal contents directly [49]. Because of the high number of commensal microorganisms present, the majority of the antigens encountered by immune cells within intestinal mucosa are nonpathogenic. Increasing evidence supports a tolerogenic phenotype of macrophages and DC in the GI tract. Macrophages isolated from colon constitutively secrete IL-10, an anti-inflammatory cytokine, and upon toll-like receptor (TLR) engagement IL-10 production is increased [54]. In fact, IL-10-deficient mice develop spontaneous colitis, but do not develop colitis when raised in germ-free conditions [55]. It is thought that intestinal macrophages mount a pro-inflammatory response upon pathogen entry into the cytosol and/or with inflammasome activation [55]. Polymorphonuclear leukocytes (PMN) are not found in significant numbers in GI mucosa, but are rapidly recruited when appropriate chemokines are released, killing invading bacteria through phagocytosis as well as release of reactive oxygen species, AMP, and proteolytic enzymes [56]. Prolonged PMN infiltration can, however, have pathologic effects and is thought to contribute to chronic mucosal damage observed in IBD patients, potentially by generating a positive feedback loop that continuously primes T cells [56]. Last, innate lymphoid cells (ILC) assist in wound healing and tissue repair by releasing the anti-inflammatory cytokine IL-22 [37,57]; however, like PMN, prolonged activation of ILC can promote disease through secretion of IL-17, which is observed in chronic inflammatory conditions [37,57]. Importantly, the intestinal mucosal immune system is tolerant to commensal bacteria and utilizes various strategies to prevent inappropriate response to these microorganisms including physical, chemical, and immunological barriers that prevent immune activation in the absence of the proper stimulus.

Chapter 2: Type 3 Muscarinic Receptors Contribute to Host Defense Against *Citrobacter rodentium* and Exert Pro-Inflammatory Effects on Macrophages

Introduction

Inflammatory bowel disease (IBD) is comprised primarily of two subtypes, UC and CD, together affecting approximately 3.6 million people in the United States (US) and Europe [58]. Despite efforts to better understand the factors that cause IBD to develop, its pathogenesis remains poorly understood. Nonetheless, it is thought that IBD is more likely to develop in genetically-predisposed hosts that possess aberrant host defensive responses to gut microbes, triggering inappropriate activation of the immune system directed at self-antigens within intestinal mucosa [59].

Macrophages are an important part of the innate and adaptive immune systems. They are resident cells within GI mucosa where they serve a homeostatic role, participating in clearance of dead cells, debris, and pathogens. Macrophage phenotype is heavily influenced by the local microenvironment. In the presence of T_H1 cytokines or LPS, macrophages become CAM and release mediators such as TNF-α, IL-1, and IL-6 to enhance destruction of microorganisms and promote leukocyte recruitment. In the presence of T_H2 cytokines, however, macrophages become AAM and promote wound healing and tissue repair. In patients with IBD, macrophages are activated inappropriately by non-pathogenic stimuli, such as self-antigens or gut commensals, and cause inflammation that is often harmful to the host [56,60]. The importance of macrophage phenotype in modulating colitis has been demonstrated in animal models where AAM are shown to reduce the severity of experimental colitis [61-64].

Cholinergic regulation of immunity, dubbed the cholinergic anti-inflammatory pathway, has been studied closely over recent years after electrical stimulation of the vagus nerve was found to inhibit TNF-α production. Clinically significant effects of increased α7 activity on macrophages include attenuation of pathologic states such as septic shock, post-operative ileus, arthritis, pancreatitis, and DSS-induced colitis [18]. In a sepsis model these effects, which are mediated by the actions of acetylcholine at the α7 NR, were attributed to acetylcholine release by splenic T cells in response to stimulation by the splenic nerve [4]. It was postulated that acetylcholine produced by T cells acts at splenic macrophages, which in turn modulate systemic TNF-α levels. Recently, the proximity of enteric nerves to mucosal antigen presenting cells within intestinal mucosa has been demonstrated suggesting the presence of a local "neuroimmune" synapse at these sites, through which cholinergic stimulation of resident immune cells can occur [27,65,66]. Although the effects of α7 activity on macrophage phenotype and function are well characterized, the contribution of MR to macrophage phenotype and function remains unclear.

Like NR, MR also respond to cholinergic stimuli. In total, 5 MR have been identified (M1R – M5R), encoded by *Chrm1-5*. MR are GPCR that mediate cholinergic neurotransmission at effector cells. Alterations in cholinergic tone can have pathologic effects on organ function as is seen in chronic obstructive pulmonary disease (COPD) and urinary retention [67]. MR have been variably linked to pro- or anti-inflammatory actions depending on the tissue and MR subtype studied [5,68,69]. Studies examining the effects of MR activity on immune regulation within the lung found that M3R activation may be pro-inflammatory whereas M1R and M2R activation may have anti-inflammatory effects [69]. Other authors have, however, suggested a pro-inflammatory role for M1R [5] indicating a lack of consensus on the impact of these receptors on immune function. Blockade of MR with atropine, a MR antagonist, in an *in vivo* model has suggested that MR as a group may be pro-inflammatory and potentially serve as a counterweight to the anti-inflammatory effects of NR [70]; however, the effects of MR-subtype specific antagonists on inflammation were not reported. As in the lung, the epithelial lining of the intestine plays a critical role in homeostasis and immune regulation. Within the GI tract, M3R is implicated in intestinal epithelial proliferation, which plays a key role in maintenance and post damage restitution of mucosal barrier function [71]. Few studies have examined the impact of these receptors on macrophage phenotype or function, particularly within the GI tract where the aberrant function of these cells has the potential to induce local and systemic disease.

Citrobacter rodentium (*C. rodentium*) is a gram-negative attaching/effacing (A/E) bacterium that transiently colonizes the colon during periods of infection evoking a highly polarized T_H1/T_H17 response [72-74]. *C. rodentium* infection serves as a model for enteropathogenic *Escherichia coli* infection in humans causing epithelial cell hyperplasia accompanied by an influx of $CD4^+$ cells as well as mucosal damage that closely mimics CD [72]. Both innate and adaptive immune responses are required for *C. rodentium* clearance [75-77]. The presence of colonic mucus is also a key factor in host defense against *C. rodentium*, as *C. rodentium*-infected *Muc2*$^{-/-}$ mice suffer mortality as high as 90% [53,78]. Since M3R is expressed on epithelial cells, including goblet cells, as well as on macrophages, we hypothesized that M3R is likely to affect *C. rodentium* clearance through direct effects on epithelial or immune cell function, or a combination of both of these factors.

The current study was designed to investigate the role of M3R on mucosal homeostasis within the colon, its contribution to host defense against the T_H1/T_H17-inducing pathogen *C. rodentium*, and its ability to modulate macrophage phenotype and function. The results of our studies demonstrate that M3R activity does not impact the ability of the host to mount a T_H1/T_H17 cytokine response to *C. rodentium*, but does affect clearance of *C. rodentium* through decreased efficacy of effector cell functions that contribute to innate immunity, specifically, regulation of mucin production by goblet cells. In addition, our studies indicate that macrophages attain a classically activated phenotype in the presence of muscarinic-specific cholinergic stimulation, an effect that is dependent on M3R; however, macrophages that do not express M3R retain their ability to differentiate into classically activated macrophages in the presence of an inflammatory stimulus (IFN-γ). These data suggest that muscarinic-specific cholinergic stimulation of macrophages has pro-inflammatory effects. We conclude that M3R facilitates clearance of the enteric pathogen *C. rodentium* through actions on goblet cells and mucus production and exerts pro-inflammatory effects on macrophages.

Methods

Animal Studies

Age and sex-matched WT and *Chrm3*$^{-/-}$ mice on a C57BL/6 background were purchased from Taconic Farms (Germantown, NY) or generously donated by Dr. Jürgen Wess of the National Institutes of Health (Bethesda, MD). Mice were housed at the United States Department of Agriculture animal facility and provided food and water *ad libitum*. Animals were euthanized using ketamine/xylazine prior to performing physiologic studies and collection and processing of tissues. Tissue samples were collected for molecular analysis, histological evaluation, and assessment of bacterial invasion. All studies were conducted in accordance with the principles set forth in the Guide for Care and Use of Laboratory Animals, Institute of Laboratory Animal Resources, National Research Council, Health and Human Services Publication (National Institutes of Health 85-23, revised 1996), and the Beltsville Area Animal Care and Use Committee (Protocol #10-003). The protocol was also approved by the Institutional Animal Care and Use Committee of the University of Maryland School of Medicine (Protocol #0110018).

Citrobacter Infection

A naladixic acid resistant mutant of *C. rodentium* strain DBS100 (American Type Culture Collection 51459; Manassas, VA) was used to inoculate WT and *Chrm3*$^{-/-}$ mice. *C. rodentium* was grown overnight in Luria-Bertani (LB) medium. The bacteria were collected by centrifugation and re-suspended in LB medium. WT and *Chrm3*$^{-/-}$ mice were infected by oral gavage with 0.2 mL of the bacterial suspension containing approximately

1.0E+10 colony forming units (CFU) of *C. rodentium*. The dose was confirmed by retrospective plating on LB agar plates containing 50 μg/mL naladixic acid.

Citrobacter Clearance and Invasion

Stool was collected from WT and *Chrm3*$^{-/-}$ mice throughout the course of *C. rodentium* infection to determine fecal bacterial content. Fecal pellets were homogenized in LB medium, diluted serially, and plated onto LB agar plates containing 50 μg/mL naladixic acid. Spleen and mesenteric lymph nodes (MLN) were collected from uninfected mice and mice 13 DPI, homogenized in LB media, and diluted serially. The presence of *C. rodentium* in spleen and MLN was determined by plating on LB agar plates. *C. rodentium* content was determined to be zero based on a colony count of zero obtained from duplicate plates inoculated with samples of undiluted fecal, MLN, or spleen homogenates. The limit of detection was assigned a colony count of 0.5.

Microsnapwell Assay for Mucosal Transepithelial Electrical Resistance

The modified microsnapwell system is a miniaturized version of the standard Ussing chamber designed to measure mucosal transepithelial electrical resistance (TEER) [79]. Decreased TEER indicates increased tissue permeability. Segments of muscle-free colon were harvested from uninfected or *C. rodentium*–infected WT and *Chrm3*$^{-/-}$ mice, stripped of both muscularis externa and serosal layers, and mounted in the microsnapwell system. A total of 250 μL DMEM containing 4.5 g/L glucose, 4 mM L-glutamine, and 1 mM nonessential amino acids was added to the mucosal side. Three milliliters of the same medium was added to the serosal side. The system was incubated at 37°C with 5%

CO_2 for 30 min to permit stabilization of pH and TEER was measured every 30 min for 180 min.

Immunoglobulin Quantification

Blood was collected by cardiac puncture and serum separated using serum-gel microfuge tubes (Sarstedt, Inc.; Newton, NC). Serum was collected by centrifugation and stored at -20°C until assayed. *C. rodentium* antigen was prepared by extracting an overnight culture of the bacteria with B-Per reagent (Thermo-Scientific; Chicago, IL) and clarified by centrifugation. The protein content of the antigen preparation was determined using the BCA protein assay (Thermo-Scientific; Chicago, IL) with BSA as the standard. Nunc MaxiSorp plates (eBioscience, Inc.; San Diego, CA) were coated overnight at 4°C with *C. rodentium* antigen at 10 µg/mL in PBS. After washing with PBS/0.05% Tween-20, plates were blocked with 5% non-fat milk for at least 1 h at room temperature. After washing, plates were incubated with serial dilutions of serum (in duplicate) in SuperBlock Blocking Buffer (Thermo-Scientific; Chicago, IL)/5% normal goat serum/0.05% Tween-20 for 30 min at 37°C. Plates were then washed with PBS/0.05% Tween-20 and incubated with a 1:10,000 dilution of biotinylated anti-mouse IgM (Antibodies, Inc.; Davis, CA) in SuperBlock Blocking Buffer/5% normal goat serum/0.05% Tween-20 for 30 minutes at 37°C. After washing with PBS/0.05% Tween-20, plates were incubated with a 1:1,000 dilution of Streptavidin-HRP (Vector Laboratories; Burlingame, CA) in SuperBlock Blocking Buffer/5% normal goat serum/0.05% Tween-20 for 30 min at 37°C. After a final wash, bound antibodies were detected by incubation with the HRP substrate 3,3',5,5'-*tetramethylbenzidine* and the color reaction was terminated by addition of 4N H_2SO_4. Plates were read at 450 nm on a SpectroMax M5 plate reader (Molecular Devices, LLC; Sunnyvale, CA).

Epithelial Proliferation

Bromodeoxyuridine (BrdU) dissolved in PBS (10 mg/0.2 mL) was injected intraperitoneally 1 h prior to euthanasia of uninfected and *C. rodentium*-infected WT and *Chrm3*$^{-/-}$ mice. Immunohistochemistry was performed utilizing formalin grade anti-BrdU antibody (Roche Diagnostics; Mannheim, Germany) diluted at 1:200 to assess epithelial proliferation. Bound antibodies were detected using a Mouse on Mouse (M.O.M.) kit (Vector Laboratories; Burlingame, CA) according to the manufacturer's instructions. The number of BrdU-positive cells per crypt was determined by counting 20 well-oriented crypts per stained section. For each mouse, BrdU-positive cells per crypt were averaged to yield a mean per animal and then averaged with mice from the same treatment group to yield a mean value per treatment group.

RNA extraction, cDNA Synthesis and Quantitative Real-Time Polymerase Chain Reaction (qRT-PCR)

Total RNA was extracted from tissue samples or bone-marrow derived macrophages (BMDM) with TRIzol reagent (Invitrogen; Carlsbad, CA) according to manufacturer's instructions. RNA integrity, quantity, and genomic DNA contamination were assessed using the Agilent Bioanalyzer 2100 and RNA 6000 Labchip kit (Agilent Technologies; Palo Alto, CA). Only those RNA samples with 28S/18S ratios between 1.5 and 2 and no DNA contamination were studied further. RNA samples (2 µg) were reverse-transcribed to cDNA using the First Strand cDNA Synthesis Kit (MBI Fermentas; Hanover, MD) with random hexamer primer.

Amplification reactions were performed on an iCycler detection system (Bio-Rad Laboratories; Hercules, CA). Primer sequences were designed using Beacon Designer 5.0 (Premier Biosoft International; Palo Alto, CA), and synthesized by the Biopolymer Laboratory of the University of Maryland. PCR was performed in 25 μL volume wells using SYBR Green Supermix (Bio-Rad Laboratories; Hercules, CA). Amplification conditions were: 95°C for 3 min, 60 cycles of 95°C for 15 s, 60°C for 15 s, and 72°C for 20 s. The fold-change in mRNA expression for targeted genes was calculated relative to respective vehicle-treated groups of mice after normalization to 18s rRNA. 18s rRNA was selected as the internal standard based on preliminary studies demonstrating no significant differences in 18s rRNA level among different groups of samples studied.

Immunofluorescence

Colons were opened longitudinally along the mesenteric border, fixed for 2 h in 4% paraformaldehyde, and embedded in paraffin blocks. Five micrometer sections affixed to glass slides were de-waxed in xylene and rehydrated in descending ethanol baths. Antigen retrieval was achieved by incubating slides in sodium citrate buffer. Nonspecific binding of antibodies was blocked with 5% normal goat serum in PBS containing 2% BSA and 0.05% Tween-20. Sections were incubated with anti-*C. rodentium*, a generous gift from Dr. P. Sherman (The Hospital for Sick Children; Toronto, Canada), overnight at 4^{o}C at a dilution of 1:300. After washing with PBS, slides were incubated with goat anti-rabbit at a dilution of 1:500 for 45 min and then washed with PBS. Slides were mounted using mounting medium containing DAPI (Sigma-Aldrich; St. Louis, MO). Images were acquired with an Axio Imager M2 microscope (Carl Zeiss Microscopy; Thornwood, NY) using ZEN Pro 2012 image acquisition software (Carl Zeiss Microscopy; Thornwood, NY).

Preparation and Treatment of Bone Marrow–Derived Macrophages

Macrophages were prepared from bone marrow mononuclear cells as previously described [80]. Mononuclear cells were obtained by flushing bone marrow from femurs, tibiae, and humeri with HyClone alpha MEM medium (Thermo-Scientific; Chicago, IL) pre-equilibrated at 37°C. Cells were cultured overnight in alpha MEM medium containing 10% FBS and 1% penicillin/streptomycin in a humidified incubator at 37°C with 5% CO_2. Non-adherent cells were collected by centrifugation after lysis of red blood cells using red blood cell lysis buffer (Sigma-Aldrich; St. Louis, MO) and mononuclear cells were counted and plated. Mature macrophages were generated by differentiating isolated mononuclear cells with 20 ng/mL rM-CSF (R&D Systems; Minneapolis, MN) for 7 d. WT or *Chrm3*$^{-/-}$ macrophages were then treated with IFN-γ, IL-4, bethanechol, atropine, or a combination of these agents for 24 h to determine their ability to attain a classically or alternatively activated phenotype.

Western Blot

BMDM were collected after 24 h treatment with vehicle, IFN-γ, or IL-4 and lysed in RIPA buffer (Thermo-Scientific; Chicago, IL) containing 1X protease inhibitor (Roche Diagnostics; Mannheim, Germany). Samples were centrifuged at 12,000 *g* at 4°C and the protein content of the resulting supernatants was determined using a BCA protein assay (Thermo-Scientific; Chicago, IL) with BSA as a standard. Fifty micrograms of each sample was subjected to SDS-PAGE using 12% Tris-glycine gels (Invitrogen; Carlsbad, CA) with Tris-glycine SDS running buffer (Invitrogen; Carlsbad, CA). After electrophoresis, proteins were transferred onto nitrocellulose membranes (Invitrogen; Carlsbad, CA). Membranes were blocked using 5% non-fat milk/Tris buffered saline plus 0.1% Tween-20 (TBS-T) overnight at 4^{o}C and subsequently probed with anti-M3R (Alomone Labs; Jerusalem, Israel) and anti-GAPDH (Abcam, Inc.; Cambridge, MA) diluted at 1:2,000 and 1:10,000, respectively, in 5% non-fat milk/TBS-T. Bound antibodies were detected using HRP-conjugated goat anti-rabbit IgG (KPL; Gaithersburg, MD) or goat anti-mouse IgG (Santa Cruz Biotechnology; Santa Cruz, CA) diluted at 1:2,000 and 1:10,000, respectively, in 5% non-fat milk/TBS-T. For detection, membranes were incubated in SuperSignal West Pico Chemiluminescent Substrate (Thermo-Scientific; Chicago, IL) and chemiluminescent bands were acquired using a Fuji Film Intelligent Dark Box with LAS-4000 software version 2.1.

Solutions and Drugs

All drugs used for physiological studies were obtained from Sigma-Aldrich (St. Louis, MO) unless otherwise indicated.

Data Analysis

For multiple comparisons, statistical analyses were performed using a one-way analysis of variance (ANOVA) with post hoc analysis for multiple comparisons. For two comparisons, statistical analyses were performed using a Student's *t*-test. Data analyses were performed using Graph Pad Prism software version 3.03. Differences between groups were considered statistically significant at p-values ≤ 0.05.

Results

M3R-Deficiency is not Associated with Alterations in Constitutive Cytokine Expression, Colon Permeability, or Microscopic Appearance

Increased expression of the T_H1/T_H17 cytokines IFN-γ, TNF-α, and IL-17 as well as the T_H2 cytokines IL-4 and IL-13 contribute to mucosal inflammation and epithelial barrier dysfunction [41,81-83]. Furthermore, perturbations in intestinal permeability are associated with a variety of autoimmune diseases including IBD [42]. We examined gene expression of T_H1/T_H17 and T_H2 cytokines in whole-tissue distal colon from *Chrm3*$^{-/-}$ mice and WT mice. Gene expression of IFN-γ, TNF-α, and IL-17 (Figure 4A) was similar in both strains, as was gene expression of the T_H2 cytokines IL-4 and IL-13 (Figure 4B). TEER, which serves as an inverse measurement of permeability, did not differ between muscle-free colon from *Chrm3*$^{-/-}$ mice and muscle-free colon from WT mice (Figures 5A & 5B). No overt differences were observed between H&E stained sections of proximal colon from WT and *Chrm3*$^{-/-}$ mice (Figure 6).

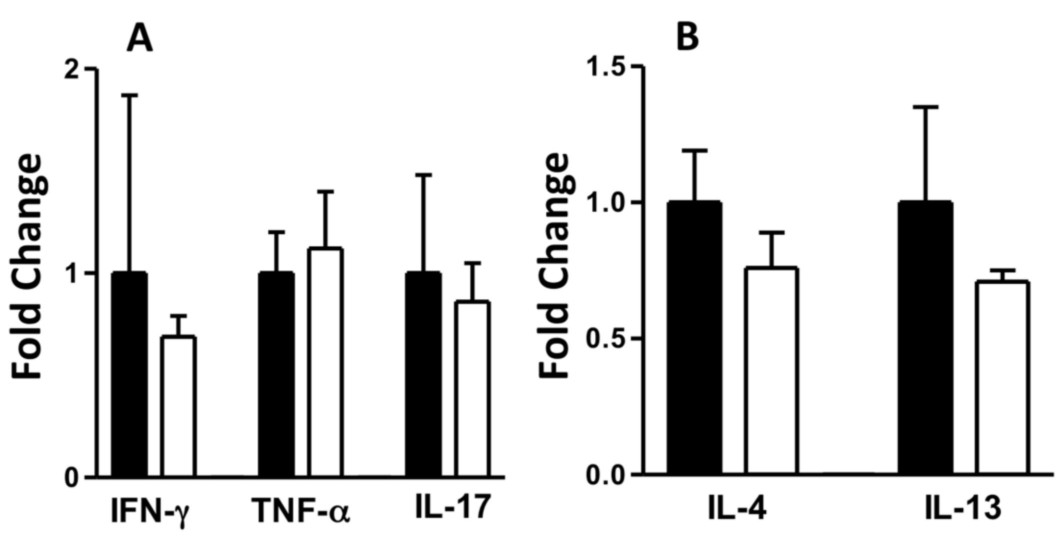

Figure 4: Gene expression of (A) T_H1/T_H17 and (B) T_H2 cytokines in WT (black bars) C57BL/6 and *Chrm3*$^{-/-}$ (white bars) C57BL/6 colon.
WT: wild-type. *Chrm3*$^{-/-}$: M3R-deficient.

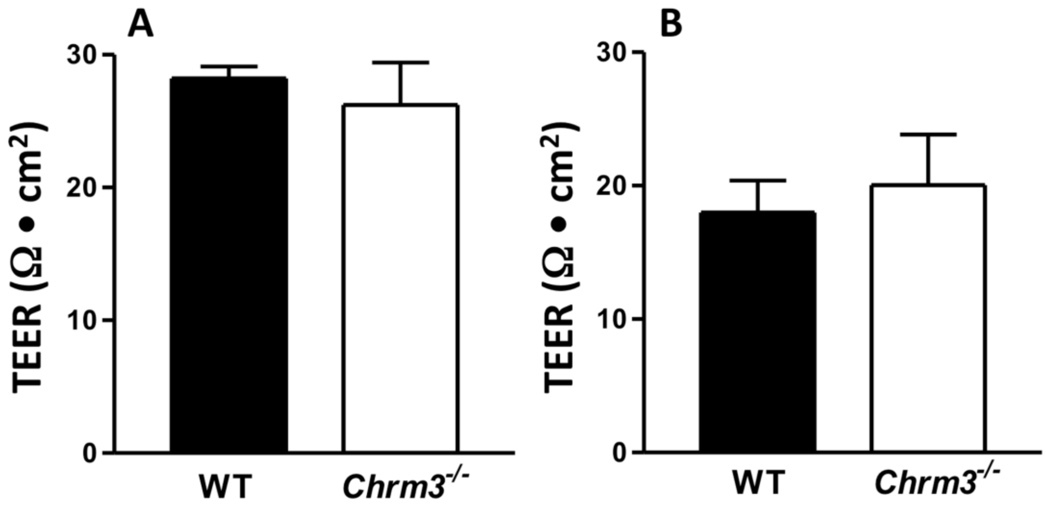

Figure 5: TEER of muscle-free WT (black bars) and *Chrm3*$^{-/-}$ (white bars) colon in (A) C57BL/6 mice and (B) SvEv x CF1 (50%:50%) mice.
WT: Wild type. *Chrm3*$^{-/-}$: M3R-deficient.

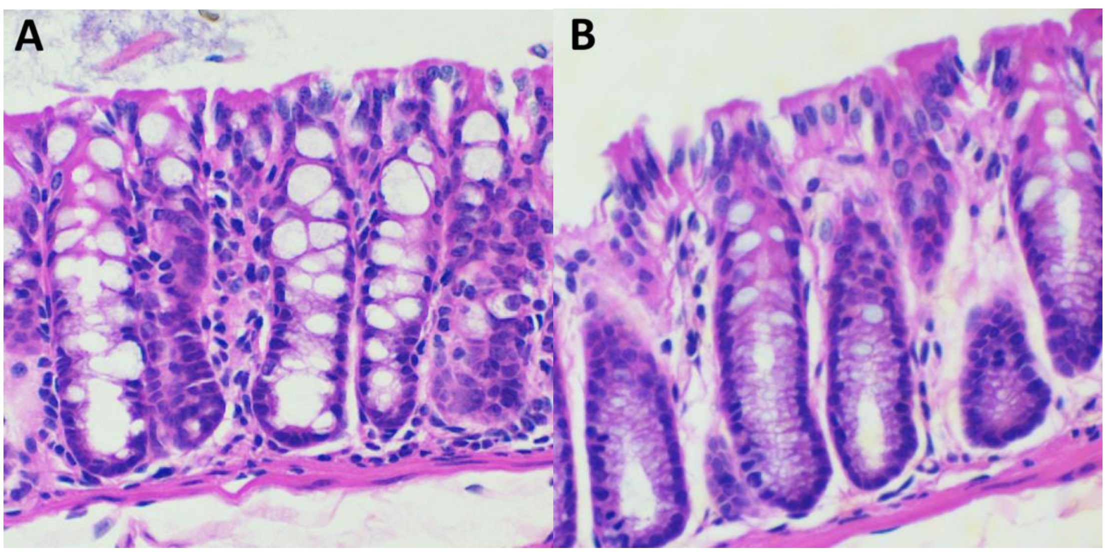

Figure 6: (A) Representative image of colon from WT mouse. (B) Representative image of colon from *Chrm3*$^{-/-}$ mouse.
WT: Wild type. *Chrm3*$^{-/-}$: M3R-deficient.

C. rodentium-Infected WT and Chrm3$^{-/-}$ Mice Lose Body Mass

Although no differences in inflammatory cytokine profile, epithelial barrier function, or histology existed between WT and *Chrm3$^{-/-}$* mice, *Chrm3$^{-/-}$* mice were shown previously to be more susceptible to DSS-induced colitis [46], suggesting that M3R exerts protective effects against chemically induced colitis. *Chrm3$^{-/-}$* mice were infected with *C. rodentium* to determine if M3R affects response to an infectious colitis. As expected, WT mice euthanized 13 DPI weighed significantly less than uninfected WT mice (Figure 7A). Similarly, *Chrm3$^{-/-}$* mice euthanized 13 DPI weighed significantly less than uninfected *Chrm3$^{-/-}$* mice (Figure 7A) with the percent change from baseline weight similar in WT and *Chrm3$^{-/-}$* mice (Figure 7B). Both WT and *Chrm3$^{-/-}$* mice 21 DPI weighed less than uninfected WT and *Chrm3$^{-/-}$* mice (data not shown). These data indicate that *C. rodentium* infection causes a decrease in body mass in both WT and *Chrm3$^{-/-}$* mice.

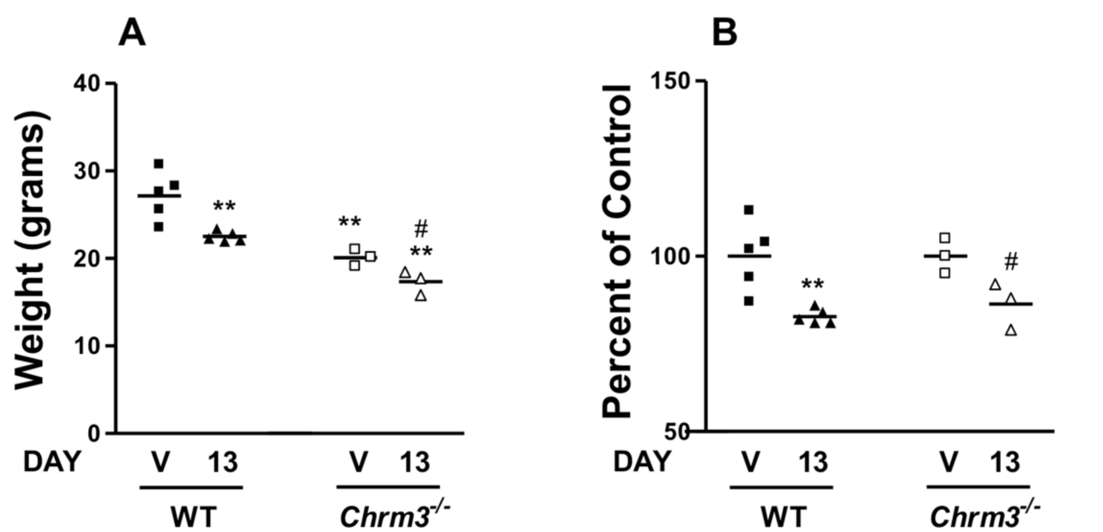

Figure 7: (A) Vehicle treated (uninfected) *Chrm3$^{-/-}$* mice weigh less than sex and age-matched vehicle-treated WT mice. WT and *Chrm3$^{-/-}$* mice experience a significant decrease in body mass at 13 DPI. (B) Both WT and *Chrm3$^{-/-}$* mice experience a similar loss of body mass when normalized to vehicle-treated WT or *Chrm3$^{-/-}$* mass.
WT: Wild type. *Chrm3$^{-/-}$*: M3R-deficient. V: vehicle. 13: 13 DPI. 21: 21 DPI. ** $p < 0.01$ vs. WT V. # $p < 0.05$ vs. *Chrm3$^{-/-}$* V.

Clearance of C. rodentium from Chrm3$^{-/-}$ Mice is Delayed

Stool was collected from WT and *Chrm3*$^{-/-}$ mice and fecal content of *C. rodentium* was determined. Fecal *C. rodentium* content was greater in stool from *Chrm3*$^{-/-}$ mice than WT mice at every time point studied (Figure 8A). In order to confirm that *C. rodentium* adherence was increased in *Chrm3*$^{-/-}$ mice, we probed colon from uninfected and *C. rodentium* infected WT and *Chrm3*$^{-/-}$ mice with an antibody directed against *C. rodentium*. First, a Western blot was performed to evaluate the ability of our polyclonal anti-*C. rodentium* antibody to detect *C. rodentium* (Figure 8B). Once specificity was confirmed, uninfected and *C. rodentium*-infected WT and *Chrm3*$^{-/-}$ colon were stained demonstrating persistent *C. rodentium* in *Chrm3*$^{-/-}$ colon 13 DPI with no discernible *C. rodentium* in WT colon at 13 DPI (Figure 9), indicating that *C. rodentium* was no longer adherent in WT colon 13 and 21 DPI or *Chrm3*$^{-/-}$ colon 21 DPI.

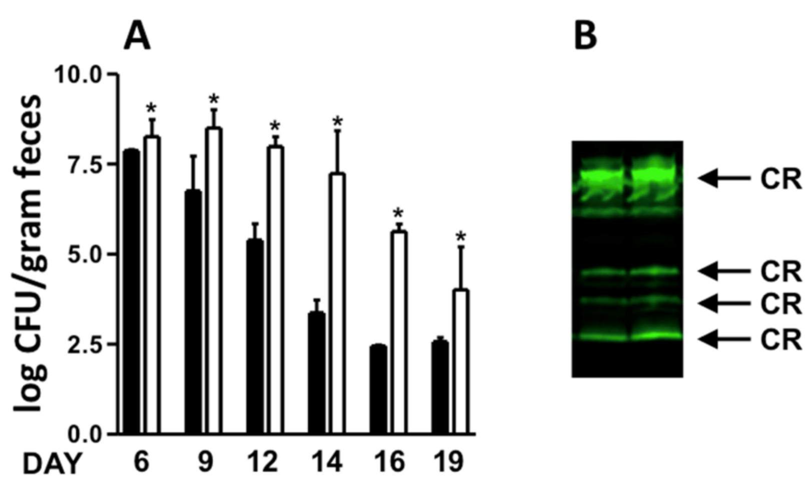

Figure 8: (A) Fecal bacterial content of *C. rodentium* infected WT (black bars) and *Chrm3*$^{-/-}$ (white bars) mice at 6, 9, 12, 14, 16, and 19 DPI. (B) Immunoblot of *C. rodentium* extract (10 µg and 20 µg, respectively) probed with rabbit polyclonal anti-*C. rodentium* antibody.
CFU: colony forming unit. WT: Wild type. *Chrm3*$^{-/-}$: M3R-deficient. * $p < 0.05$ vs. WT. CR: *C. rodentium*.

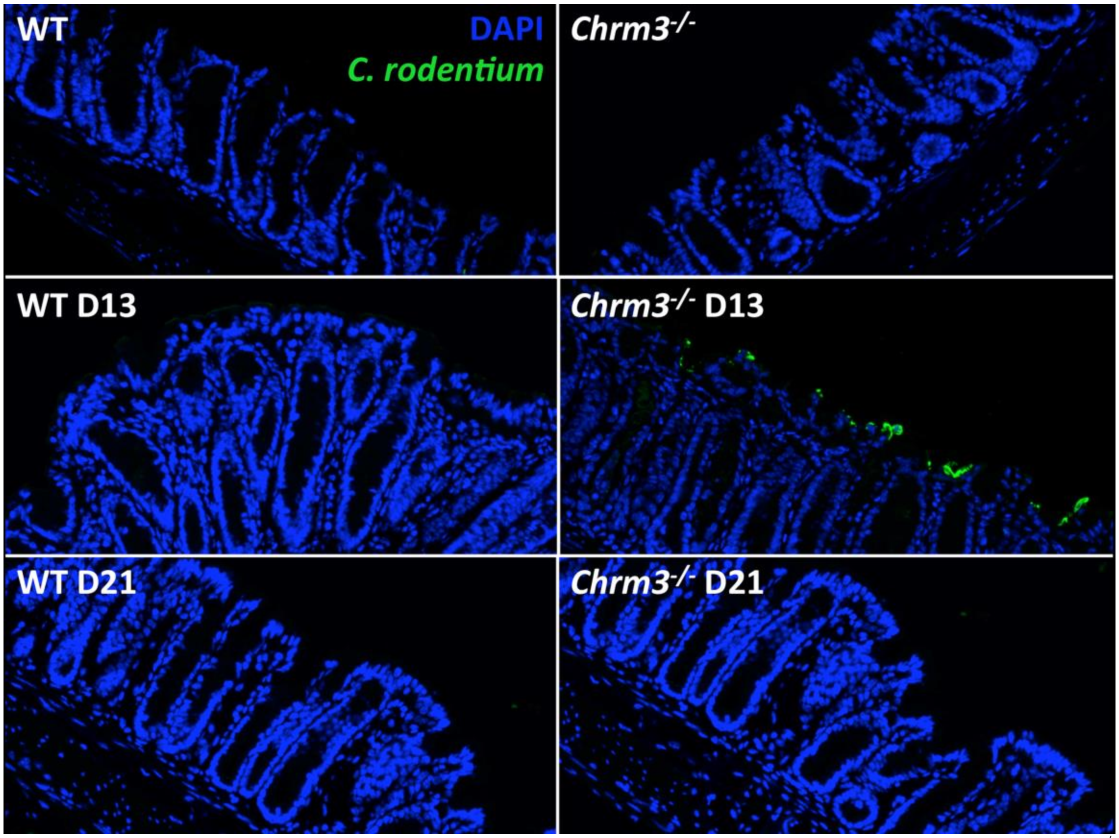

Figure 9: Immunofluorescent staining demonstrating persistent adherence of *C. rodentium* in *Chrm3*$^{-/-}$ colon mucosa 13 DPI. Uninfected WT and *Chrm3*$^{-/-}$ mucosa serve as negative controls. *C. rodentium* is cleared by 21 DPI in both WT and *Chrm3*$^{-/-}$ mucosa.
WT: Wild type. *Chrm3*$^{-/-}$: M3R-deficient. DAPI: 4',6-diamidino-2-phenylindole.

C. rodentium Infected Chrm3$^{-/-}$ Mice Have Increased Spleen Mass

We determined spleen weight normalized to body weight of *C. rodentium*-infected WT and *Chrm3*$^{-/-}$ mice as an index of immune response. Spleen weight per body weight was significantly greater in *Chrm3*$^{-/-}$ mice 13 DPI when compared to WT mice 13 DPI or uninfected *Chrm3*$^{-/-}$ mice (Figure 10). Additionally, spleen weight per body weight of *Chrm3*$^{-/-}$ mice 13 DPI was significantly greater than uninfected *Chrm3*$^{-/-}$ mice. These data indicate that *Chrm3*$^{-/-}$ mice mount an amplified immune response to *C. rodentium* compared to WT mice.

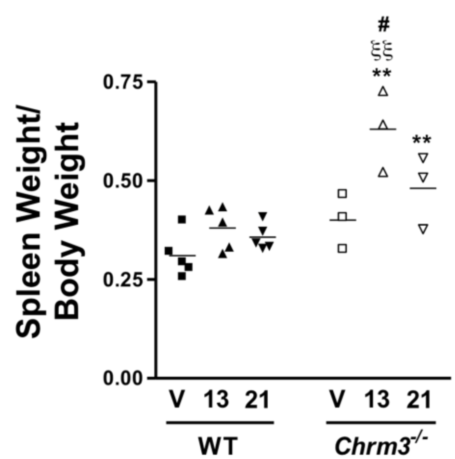

Figure 10: Spleen weight per body weight in *C. rodentium* infected *Chrm3*$^{-/-}$ mice 13 DPI is significantly increased compared to spleen weight per body weight in WT mice 13 DPI and uninfected *Chrm3*$^{-/-}$ mice.
WT: Wild type. *Chrm3*$^{-/-}$: M3R-deficient. V: vehicle. 13: 13 DPI. 21: 21 DPI. ** $p < 0.01$ vs. respective WT control. ξξ $p < 0.01$ vs. WT V. # $p < 0.05$ vs. *Chrm3*$^{-/-}$ V.

Bacterial Invasion is Amplified in Chrm3$^{-/-}$ Mice

Given the increased spleen mass observed in *C. rodentium*-infected *Chrm3*$^{-/-}$ mice, we evaluated MLN and spleen for the presence of *C. rodentium* in these organs. *C. rodentium* was not detected in MLN of WT or *Chrm3*$^{-/-}$ mice 13 DPI, but was detected in spleen of WT and *Chrm3*$^{-/-}$ mice 13 DPI. Bacterial invasion was present in only 1 of 4 WT spleens, but 3 of 4 *Chrm3*$^{-/-}$ spleens (Figure 11), indicating increased susceptibility to bacterial translocation in *Chrm3*$^{-/-}$ mice.

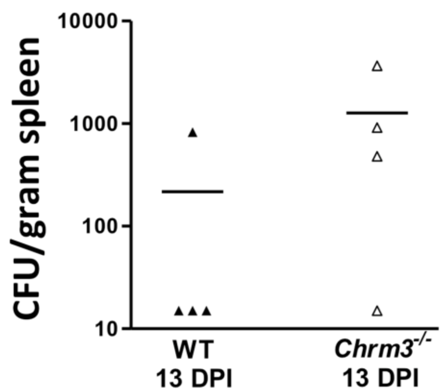

Figure 11: *C. rodentium* was detected in spleen of 1 of 4 WT mice and 3 of 4 *Chrm3*$^{-/-}$ mice 13 DPI.
CFU: colony forming unit. WT: Wild type. *Chrm3*$^{-/-}$: M3R-deficient. V: vehicle.

Cytokine Response is Amplified in C. rodentium-Infected Chrm3$^{-/-}$ Mice

C. rodentium induces a stereotypic T_H1/T_H17 response in infected rodents [72-74]. We determined cytokine expression in uninfected and *C. rodentium*-infected WT and *Chrm3*$^{-/-}$ whole-tissue colon at 13 and 21 DPI. The expression of the T_H1/T_H17 cytokines *IFN-γ*, *TNF-α*, and *IL-17A* were all significantly upregulated at 13 DPI in *Chrm3*$^{-/-}$ colon compared to 13 DPI in WT colon and to uninfected *Chrm3*$^{-/-}$ colon (Figure 12). In addition, *Nos-2* expression was upregulated significantly at 13 DPI in *Chrm3*$^{-/-}$ colon mucosa compared to WT colon and to uninfected *Chrm3*$^{-/-}$ colon (Figure 13), indicating that *in vivo Chrm3*$^{-/-}$ macrophages appropriately attain a classically activated phenotype when exposed to T_H1/T_H17 cytokines. The amplified T_H1/T_H17 response in *Chrm3*$^{-/-}$ colon suggested that these mice do not have a defect in T cell recruitment. Gene expression of the T cell marker *CD3* suggests that T cell recruitment is amplified in *C. rodentium* infected *Chrm3*$^{-/-}$ mucosa (Figure 14).

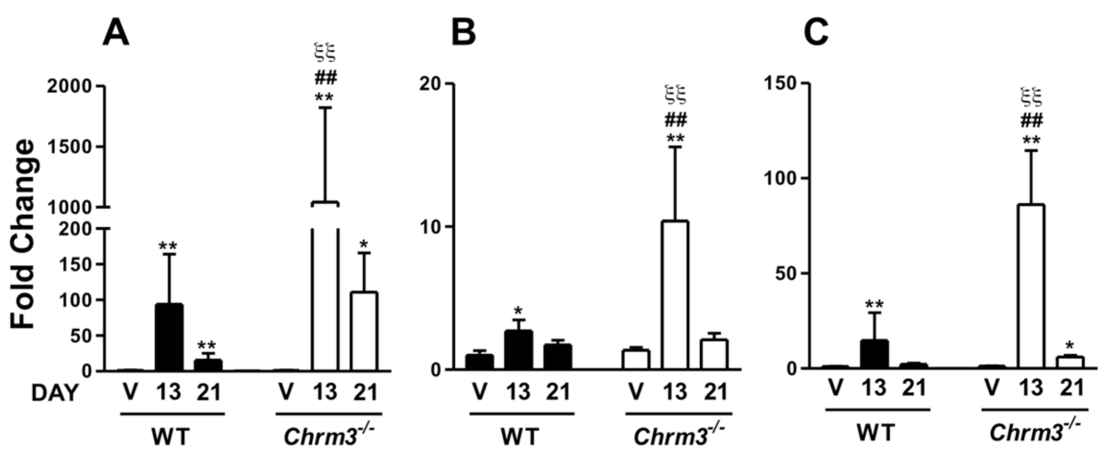

Figure 12: (A) Gene expression of IFN-γ in WT (black bars) and *Chrm3*$^{-/-}$ (white bars) uninfected and *C. rodentium*-infected colon. (B) Gene expression of TNF-α in WT (black bars) and *Chrm3*$^{-/-}$ (white bars) uninfected and *C. rodentium*-infected colon. (C) Gene expression of IL-17A in WT (black bars) and *Chrm3*$^{-/-}$ (white bars) uninfected and *C. rodentium*-infected colon.
WT: Wild type. *Chrm3*$^{-/-}$: M3R-deficient. V: vehicle. 13: 13 DPI. 21: 21 DPI. ** $p < 0.01$ vs. WT vehicle. * $p < 0.05$ vs. WT vehicle. ## $p < 0.01$ vs. WT 13 DPI. ξξ $p < 0.01$ vs. *Chrm3*$^{-/-}$ V.

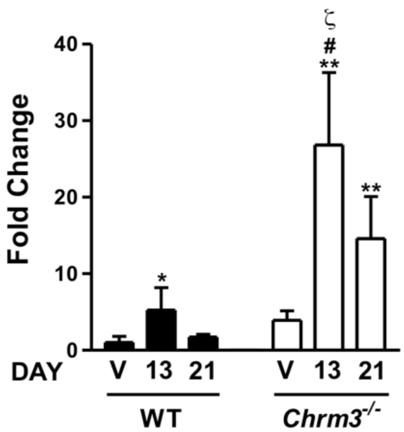

Figure 13: Gene expression of *Nos-2* in WT (black bars) and *Chrm3*$^{-/-}$ (white bars) uninfected and *C. rodentium*-infected colon. WT: Wild type. *Chrm3*$^{-/-}$: M3R-deficient. V: vehicle. 13: 13 DPI. 21: 21 DPI. ** $p < 0.01$ vs. WT vehicle. * $p < 0.05$ vs. WT vehicle. # $p < 0.05$ vs. WT 13 DPI. ξ $p < 0.05$ vs. *Chrm3*$^{-/-}$ vehicle.

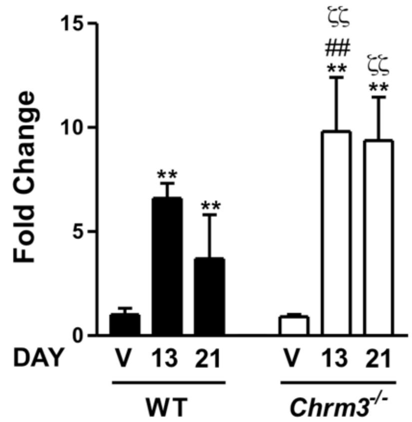

Figure 14: Gene expression of *CD3* in WT (black bars) and *Chrm3*$^{-/-}$ (white bars) uninfected and *C. rodentium*-infected colon. WT: Wild type. *Chrm3*$^{-/-}$: M3R-deficient. V: vehicle. 13: 13 DPI. 21: 21 DPI. ** $p < 0.01$ vs. WT vehicle. ## $p < 0.01$ vs. WT 13 DPI. ξξ $p < 0.01$ vs. *Chrm3*$^{-/-}$ vehicle.

Epithelial Proliferation is Enhanced in $Chrm3^{-/-}$ Colon

Mucosal proliferation serves multiple purposes and is considered part of host immune defense in the setting of infectious colitis [84]. As a result, we assessed the ability of colon mucosa from *$Chrm3^{-/-}$* mice to proliferate in response to *C. rodentium*. BrdU was injected prior to euthanasia to label proliferating cells. When compared to WT mucosa, *$Chrm3^{-/-}$* mucosa 13 DPI exhibits greater BrdU staining than WT mucosa 13 DPI (Figure 15) indicating that epithelial proliferation is enhanced in *$Chrm3^{-/-}$* colon. By 21 DPI, BrdU staining in WT and *$Chrm3^{-/-}$* mucosa was similar and approached basal levels (Figure 15). BrdU-positive cells per crypt were counted and significantly more BrdU-positive cells per crypt were present in WT mucosa 13 DPI compared to uninfected WT mucosa. Similarly, there were significantly more BrdU-positive cells per crypt in *$Chrm3^{-/-}$* mucosa 13 DPI compared to uninfected *$Chrm3^{-/-}$* mucosa as well as WT mucosa 13 DPI (Figures 15 & 16). These data demonstrate that epithelial cell proliferation in the colon of *C. rodentium*-infected *$Chrm3^{-/-}$* mice is amplified at 13 DPI.

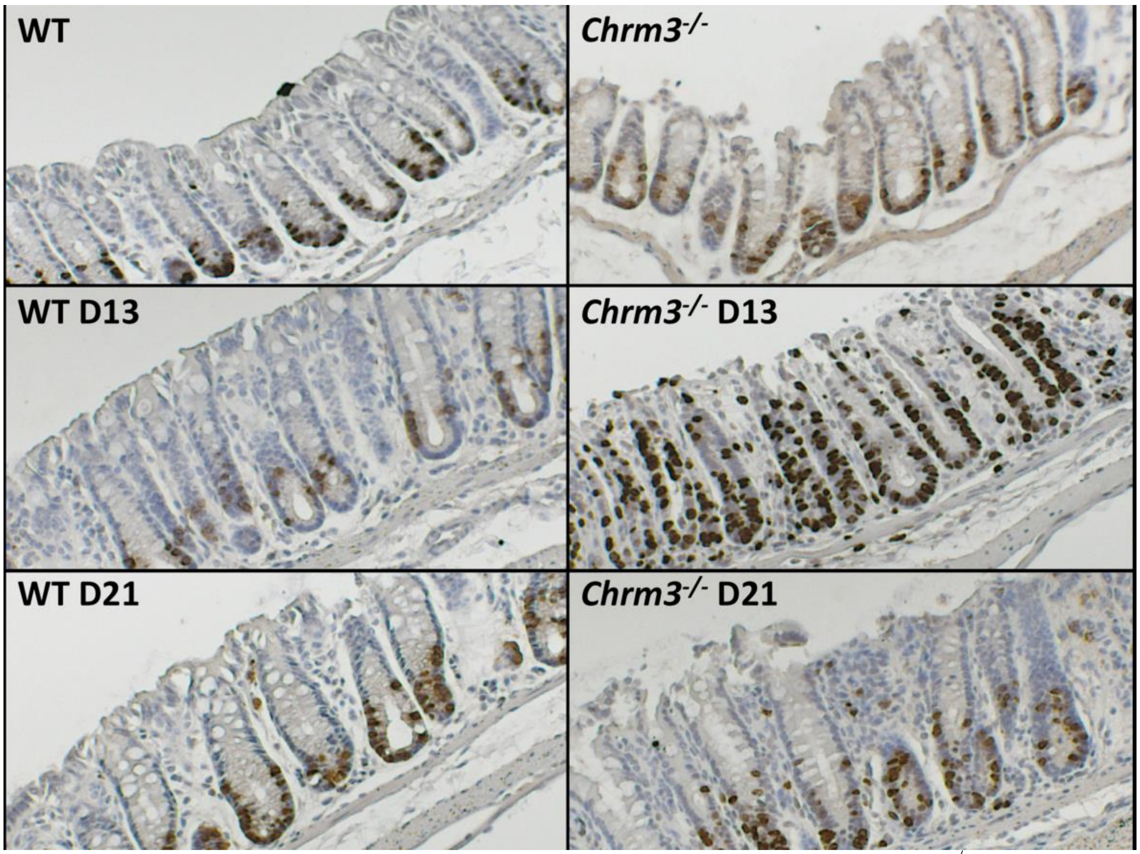

Figure 15: BrdU-labeled cells in uninfected and *C. rodentium*-infected WT and $Chrm3^{-/-}$ colon. Relative number of BrdU-positive cells is increased in $Chrm3^{-/-}$ colon 13 DPI.
WT: Wild type. $Chrm3^{-/-}$: M3R-deficient. BrdU: bromodeoxyuridine.

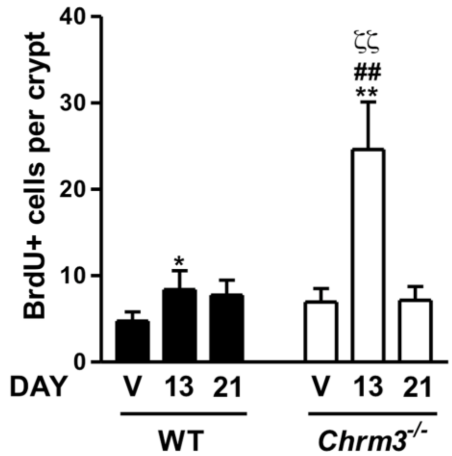

Figure 16: Mean ± SEM of BrdU-positive cells per crypt in uninfected and *C. rodentium*-infected WT (black bars) and *Chrm3*$^{-/-}$ (white bars) colon mucosa.
WT: Wild type. *Chrm3*$^{-/-}$: M3R-deficient. SEM: Standard error. V: vehicle. 13: 13 DPI. 21: 21 DPI. ** $p < 0.01$ vs. WT vehicle. * $p < 0.05$ vs. WT vehicle. ## $p < 0.01$ vs. WT 13 DPI. ξξ $p < 0.01$ vs. *Chrm3*$^{-/-}$ vehicle.

Mucus Production

The intestinal mucus layer, produced by epithelial goblet cells, contributes to host defense by inhibiting the ability of pathogens to adhere to intestinal and colonic mucosa [85]. The number of goblet cells per crypt decreased in response to *C. rodentium* infection in *Chrm3*$^{-/-}$ mucosa 13 DPI compared to uninfected *Chrm3*$^{-/-}$ mucosa, but did not differ between WT mucosa 13 DPI and uninfected WT mucosa (Figures 17A & 19). Gene expression of *CLCA3*, a calcium activated chloride channel that is a recognized marker of goblet cell hyperplasia [86], was significantly lower in *Chrm3*$^{-/-}$ colon 13 DPI compared to uninfected *Chrm3*$^{-/-}$ colon; however, gene expression of *CLCA3* in WT colon 13 DPI did not differ from uninfected WT colon (Figure 17B). Mucin-2, encoded by *Muc2*, is the primary mucin that forms the mucus layer in the small intestine and colon [87,88]. Expression of *Muc2* was decreased significantly in *Chrm3*$^{-/-}$ colon 13 DPI

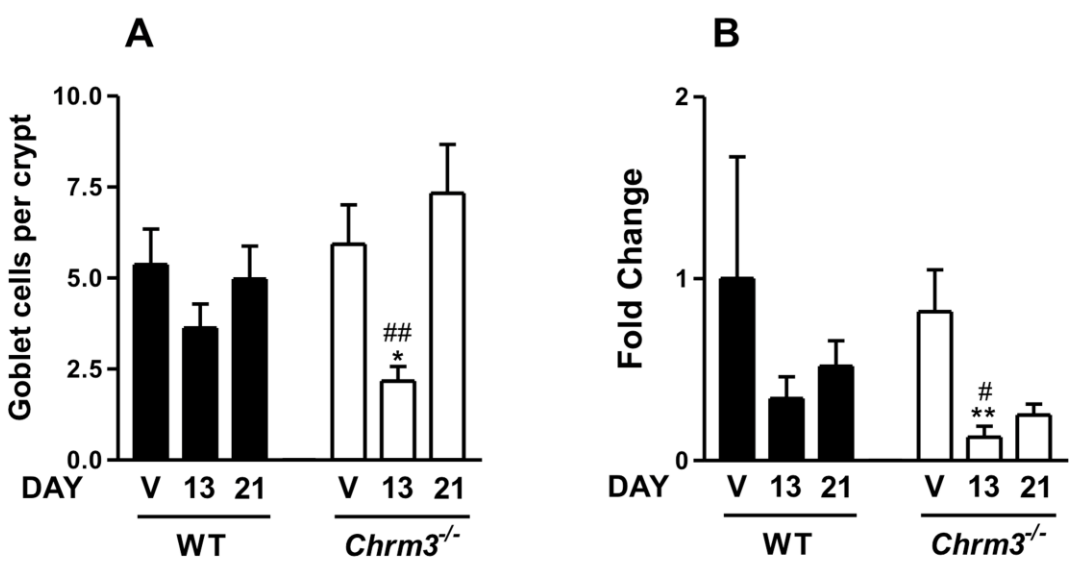

Figure 17: (A) Goblet cells per crypt in uninfected and *C. rodentium*-infected WT (black bars) and *Chrm3*$^{-/-}$ (white bars) mice. (B) Gene expression of CLCA3 in muscle-free WT (black bars) and *Chrm3*$^{-/-}$ (white bars) uninfected and *C. rodentium*-infected colon.
WT: Wild type. *Chrm3*$^{-/-}$: M3R-deficient. V: vehicle. 13: 13 DPI. 21: 21 DPI. ** $p < 0.01$ vs. WT vehicle. * $p < 0.05$ vs. WT vehicle. ## $p < 0.01$ vs. *Chrm3*$^{-/-}$ vehicle. ## $p < 0.05$ vs. *Chrm3*$^{-/-}$ vehicle.

compared to uninfected *Chrm3*$^{-/-}$ colon, but did not differ between WT colon 13 DPI and WT uninfected colon (Figure 18A). *Muc5AC* is upregulated during parasitic nematode infection [89]; however, no upregulation of *Muc5AC* occurred in either WT or *Chrm3*$^{-/-}$ *C. rodentium*-infected colon (Figure 18B). These data demonstrate differential expression of mucins in WT and *Chrm3*$^{-/-}$ colon in response to *C. rodentium* infection.

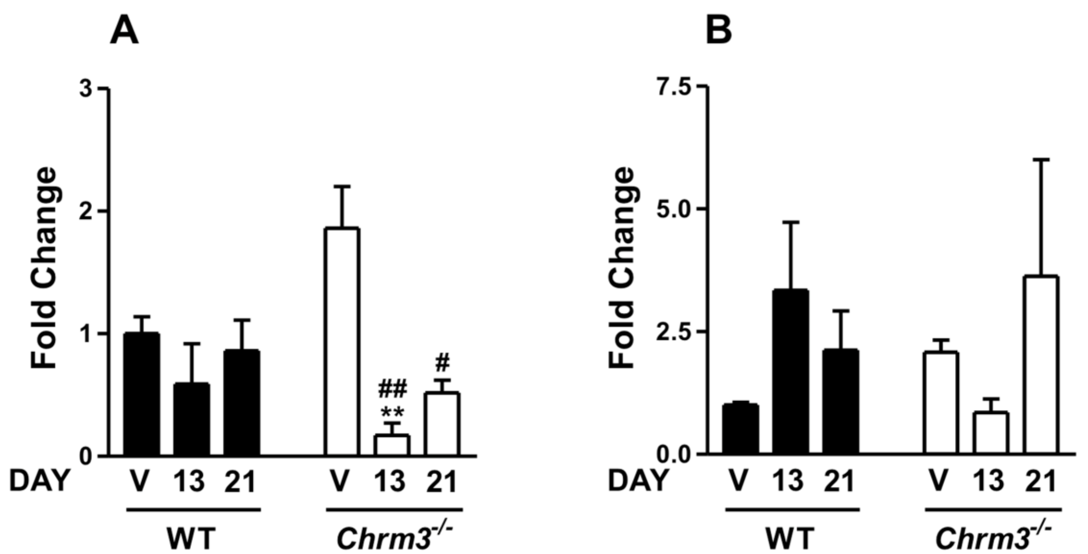

Figure 18: (A) Gene expression of *Muc2* in WT (black bars) and *Chrm3*$^{-/-}$ (white bars) uninfected and *C. rodentium*-infected colon. (B) Gene expression of *Muc5AC* in WT (black bars) and *Chrm3*$^{-/-}$ (white bars) uninfected and *C. rodentium*-infected colon.
WT: Wild type. *Chrm3*$^{-/-}$: M3R-deficient. V: vehicle. 13: 13 DPI. 21: 21 DPI. ** $p < 0.01$ vs. WT vehicle. # $p < 0.05$ vs. *Chrm3*$^{-/-}$ vehicle. ## $p < 0.01$ vs. *Chrm3*$^{-/-}$ vehicle.

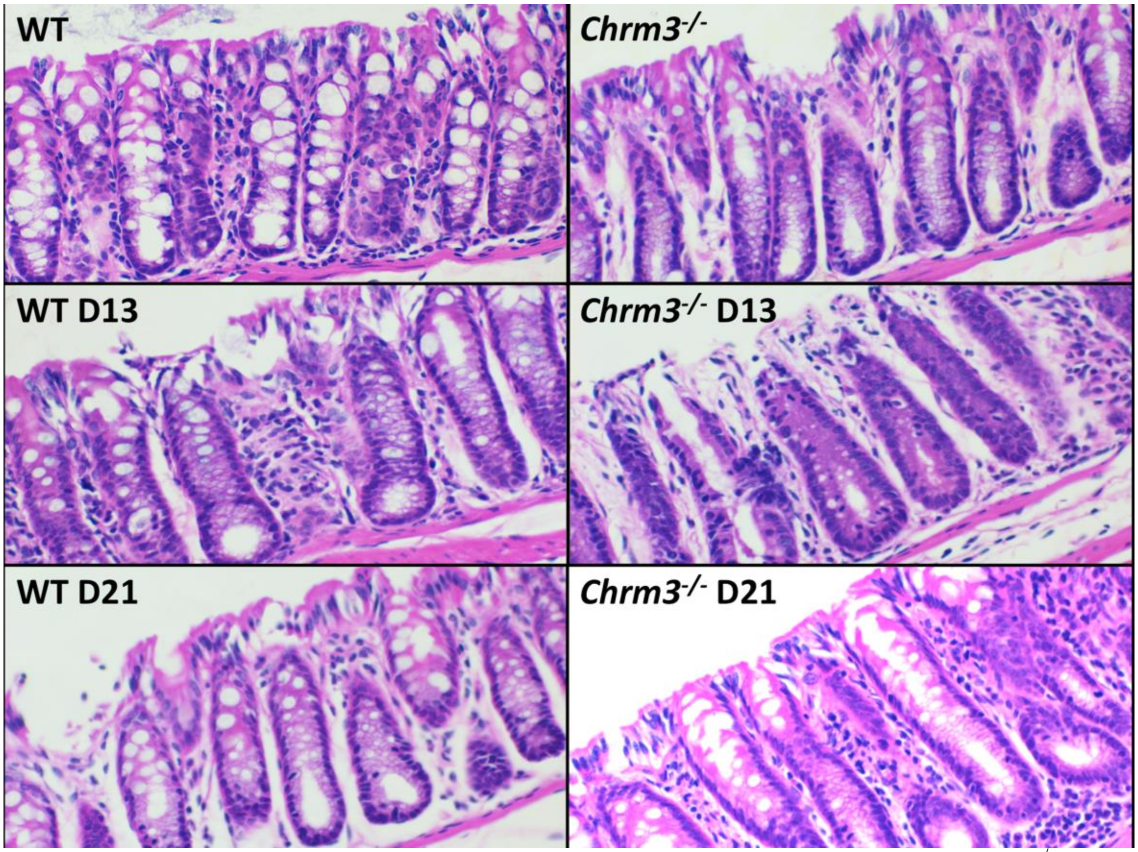

Figure 19: H&E stained sections of uninfected and *C. rodentium*-infected WT and *Chrm3*$^{-/-}$ colon. Relative number of goblet cells is decreased at 13 DPI in both WT and *Chrm3*$^{-/-}$ colon, but is more pronounced in *Chrm3*$^{-/-}$ colon 13 DPI.
WT: Wild type. *Chrm3*$^{-/-}$: M3R-deficient. H&E: hematoxylin and eosin.

Immunoglobulin Production

A functioning adaptive immune system including B cells and immunoglobulin production are required for clearance of *C. rodentium* [76]. Serum was collected from uninfected and *C. rodentium*-infected WT and *Chrm3*$^{-/-}$ mice to determine if alterations in immunoglobulin levels were associated with delayed clearance of *C. rodentium*. Serum levels of IgM were similar in uninfected and *C. rodentium*-infected WT and *Chrm3*$^{-/-}$ mice, indicating that *Chrm3*$^{-/-}$ mice have functional B cells that respond appropriately to *C. rodentium* infection (Figure 20).

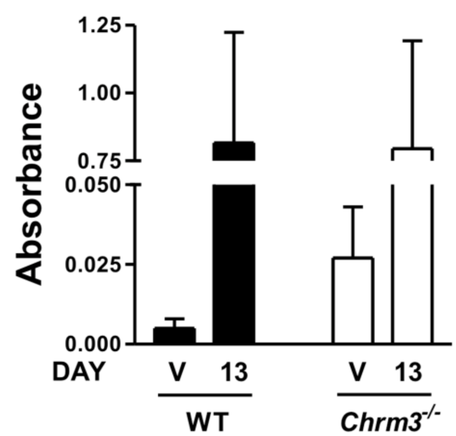

Figure 20: (A) Relative serum levels of IgM in WT (black bars) and *Chrm3*$^{-/-}$ (white bars) uninfected and *C. rodentium*-infected mice. WT: Wild type. *Chrm3*$^{-/-}$: M3R-deficient. V: vehicle. 13: 13 DPI.

WT Macrophages Express Cholinergic Receptors

Macrophages are a critical component of the innate immune system, contribute to tolerance to commensals, and participate in host defense. BMDM were generated to investigate the effects of M3R-deficiency on macrophage phenotype and function. Flow cytometry was used to confirm that bone marrow cells differentiated in the presence of M-CSF were macrophages by determining the proportion of cells expressing both CD11b and F4/80. Approximately 95% of cells expressed both CD11b and F4/80 (Figure 21), indicating that the cell population was highly enriched in macrophages. Using RT-PCR, we confirmed that BMDM express genes for M1R-M4R as well as α7 NR (Figure 22).

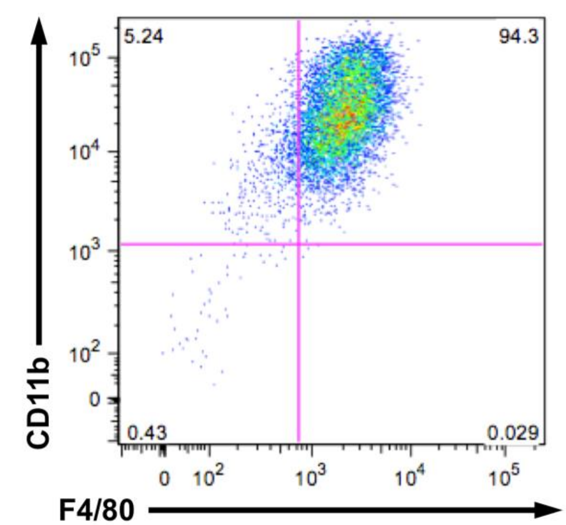

Figure 21: Bone marrow cells differentiated in M-CSF for 7 days that express CD11b and F4/80.

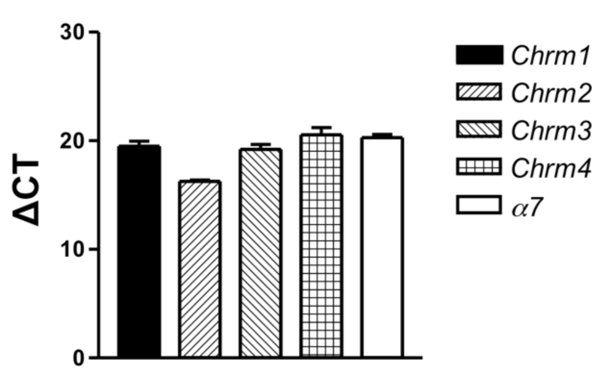

Figure 22: WT BMDM gene expression of *Chrm1*, *2*, *3*, *4* and *α7* nicotinic receptor. *Chrm5* was not detected.

Expression of M3R is Increased by Muscarinic Specific Stimulation of WT Macrophages as well as by IFN-γ Treatment of WT Macrophages

Treatment of WT BMDM with nanomolar range doses of bethanechol, a muscarinic-specific agonist, upregulates gene expression of M3R (Figure 23). Gene expression of M3R was also increased by treatment with the T_H1 cytokine IFN-γ (Figure 24A). Treatment with the T_H2 cytokine IL-4 did not affect M3R gene expression. IFN-γ treatment did not affect gene expression of other muscarinic receptors expressed by macrophages, nor did it affect gene expression of the α7 nicotinic receptor (Figure 24B). In addition, protein expression of M3R increased in BMDM treated with IFN-γ when compared to BMDM

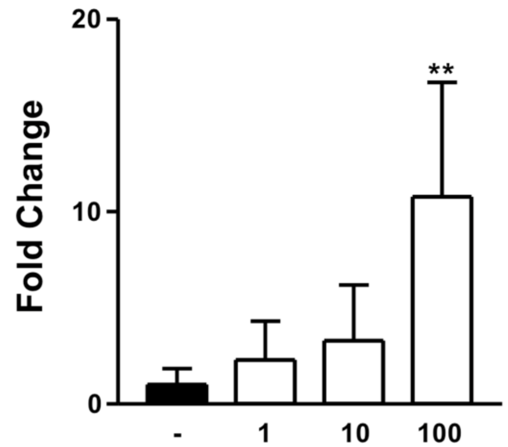

Figure 23: Gene expression of *Chrm3* in WT BMDM treated with vehicle (black bar) or bethanechol 1-100 nM (white bars).
** $p < 0.01$ vs. WT vehicle.

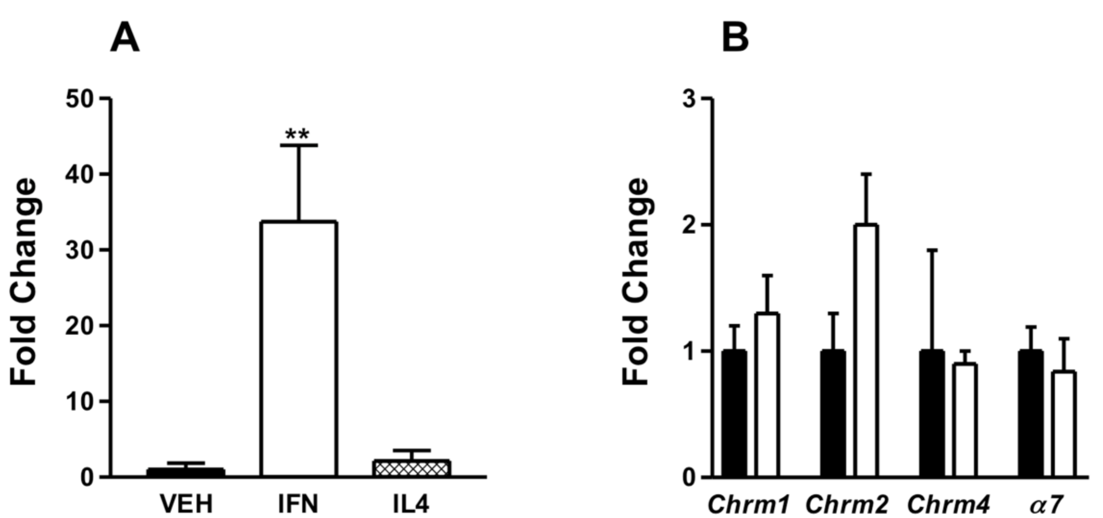

Figure 24: (A) Gene expression of *Chrm3* in vehicle, IFN-γ (10 ng/mL), and IL-4 (20 ng/mL) treated WT BMDM. (B) Gene expression of *Chrm1*, *Chrm2*, *Chrm4*, and *α7* in vehicle (black bars) and IFN-γ (10 ng/mL, white bars) treated WT BMDM. ** $p < 0.01$ vs. WT vehicle.

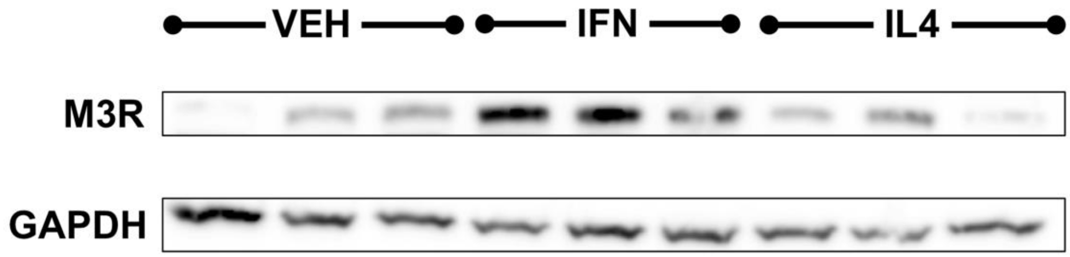

Figure 25: Immunoblot demonstrating expression of M3R in vehicle, IFN-γ (10 ng/mL), and IL-4 (20 ng/mL) treated BMDM. VEH: vehicle. IFN: interferon-γ. IL4: IL-4

treated with vehicle or IL-4 (Figure 25). These data demonstrate that M3R is upregulated not only in response to muscarinic specific stimulation of macrophages, but also by exposure to the T_H1 cytokine IFN-γ.

Muscarinic Specific Stimulation of Macrophages Induces Development of a Classically Activated Phenotype via M3R

Cholinergic tone exerts anti-inflammatory effects on macrophages [27,66,90]; however, the effect of muscarinic specific tone on macrophages has not been established. Expression of *Nos-2*, a marker for CAM, was increased significantly in WT BMDM

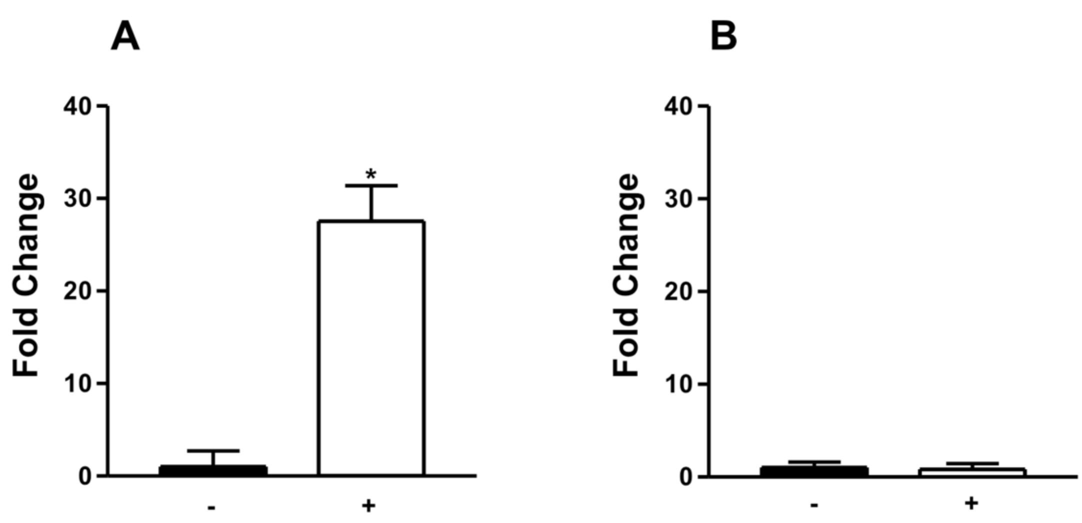

Figure 26: (A) Gene expression of *Nos-2* in WT BMDM treated with vehicle (black bars) or bethanechol 100 nM (white bars). (B) Gene expression of *Nos-2* in *Chrm3*$^{-/-}$ BMDM treated with vehicle (black bars) or bethanechol 100 nM (white bars).

treated with physiologic doses of bethanechol indicating that WT BMDM differentiate into CAM in the setting of muscarinic stimulation (Figure 26A). *Nos-2* expression was unchanged in *Chrm3*$^{-/-}$ BMDM treated with the same dose of bethanechol (Figure 26B). Furthermore, treatment of WT BMDM with atropine, a muscarinic-specific antagonist, is associated with decreased gene expression of *Nos-2* (Figure 27A). *Nos-2* gene expression did not change with atropine treatment of *Chrm3*$^{-/-}$ BMDM (Figure 27B) further demonstrating that muscarinic-specific stimulation induces development of CAM.

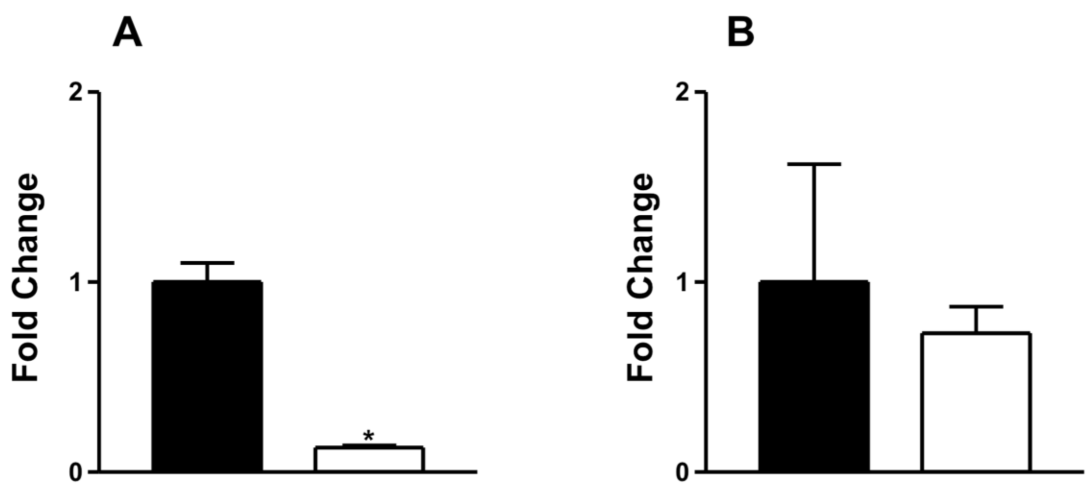

Figure 27: (A) Gene expression of *Nos-2* in WT BMDM treated with vehicle (black bars) or atropine 50 nM (white bars). (B) Gene expression of *Nos-2* in *Chrm3*$^{-/-}$ BMDM treated with vehicle (black bars) or atropine 50 nM (white bars).
WT: Wild type. *Chrm3*$^{-/-}$: M3R-deficient. * $p < 0.05$ vs. WT vehicle.

Chrm3$^{-/-}$ *Macrophages Retain Their Ability to Attain a Classically Activated Phenotype in the Presence of Interferon-*γ

Macrophages exposed to T_H1 cytokines such as IFN-γ attain a CAM phenotype [91]. As expected, gene expression of *Nos-2* increased significantly when WT BMDM were treated with IFN-γ (Figure 28A). Similarly, gene expression of *Nos-2* also increased significantly when *Chrm3*$^{-/-}$ BMDM were treated with IFN-γ (Figure 28B), indicating that

M3R is not required for BMDM to attain a CAM phenotype in the presence of IFN-γ. These data indicate that *Chrm3*$^{-/-}$ BMDM retain their ability to differentiate into CAM in the setting of a cytokine stimulus (IFN-γ), but their ability to differentiate into CAM due to a muscarinic stimulus is dependent on M3R.

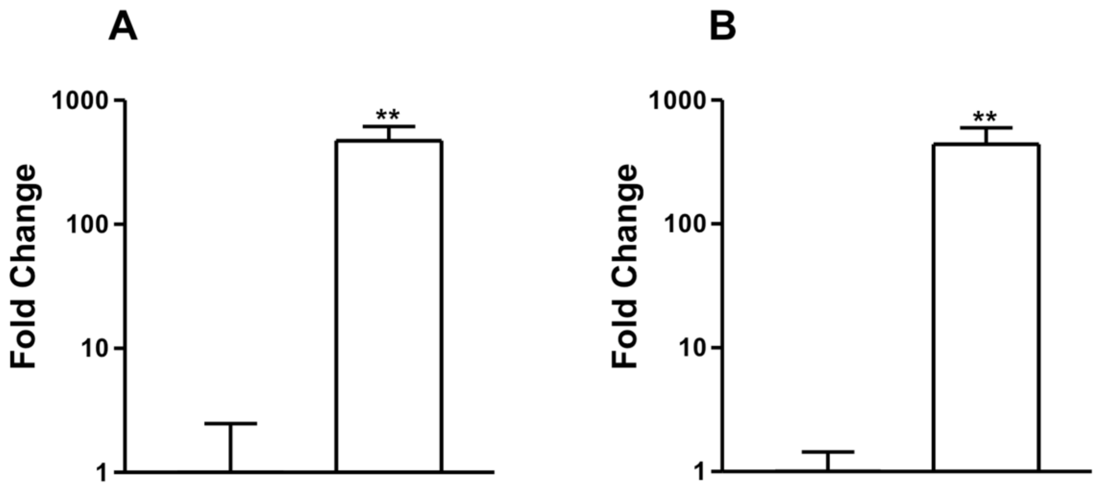

Figure 28: (A) Gene expression of *Nos-2* in WT BMDM treated with vehicle or IFN-γ (10 ng/mL, white bars). (B) Gene expression of *Nos-2* in *Chrm3*$^{-/-}$ BMDM treated with vehicle (black bars) or IFN-γ (10 ng/mL, white bars).
** $p < 0.01$ vs. WT vehicle.

Muscarinic Stimulation Acts Synergistically with Interferon-γ on Macrophages to Promote Development of a Classically Activated Macrophage Phenotype

Finally, we examined the ability of muscarinic stimulation to amplify the response of BMDM to IFN-γ. Gene expression of *Nos-2* in WT BMDM treated with bethanechol and IFN-γ increased when compared to treatment with IFN-γ alone (Figure 29A). This effect was not observed in *Chrm3*$^{-/-}$ BMDM (Figure 28B). Treating BMDM with atropine in addition to IFN-γ and bethanechol abrogated bethanechol-induced upregulation of *Nos-2* in WT BMDM (Figure 28A). Treatment of *Chrm3*$^{-/-}$ BMDM with atropine in addition to IFN-γ and bethanechol did not affect *Nos-2* gene expression (Figure 29B).

These data indicate that muscarinic specific stimulation potentiates development of a CAM phenotype in IFN-γ treated WT BMDM and that this effect is dependent on M3R expression.

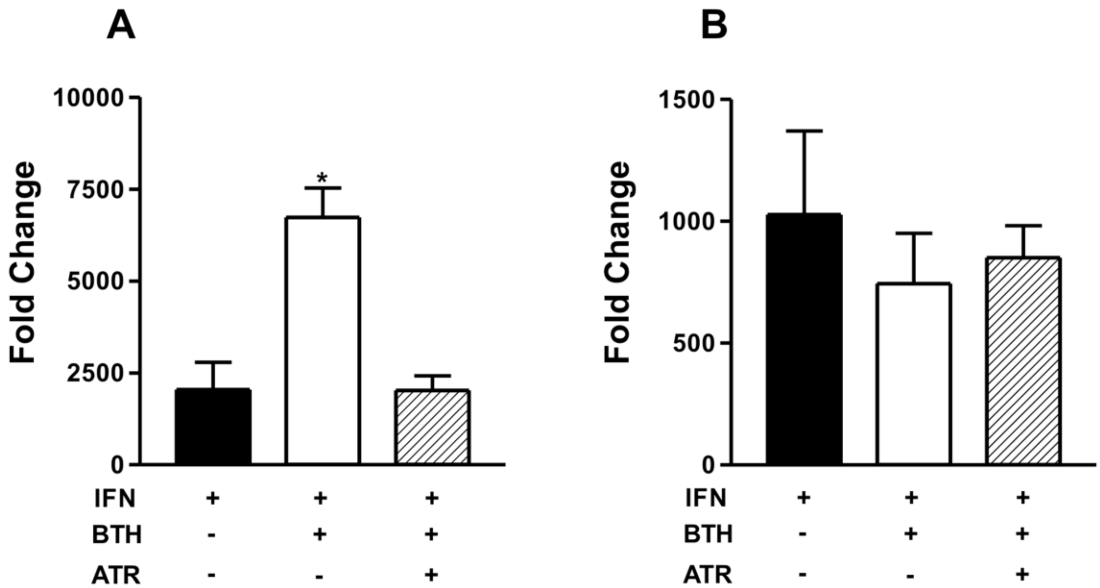

Figure 29: (A) Gene expression of *Nos-2* in WT BMDM treated with IFN-γ 10 ng/mL (black bars), IFN-γ 10 ng/mL and bethanechol 100 nM (white bars), and IFN-γ 10 ng/mL, bethanechol 10 nM, and atropine 50 nM (hatched bars). (B) Gene expression of *Nos-2* in *Chrm3*$^{-/-}$ BMDM treated with IFN-γ 10 ng/mL (black bars), IFN-γ 10 ng/mL and bethanechol 100 nM (white bars), and IFN-γ 10 ng/mL, bethanechol 10 nM, and atropine 50 nM (hatched bars).
WT: Wild type. *Chrm3*$^{-/-}$: M3R-deficient. IFN: interferon-γ. BTH: bethanechol. ATR: atropine.
* $p < 0.05$ vs. IFN-γ.

Discussion

Our study demonstrates a previously undescribed role for M3R in host defense against infectious colitis through modulation of mucus production. The importance of the colonic mucus layer in host defense against *C. rodentium* is established and our results complement prior findings demonstrating that *Muc2*$^{-/-}$ mice suffer from increased mortality when infected with *C. rodentium* [53]. In addition, our data suggests a pro-inflammatory role for M3R on macrophage phenotype, which represents an alternate mechanism for modulating macrophage function via cholinergic signaling in addition to the previously described anti-inflammatory role of α7.

In this study we demonstrate that clearance of *C. rodentium* from *Chrm3*$^{-/-}$ mice is delayed despite an amplified T_H1/T_H17 cytokine response. The delay in bacterial clearance observed in *Chrm3*$^{-/-}$ mice suggested by stool bacterial counts was confirmed by demonstrating persistent adherence of *C. rodentium* to colonic mucosa as well as crypt hyperproliferation 13 DPI in *Chrm3*$^{-/-}$ colon when compared to WT colon. Coincident with these changes is a 91% decrease in *Muc2* expression from baseline in *C. rodentium*-infected *Chrm3*$^{-/-}$ colon, but only a 41% decrease in *Muc2* expression in *C. rodentium*-infected WT colon. The critical role of Muc2 in controlling pathogen burden within the colon is established [53,78]. Goblet cells, which secrete mucin, respond to various stimuli and release mucin according to two different processes – simple and compound exocytosis [92]. Simple exocytosis occurs in a constitutive, basal fashion whereas compound exocytosis is the result of exposure to various secretagogues, including neurotransmitters (such as acetylcholine), hormones, neuropeptides, and cytokines. In addition, the thickness of the intestinal mucus layer is directly proportional to goblet cell number and size [93], indicating that *Chrm3*$^{-/-}$ mice are likely to have a thinner mucus layer than WT controls. Unfortunately, direct measurements of this layer are technically challenging as traditional fixation methods result in mucus detachment [92].

The ability of cholinergic tone to trigger mucin release from goblet cells has been demonstrated previously [94]. Considering the importance of mucus in host defense against enteric pathogens, our data strongly suggest a role for muscarinic signaling, specifically via M3R, in the release of mucin from goblet cells. The fact that *Chrm3*$^{-/-}$ mice do not succumb to *C. rodentium*-infection indicates that M3R is not required for clearance of *C. rodentium*, but that it does facilitate its clearance. These studies link delayed clearance of *C. rodentium* from *Chrm3*$^{-/-}$ mice to impaired mucin production, likely a consequence of disrupted cholinergic signaling at goblet cells due to genetic ablation of M3R, establishing a role for M3R in innate host defense.

In addition to the contribution of M3R to innate immunity via its actions on goblet cells, our studies demonstrate that M3R modulates macrophage phenotype and function. Discussion of the effects of cholinergic tone on macrophage signaling has focused predominantly on its anti-inflammatory effects via activation of α7 [9,10,25,27,95-97], thereby decreasing inflammation associated with a variety of conditions including pancreatitis, post-operative ileus, sepsis, and experimental colitis. In contrast, there is little information on the ability of MR to alter inflammation, although some studies have suggested that muscarinic specific stimulation of alveolar macrophages may have pro-inflammatory effects [98]. In isolated BMDM, we demonstrate that physiologic levels of muscarinic stimulation are capable of inducing a CAM phenotype, an effect that is dependent on the presence of M3R. Interestingly, stimulation with IFN-γ increases M3R gene expression, suggesting a role for M3R in immune regulation of macrophage function. When macrophages were exposed to both inflammatory and muscarinic stimuli, a more robust upregulation of *Nos-2* was observed, indicating greater skewing towards CAM than what was observed with IFN-γ treatment alone. It is well established that cholinergic tone exerts a net anti-inflammatory effect on macrophages (Figure 30A). Our *in vitro* data, however, indicate that IFN-γ upregulates expression of M3R on macrophages. This likely increases the proportion of cholinergic tone received by M3R, which may act to counter-balance the anti-inflammatory effects of α7 (Figure 30B), preventing or limiting the development of AAM. These dichotomous actions of cholinergic signaling may have important consequences for maintaining the host's ability to respond appropriately to pathogens as *in vitro* α7 specific stimulation ameliorates release of inflammatory mediators [99], but *in vivo* is associated with worsening of experimental colitis [8].

Taken together, our studies indicate a previously undescribed role for M3R in modulation of and response to inflammation. Further work remains with respect to characterizing the *in vivo* effects of M3R ablation on response to colitis. Depleting macrophages from WT mice and reconstituting them with *Chrm3*$^{-/-}$ macrophages will help us better understand the role of M3R on response to experimental models of colitis and could potentially identify avenues for further research in an area that remains relatively unexplored.

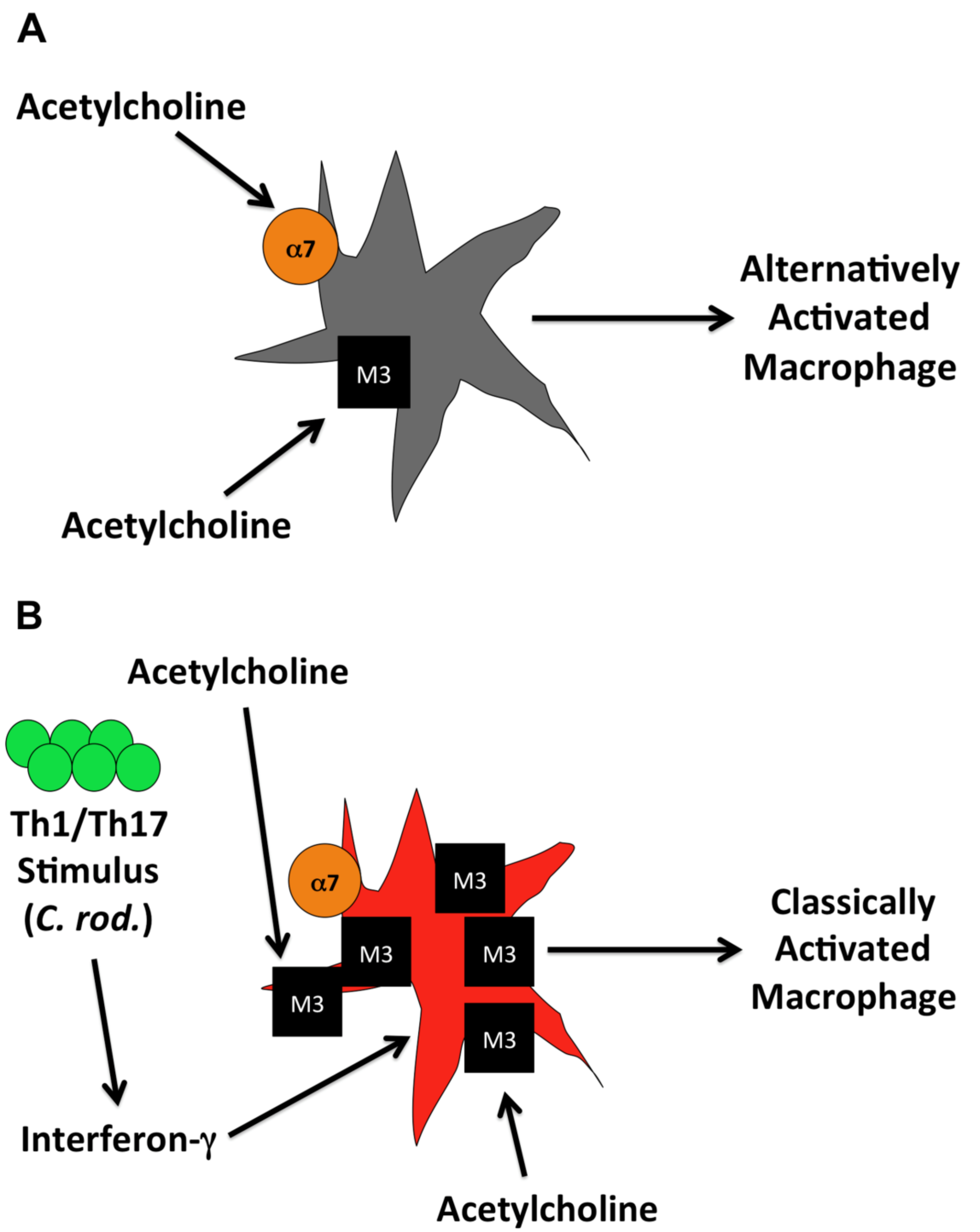

<u>Figure 30</u>: Proposed model of effects of M3R on macrophage phenotype. (A) In the absence of an inflammatory stimulus, acetylcholine acts at both α7 and M3R with net effect driving the macrophage towards an alternatively activated phenotype. (B) In the presence of T_H1/T_H17 cytokines, M3R expression on macrophages is increased and acetylcholine acts at relatively greater number of M3R, causing the macrophage to attain a more classically activated phenotype (or a less alternatively activated phenotype).
α7: alpha 7 nicotinic receptor. M3: type 3 muscarinic receptor. C. rod: *C. rodentium*

Chapter 3: Type 3 Muscarinic Receptors Contribute to Mucosal Homeostasis, Clearance of *Nippostrongylus brasiliensis*, and Expression of Th2 Cytokines

Introduction

In recent years there have been extensive studies exploring the role of vagal tone and cholinergic signaling in the modulation of systemic [10,25,95,100] and local [9,27,66] inflammation. The α7 NR has been identified as the primary receptor responsible for transducing these anti-inflammatory signals from the vagus through local nerves [10]. Trials are underway currently to determine if manipulation of vagal tone, either by physiologic means (e.g. exercise) [6,96] or the use of implanted nerve stimulators [11,101,102] attenuates local and/or systemic inflammatory conditions. Unfortunately, attempts to develop pharmacologic means of targeting α7 have not been successful [8], generating uncertainty about whether manipulation of this receptor will be successful in clinical applications.

Interactions between enteric nematodes and their mammalian hosts have co-evolved to benefit both organisms. Nematodes cause disease in infected hosts, but a significant proportion of those infected tolerate colonization without any significant ill-effects [103,104]. Evidence suggests that nematode infection protects against autoimmune diseases including type 1 diabetes [105], rheumatoid arthritis [106], multiple sclerosis [107], and CD [108]. The mammalian host responds to the presence of enteric nematodes by generating a T_H2 response, characterized by the production of cytokines such as IL-4, IL-5, IL-10, and IL-13 [109,110]. Along with increased production of T_H2 cytokines, several characteristic T_H2-dependent physiologic changes that facilitate nematode expulsion occur including smooth muscle hypercontractility, increased epithelial permeability, decreased epithelial secretion, decreased glucose absorption, and goblet cell expansion [82,103,111-113].

The current study was designed to investigate the role of M3R on mucosal homeostasis in the small intestine as well as its contribution to host defense against the T_H2-inducing pathogen *N. brasiliensis*. The results of our studies demonstrate that M3R contributes to mucosal homeostasis in the absence of enteric nematode infection as well as to T_H2 cytokine mediated expulsion of *N. brasiliensis*. The inability of *Chrm3*$^{-/-}$ mice to mount an appropriate cytokine response to *N. brasiliensis* implicates this receptor as a significant contributor to the T_H2 response in enteric nematode infection. Furthermore, IL4 treatment of *Chrm3*$^{-/-}$ macrophages results in exaggerated development of AAM, suggesting that M3R may exert counter regulatory effects on macrophages to prevent extreme alternative activation of macrophages, potentially contributing to the maintenance of an appropriate balance between CAM and AAM. We conclude that M3R activity not only contributes to barrier function and mucosal homeostasis in small intestine, but also facilitates generation of a T_H2 cytokine response to enteric nematode infection.

Methods

Animal Studies

Age and sex-matched WT and *Chrm3*$^{-/-}$ on a C57BL/6 background as well as WT and *Chrm3*$^{-/-}$ mice on a 129/SvEv x CF1 (50%:50%) background were purchased from Taconic Farms (Germantown, NY) or generously donated by Dr. Jürgen Wess of the National Institutes of Health (Bethesda, MD). Mice were housed at the United States Department of Agriculture animal facility and provided food and water *ad libitum*. Animals were euthanized using ketamine/xylazine prior to performing physiologic studies and collection and processing of tissues. Tissue samples were collected for molecular analysis, histological evaluation, and assessment of continuing nematode infection. All studies were conducted in accordance with the principles set forth in the Guide for Care and Use of Laboratory Animals, Institute of Laboratory Animal Resources, National Research Council, Health and Human Services Publication (National Institutes of Health 85-23, revised 1996), and the Beltsville Area Animal Care and Use Committee (Protocol #10-003). The protocol was also approved by the Institutional Animal Care and Use Committee of the University of Maryland School of Medicine (Protocol #0110018).

Nippostrongylus Infection and Worm Expulsion

Infective, third stage *N. brasiliensis* (specimens on file at the U.S. National Parasite Collection, U.S. National Helminthological Collection, Collection 81930; Beltsville, MD) larvae (L_3) were propagated and stored at room temperature in fecal/charcoal/peat moss culture plates as previously described [112]. Age and sex-matched groups of WT and *Chrm3*$^{-/-}$ mice were inoculated subcutaneously with 500 L_3 and studied five to nine days later. Stool was collected from WT and *Chrm3*$^{-/-}$ mice throughout the course of *N. brasiliensis* infection to determine fecal egg content. After euthanasia, proximal small intestine (duodenum) from WT and *Chrm3*$^{-/-}$ mice was collected and nematodes residing within were counted directly.

In vitro Smooth Muscle and Epithelial Cell Function

Smooth muscle contractility was measured as described previously [112]. Response to acetylcholine (10 nM to 0.1 mM) and the amplitude of spontaneous contractions were determined. Tension was expressed as force per cross-sectional area [114]. Responses from all tissue segments exposed to acetylcholine from an individual animal were averaged resulting in a mean response per animal and then averaged to yield a mean value per group.

Ussing Chambers

One cm segments of jejunal mucosa were stripped of muscularis externa and mounted in Ussing chambers with 0.126 cm^2 of the epithelium exposed to 10 mL of Krebs' buffer. The potential difference across the tissue was measured using agar-salt bridges and electrodes. Every 50 s, the tissue was short circuited at 1 volt (V) (World Precision Instruments DVC 1000 voltage clamp; Sarasota, FL) for 2 s to allow calculation of tissue resistance utilizing Ohm's law (V = IR). In addition, the short circuit current (I_{sc}) was monitored continuously. Basal I_{sc}, representing the net ion flux at baseline, and tissue resistance, an indication of tissue permeability, were determined after a 15 min period of equilibration. Following a second 15 min period of equilibration, concentration-dependent changes in I_{sc} were measured in response to the cumulative addition of glucose or bethanechol to the mucosal side. For all tissue segments taken from an individual mouse (n = 3–4 per mouse), resistance, basal I_{sc}, and changes in I_{sc} in response to glucose or bethanechol were averaged to yield a mean response per animal and then averaged to yield a mean value per group.

Microsnapwell Assay for Mucosal Transepithelial Electrical Resistance

The modified microsnapwell system is a miniaturized version of the standard Ussing chamber designed to measure mucosal transepithelial electrical resistance (TEER) [79]. Decreases in TEER indicate increased tissue permeability. Segments of small intestine were harvested from uninfected or *N. brasiliensis*–infected WT and *Chrm3*$^{-/-}$ mice, stripped of both muscularis externa and serosal layers, and mounted in the microsnapwell system. A total of 250 μL DMEM containing 4.5 g/L glucose, 4 mM L-glutamine, and 1 mM nonessential amino acids was added to the mucosal side. Three milliliters of the same medium was added to the serosal side. The system was incubated at 37°C with 5% CO_2 for 30 min to permit stabilization of pH and TEER was measured every 30 min for 180 min.

Preparation and Treatment of Bone Marrow–Derived Macrophages

Macrophages were prepared from bone marrow mononuclear cells as previously described [80]. Mononuclear cells were obtained by flushing bone marrow from femurs, tibias, and humeri with HyClone alpha MEM medium (Thermo-Scientific; Chicago, IL) pre-equilibrated at 37°C. Cells were cultured overnight in alpha MEM medium containing 10% FBS and 1% penicillin/streptomycin in a humidified incubator at 37°C with 5% CO_2. Non-adherent cells were collected by centrifugation after lysis of red blood cells using red blood cell lysis buffer (Sigma-Aldrich; St. Louis, MO) and mononuclear cells were counted and plated. Mature macrophages were generated by differentiating isolated mononuclear cells with 20 ng/mL rM-CSF (R&D Systems; Minneapolis, MN) for 7 d. WT or *Chrm3*$^{-/-}$ macrophages were then treated with IFN-γ, IL-4, or bethanechol for 24 h to determine their ability to attain a classically or alternatively activated phenotype.

RNA Extraction, cDNA synthesis and quantitative real-time polymerase chain reaction (qRT-PCR)

Total RNA was extracted from tissue samples or bone-marrow derived macrophages (BMDM) with TRIzol reagent (Invitrogen; Carlsbad, CA) according to manufacturer's instructions. RNA integrity, quantity, and genomic DNA contamination were assessed using the Agilent Bioanalyzer 2100 and RNA 6000 Labchip kit (Agilent Technologies; Palo Alto, CA). Only those RNA samples with 28S/18S ratios between 1.5 and 2 and no DNA contamination were studied further. RNA samples (2 µg) were reverse-transcribed to cDNA using the First Strand cDNA Synthesis Kit (MBI Fermentas; Hanover, MD) with random hexamer primer.

Amplification reactions were performed on an iCycler detection system (Bio-Rad Laboratories; Hercules, CA). Primer sequences were designed using Beacon Designer 5.0 (Premier Biosoft International; Palo Alto, CA), and synthesized by the Biopolymer Laboratory of the University of Maryland. PCR was performed in 25 µL volume wells using SYBR Green Supermix (Bio-Rad Laboratories; Hercules, CA). Amplification conditions were: 95°C for 3 min, 60 cycles of 95°C for 15 s, 60°C for 15 s, and 72°C for 20 s. The fold-change in mRNA expression for targeted genes was calculated relative to respective vehicle-treated groups of mice after normalization to 18s rRNA. 18s rRNA was selected as the internal standard based on preliminary studies demonstrating no significant differences in 18s rRNA level among different groups of samples studied.

Histology

Colons were opened longitudinally along the mesenteric border, fixed for 2 h in 4% paraformaldehyde, and embedded in paraffin blocks. Tissue was processed, cut in 5 μm sections, affixed to glass slides, and stained with H&E by Histoserv, Inc. (Germantown, MD). Images were acquired with an Axio Imager M2 microscope (Carl Zeiss Microscopy; Thornwood, NY) using ZEN Pro 2012 image acquisition software (Carl Zeiss Microscopy; Thornwood, NY).

Solutions and Drugs

All drugs used for physiological studies were obtained from Sigma-Aldrich (St. Louis, MO) unless otherwise indicated.

Data Analysis

For multiple comparisons, statistical analyses were performed using a one-way analysis of variance (ANOVA) with post hoc analysis for multiple comparisons. For two comparisons, statistical analyses were performed using a Student's *t*-test. Data analyses were performed using Graph Pad Prism software version 3.03. Differences between groups were considered statistically significant at p-values ≤ 0.05.

Results

Permeability and Proinflammatory Cytokine Expression are Increased in Chrm3$^{-/-}$ Intestine

We measured TEER of muscle-free small intestine from WT and *Chrm3*$^{-/-}$ mice in order to determine if differences in constitutive permeability exist in the absence of M3R. TEER was significantly decreased in *Chrm3*$^{-/-}$ small intestine obtained from 129S6/SvEv:CF1 (50%:50%) mice when compared to WT small intestine (Figure 31A). TEER was also significantly decreased in *Chrm3*$^{-/-}$ small intestine from C57BL/6 mice when compared to WT small intestine (Figure 31B), demonstrating that decreased TEER in *Chrm3*$^{-/-}$ mice was due to genetic ablation of M3R and not a unique property associated with either the 129S6/SvEv:CF1 (50%:50%) or C57BL/6 background. Flux of FITC-dextran across small intestine mucosa was also measured to verify the permeability defect suggested by TEER measurements. Dextran flux was significantly greater across

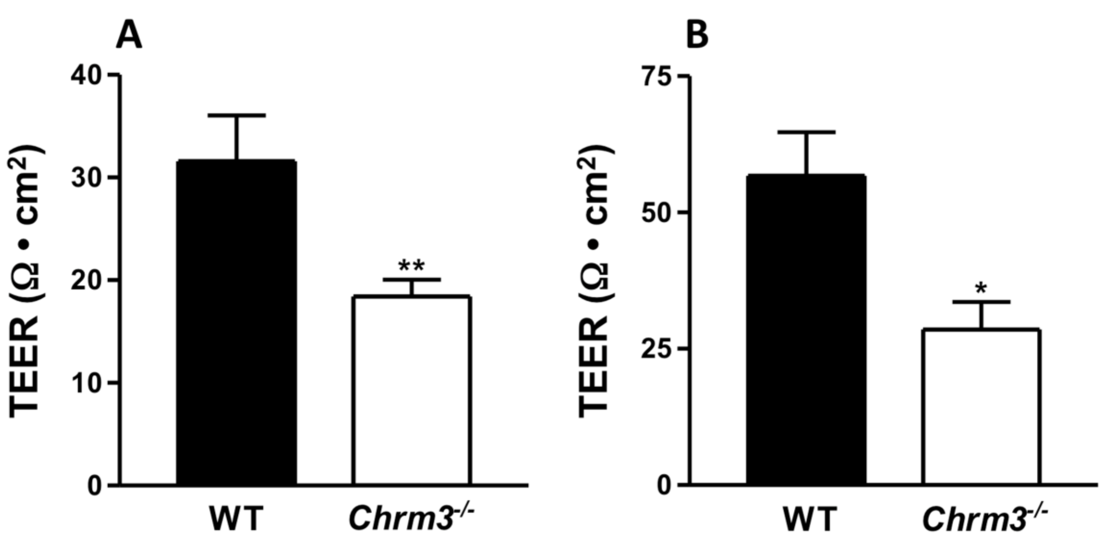

Figure 31: (A) TEER of muscle-free small intestine from WT and *Chrm3*$^{-/-}$ 129S6/SvEv:CF1 (50%:50%) mice. (B) TEER of muscle-free small intestine from WT and *Chrm3*$^{-/-}$ C57BL/6 mice. TEER: Transepithelial electrical resistance. ** $p < 0.01$ vs. WT. * $p < 0.05$ vs. WT.

Chrm3$^{-/-}$ small intestine than WT small intestine (Figure 32). Together, these data indicate that M3R contributes to barrier function and promotes stability of the paracellular pathway within the small intestine.

Expression of T_H1/T_H17 and T_H2 cytokines was measured to determine if changes in permeability were associated with alterations in basal cytokine profiles. In muscle-free small intestine from 129S6/SvEv:CF1 (50%:50%) mice, genetic ablation of M3R was associated with upregulation of *IFN-γ* and *TNF-α* (Figure 33A). Similarly, expression of *IFN-γ* and *TNF-α* was increased in muscle-free small intestine from *Chrm3*$^{-/-}$ C57/BL6 mice (Figure 33B). *IL-17A* expression was also increased in muscle-free small intestine from *Chrm3*$^{-/-}$ C57/BL6 mice. (Figure 33B). In addition, expression of the T_H2 cytokines *IL-4* and *IL-13* was measured (Figure 33C). *IL-13* was significantly down-regulated in 129S6/SvEv:CF1 (50%:50%) *Chrm3*$^{-/-}$ small intestine (Figure 33C), but this was not observed in *Chrm3*$^{-/-}$ C57/BL6 mice (data not shown). *IL-4* was unaltered in either WT background strain. Together, these data indicate that genetic ablation of M3R is associated with upregulation of pro-inflammatory T_H1/T_H17 cytokines in uninfected small intestine.

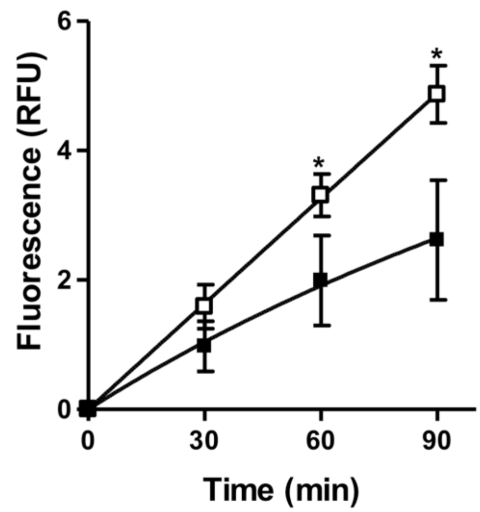

Figure 32: Flux of 4 kDa FITC-dextran across WT (closed squares) and *Chrm3*$^{-/-}$ (open squares) muscle-free smooth intestine at various time points.
kDa: kilo Dalton * $p < 0.05$ vs. WT.

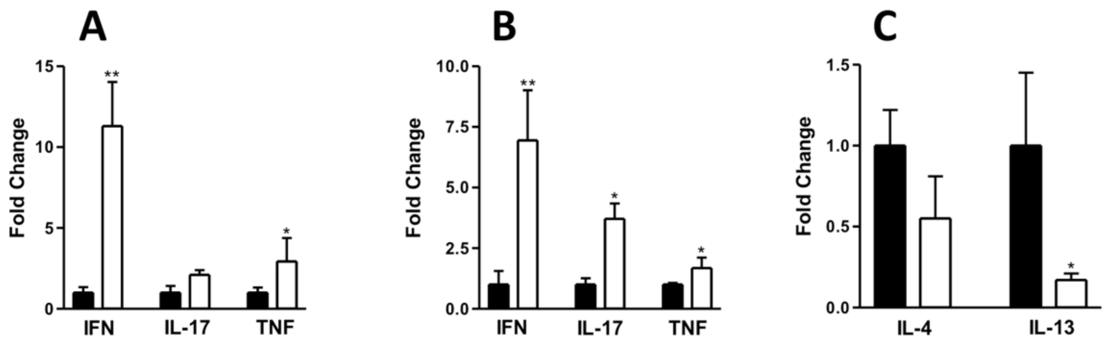

Figure 33: Gene expression of (A) *IFN-γ* (IFN), *IL-17A* (IL-17) and *TNF-α* (TNF) in WT (black bars) and *Chrm3*$^{-/-}$ (white bars) 129S6/SvEv:CF1 (50%:50%) mice, (B) *IFN-γ* (IFN), *IL-17A* (IL-17) and *TNF-α* (TNF) in WT (black bars) and *Chrm3*$^{-/-}$ (white bars) C57BL/6 mice, and (C) *IL-4* (IL-4) and *IL-13* (IL-13) in WT (black bars) and *Chrm3*$^{-/-}$ (white bars) 129S6/SvEv:CF1 (50%:50%) mice.
WT: Wild type. *Chrm3*$^{-/-}$: M3R-deficient. * $p < 0.05$ vs. WT. ** $p < 0.01$ vs. WT.

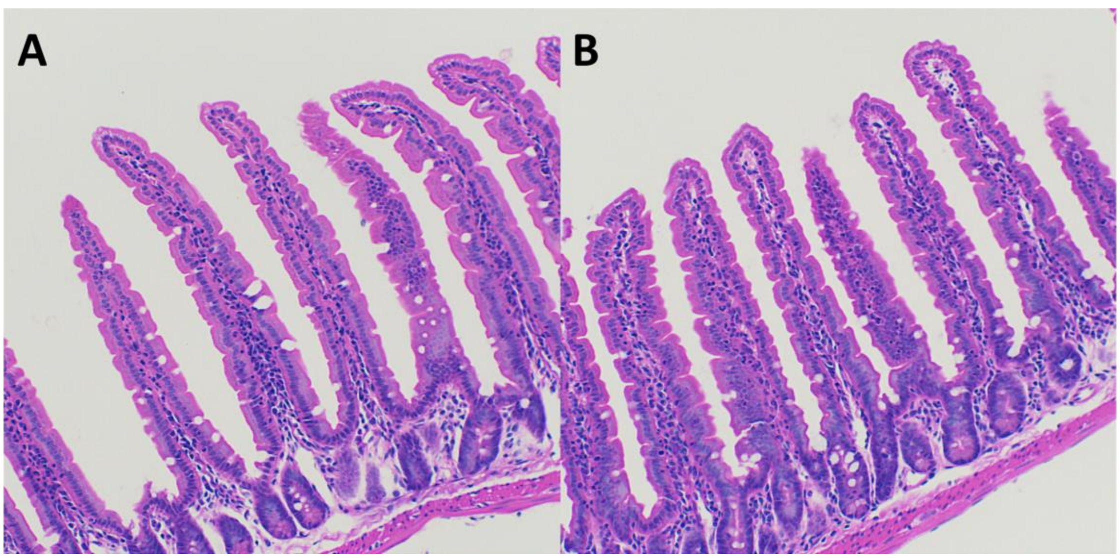

Figure 34: Representative sections of H&E stained small intestine from (A) WT C57BL/6 mice and (B) *Chrm3*$^{-/-}$ C57BL/6 mice.
H&E: hematoxylin and eosin.

Given the alterations in TEER and upregulation of T_H1/T_H17 cytokines observed in *Chrm3*$^{-/-}$ mice, we next evaluated H&E stained sections of small intestine from WT and *Chrm3*$^{-/-}$ mice. No significant differences in intestinal architecture exist between WT and *Chrm3*$^{-/-}$ small intestine (Figure 34).

Clearance of N. brasiliensis from Chrm3$^{-/-}$ Mice is Impaired

WT and *Chrm3*$^{-/-}$ mice were infected with *N. brasiliensis* and studied 5-9 DPI. Fecal egg content was determined 9 DPI. Feces from *Chrm3*$^{-/-}$ mice had a significantly higher egg burden than feces from WT mice (Figure 35A). To confirm that the higher egg count observed in *Chrm3*$^{-/-}$ mice was due to a higher intestinal worm burden, nematodes residing within the proximal small bowel (duodenum) of WT and *Chrm3*$^{-/-}$ mice were counted (Figure 35B). The number of nematodes within the proximal small intestine was significantly greater in *Chrm3*$^{-/-}$ mice than in WT mice. These data indicate that clearance of the enteric nematode *N. brasiliensis* is delayed in *Chrm3*$^{-/-}$ mice.

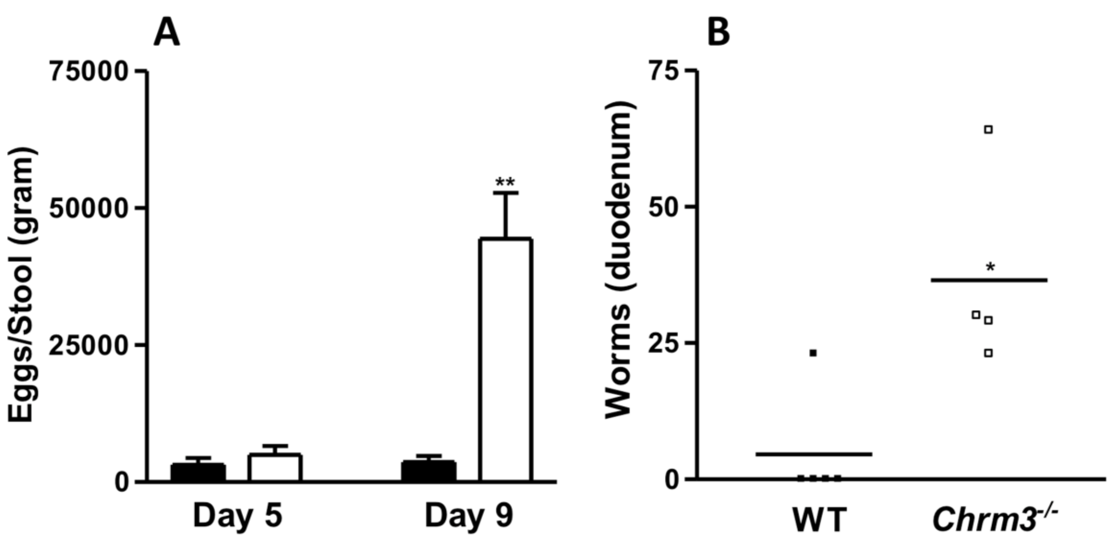

Figure 35: (A) Fecal egg content at 9 DPI from WT (black bars) and *Chrm3*$^{-/-}$ (white bars) mice. (B) Nematode count within the proximal small intestine (duodenum) at 9 DPI.
** $p < 0.01$ vs. WT. * $p < 0.05$ vs. WT.

Upregulation of T_H2 Cytokines is Inhibited in N. brasiliensis-Infected Chrm3$^{-/-}$ Small Intestine

Enteric nematode infection elicits a stereotypic T_H2 cytokine response in murine small intestine [115]. Expression of T_H2 and T_H1/T_H17 cytokines from small intestine of WT and *Chrm3*$^{-/-}$ mice was measured using RT-PCR. In *N. brasiliensis*-infected WT small intestine both *IL-4* and *IL-13* were significantly upregulated (Figures 36A & 36B) as expected. However, in *N. brasiliensis*-infected *Chrm3*$^{-/-}$ small intestine upregulation of *IL-4* and *IL-13* was abrogated (Figures 36A & 36B). Expression of T_H1/T_H17 cytokines was also determined. *IFN-γ* was upregulated modestly in *N. brasiliensis*-infected *Chrm3*$^{-/-}$ mucosa; however, neither *TNF-α* nor *IL-17* was upregulated in *N. brasiliensis*-infected *Chrm3*$^{-/-}$ mucosa (Figure 36C). Gene expression of *CD3* was similar in WT and *Chrm3*$^{-/-}$ mice, indicating T cell recruitment is intact in *Chrm3*$^{-/-}$ mice (data not shown). These data indicate that genetic ablation of M3R is associated with impaired generation of T_H2 cytokines in response to enteric nematode infection.

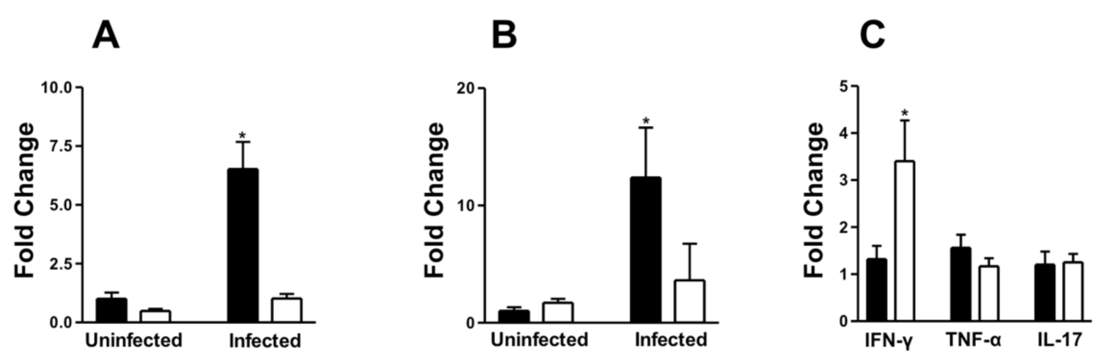

Figure 36: Gene expression of (A) IL-13 and (B) IL-4 in uninfected and *N. brasiliensis*-infected WT (black bars) and *Chrm3*$^{-/-}$ (white bars) intestine. Gene expression of (C) T_H1/T_H17 cytokines in infected WT (black bars) and *Chrm3*$^{-/-}$ (white bars) intestine.
** $p < 0.01$ vs. WT. * $p < 0.05$ vs. WT.

Alternative Activation of Macrophages is Inhibited in N. brasiliensis-Infected Chrm3$^{-/-}$ *Small Intestine*

We examined the ability of *Chrm3*$^{-/-}$ macrophages to respond *in vivo* to *N. brasiliensis* infection or *in vitro* to IL-4 treatment. As expected, in WT mice *N. brasiliensis* infection induced an influx of AAM that express arginase-1 (*Arg-1*). In contrast, *Arg-1* was not upregulated in *N. brasiliensis*-infected *Chrm3*$^{-/-}$ mice (Figure 37). *In vitro* studies were performed to further characterize the relationship between M3R and T_H1/T_H2 cytokines with respect to macrophage differentiation. Although IFN-γ treatment resulted in increased gene expression of M3R, treatment with IL-4 was not associated with any change in M3R gene expression (Figure 38). Treatment of WT BMDM with bethanechol, a muscarinic-specific agonist, resulted in decreased expression of *Arg-1* (Figure 39). As expected, treatment of WT BMDM with IL-4 induced a significant increase in *Arg-1* expression (Figure 40), indicating that WT BMDM appropriately develop the AAM phenotype in the presence of IL-4. Treatment of *Chrm3*$^{-/-}$ BMDM with IL-4 also induced an increase in *Arg-1*; however, this increase was significantly greater

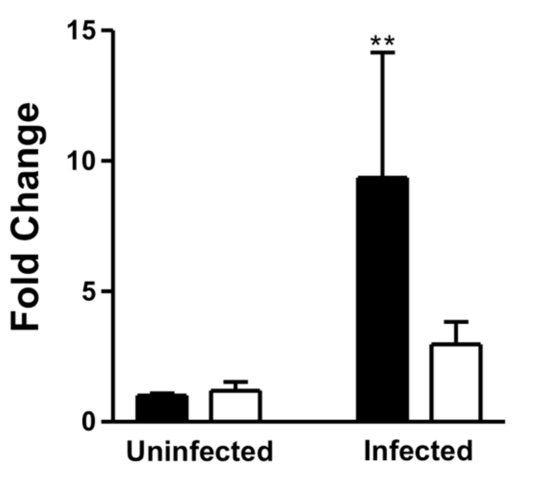

Figure 37: Gene expression of *Arg-1* in uninfected and *N. brasiliensis*-infected WT (black bars) and *Chrm3*$^{-/-}$ (white bars) small intestine.
**p < 0.01 WT uninfected

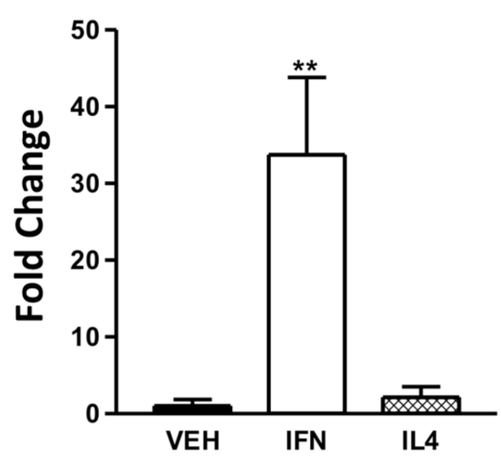

Figure 38: Gene expression of *Chrm3* in vehicle, IFN-γ (10 ng/mL), and IL-4 (20 ng/mL) treated WT BMDM.
** p < 0.01 vs. vehicle

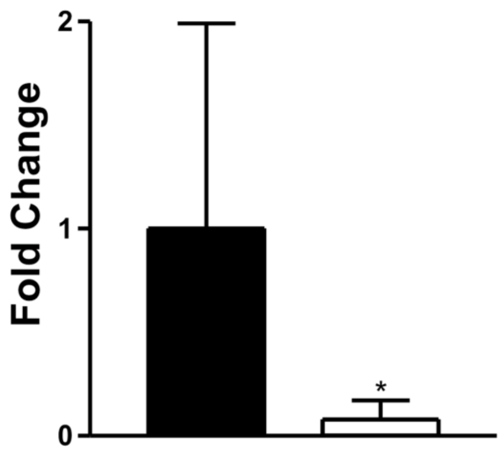

Figure 39: Gene expression of *Arg-1* in WT BMDM treated with vehicle (black bar) or bethanechol (100 nM, white bar).
*p < 0.05 WT vehicle.

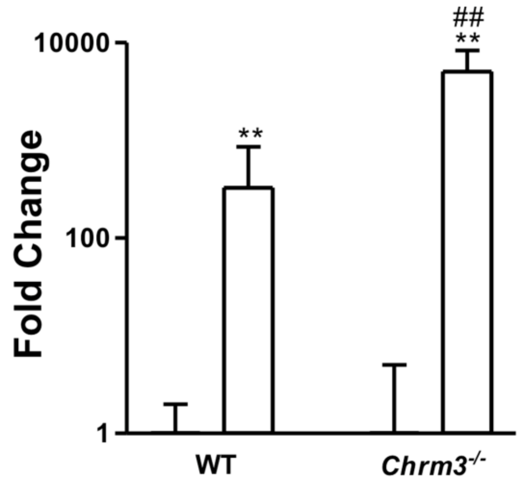

Figure 40: Gene expression of *Arg-1* in WT or *Chrm3*$^{-/-}$ BMDM treated with vehicle or IL4 (20 ng/mL, white bars).
** p < 0.01 vs. vehicle. ## p < 0.01 vs. WT IL4.

than the upregulation of *Arg-1* observed in IL-4-treated WT BMDM (Figure 40). These data indicate that *Chrm3*$^{-/-}$ macrophages retain their ability to respond to a T_H2 stimulus and suggest that constitutive M3R activity may provide a counter regulatory effect to control the degree of AAM development.

T_H2-Dependent Changes in Gut Function are Not Observed in N. brasiliensis-Infected Chrm3$^{-/-}$ *mice*

Upregulation of the T_H2 cytokines IL-4 and IL-13 induces characteristic changes in intestinal physiology generating several stereotypic functional changes (increased permeability, smooth muscle hypercontractility, decreased epithelial secretion, decreased fluid absorption, and goblet cell expansion) that promote nematode expulsion [82,109-112,115]. These changes depend on generation of T_H2 cytokines [109] and transcription of STAT6-dependent genes [82,111,116].

As expected, small intestinal TEER decreased significantly in *N. brasiliensis*-infected WT mice, consistent with increased epithelial permeability (Figure 41A). This decrease was not observed in small intestine from *N. brasiliensis*-infected *Chrm3*$^{-/-}$ mice (Figure 41A). Similarly, smooth muscle hypercontractility in response to acetylcholine stimulation was observed in *N. brasiliensis*-infected WT mice, but was not observed in smooth muscle from *N. brasiliensis*-infected *Chrm3*$^{-/-}$ mice (Figure 41B). Acetylcholine induced epithelial secretion was decreased significantly in *N. brasiliensis*-infected WT mice (Figure 41C), but again, this effect was absent from *N. brasiliensis*-infected *Chrm3*$^{-/-}$ mice (Figure 41C). Glucose stimulated epithelial absorption was also decreased significantly in *N. brasiliensis*-infected WT mice (Figure 41D), but this change was not observed in small intestine from *N. brasiliensis*-infected *Chrm3*$^{-/-}$ mice (Figure 41D). Finally, goblet cell expansion occurred in *N. brasiliensis*-infected WT mice, but did not occur in *N. brasiliensis*-infected *Chrm3*$^{-/-}$ mice (Figure 42). Together these data demonstrate that stereotypic physiologic changes induced by enteric nematode infection are not observed in *Chrm3*$^{-/-}$ mice, emphasizing the dependence of these changes in gut function on generation of T_H2 cytokines.

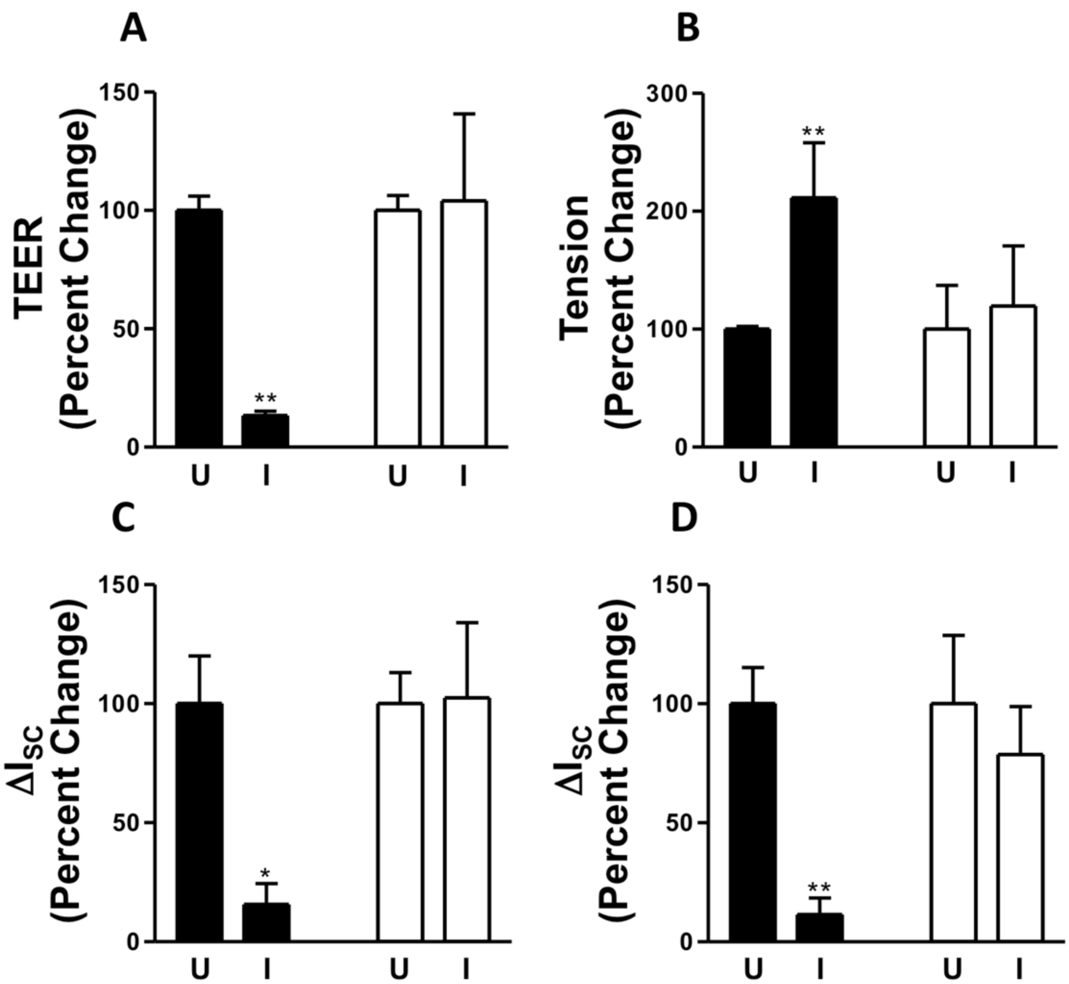

Figure 41: (A) Percent change in TEER in uninfected and *N. brasiliensis*-infected (9 DPI) WT (black bars) and *Chrm3*$^{-/-}$ (white bars) mice. (B) Percent change in smooth muscle contraction in response to acetylcholine 100 μM in uninfected and *N. brasiliensis*-infected (9 DPI) WT (black bars) and *Chrm3*$^{-/-}$ (white bars) mice. (C) Percent change in epithelial secretion in response to acetylcholine 100 μM in uninfected and *N. brasiliensis*-infected (9 DPI) WT (black bars) and *Chrm3*$^{-/-}$ (white bars) mice. (D) Percent change in epithelial absorption in response to glucose 40 μM in uninfected and *N. brasiliensis*-infected (9 DPI) WT (black bars) and *Chrm3*$^{-/-}$ (white bars) mice.

** $p < 0.01$ vs. WT uninfected. * $p < 0.05$ vs. WT uninfected.

TEER: transepithelial electrical resistance. ΔI_{SC}: change in short-circuit current.

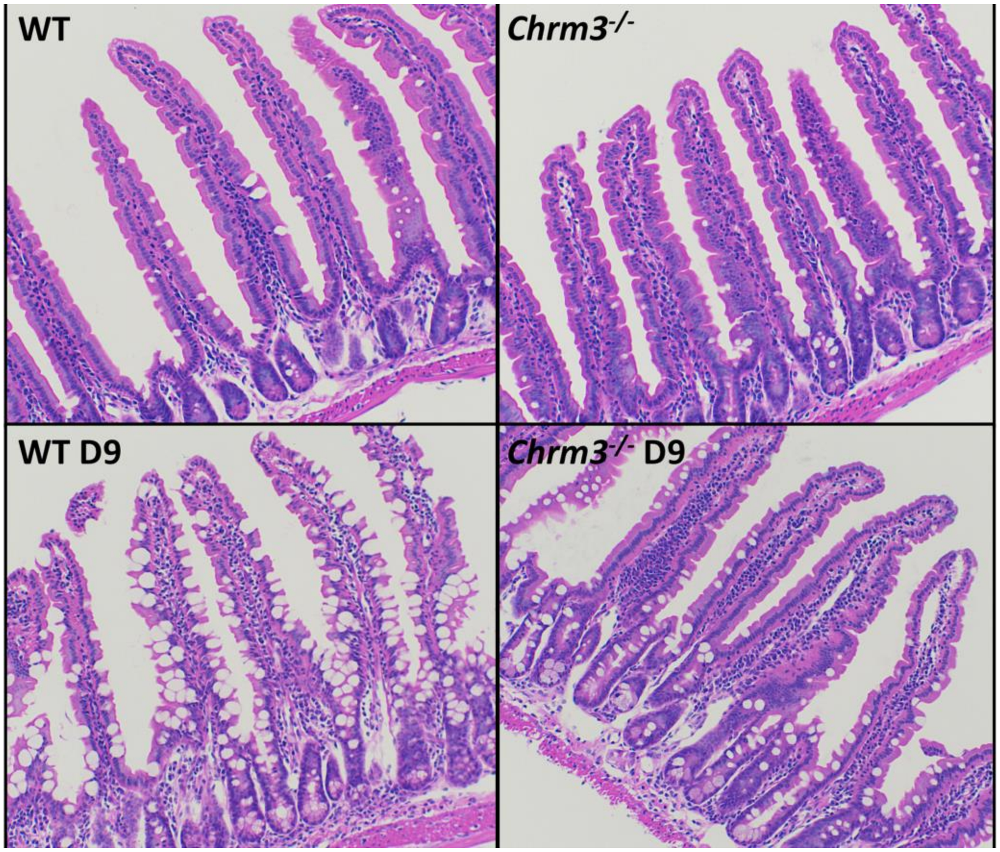

Figure 42: Representative H&E-stained sections of ileum from uninfected and *N. brasiliensis*-infected WT and *Chrm3*$^{-/-}$ mice demonstrating goblet cell expansion in WT small intestine 9 DPI, but not in *Chrm3*$^{-/-}$ small intestine 9 DPI.
WT: Wild type. *Chrm3*$^{-/-}$: M3R-deficient. D9: 9 days post-infection. H&E: hematoxylin and eosin.

Discussion

These data demonstrate that generation of a T_H2 immune response in GI mucosa in the setting of enteric nematode infection is dependent on M3R. In the absence of T_H2 cytokines, *N. brasiliensis*-infected *Chrm3*$^{-/-}$ mice do not develop stereotypic T_H2-dependent physiologic changes such as smooth muscle hypercontractility, increased epithelial permeability, decreased mucosal secretion and absorption, or goblet cell expansion. At present, the defect underlying the impaired ability of *Chrm3*$^{-/-}$ mice to generate T_H2 cytokines in the setting of nematode infection is not clear, although it is possible that T cells, which express M3R [5,7,117], may not respond appropriately to T_H2-inducing stimuli. Alternatively, antigen presentation or T cell activation may be impaired in *Chrm3*$^{-/-}$ mice; however, *Chrm3*$^{-/-}$ mice are able to mount a T_H1/T_H17 response in the setting of a T_H1/T_H17 stimulus (Figure 12), suggesting that M3R activity specifically modulates the development of a T_H2 response, but not a T_H1/T_H17 response.

A recently published article examined the contribution of M3R to airway remodeling in a murine model [118]. In this study, Kistemaker *et al.* examined a variety of physiologic parameters including smooth muscle thickening and airway remodeling. They observed a 35-40% decrease in these parameters in *Chrm3*$^{-/-}$ mice when compared to WT, *Chrm1*$^{-/-}$, and *Chrm2*$^{-/-}$ mice, which served as controls. Interestingly, the authors report similar or higher levels of T_H2 cytokines in *Chrm3*$^{-/-}$ mice compared to WT, *Chrm1*$^{-/-}$, and *Chrm2*$^{-/-}$ mice. In our study we observed none of the expected physiologic changes in response to *N. brasiliensis* infection, most likely due to abrogated upregulation of T_H2 cytokines (Figure 43). The reason for attenuated smooth muscle thickening and airway remodeling observed by Kistemaker *et al.* in *Chrm3*$^{-/-}$ mice could not be attributed to an impaired immune response as they detected T_H2 cytokines in response to ovalbumin stimulation. The inability to generate T_H2 cytokines within small intestine in response to nematode infection suggests that generation of T_H2 cytokines may be region or stimulus specific. Interestingly, a different study reported markedly reduced levels of IL-4, IL-5, and eotaxin in ovalbumin stimulated mice treated with bencycloquidium bromide, a M3R antagonist being considered for use in asthma [68], also supporting a role for M3R activity in the generation of T_H2 cytokines.

Enteric nematode infection has been linked to decreased incidence of autoimmune disease, including IBD, as well as decreased colitis severity in murine models [119,120]. In addition to stimulating production of T_H2 cytokines, enteric nematode infection triggers recruitment of a variety of immune cells including mast cells, eosinophils, basophils, and macrophages [121]. The lack of AAM in *N. brasiliensis*-infected *Chrm3*$^{-/-}$ mice can be attributed directly to impaired upregulation of T_H2 cytokines. Our *in vitro* data, however, demonstrate that M3R affects macrophage phenotype in response to a T_H2 stimulus (IL-4), with enhanced expression of *Arg-1* in the absence of M3R. M3R is one of at least two cholinergic receptors, the other being α7, capable of modulating macrophage phenotype and function. Although further studies are required, it is plausible that cholinergic tone affects macrophage phenotype at both α7 and M3R, with α7 driving macrophages towards an AAM phenotype and M3R acting in a counter regulatory fashion preventing extreme AAM polarization. This may explain, in part, why mice with DSS-induced colitis develop an exacerbation of their colitis and increased expression of pro-inflammatory cytokines after treatment with either of two α7 specific agonists [8].

Our studies also demonstrate that M3R contributes to barrier function and mucosal homeostasis in uninfected small intestine in addition to its role in the response to enteric nematode infection and modulation of macrophage phenotype and function. Prior reports link M3R activity to transcellular transport of macromolecules [122], but the role of M3R in maintenance of intestinal barrier function has not been demonstrated previously. In addition to increased permeability in small intestine of *Chrm3*$^{-/-}$ mice, expression of pro-inflammatory T_H1/T_H17 cytokines is upregulated. It has been suggested that defects in barrier function precede the development of pathologic inflammatory conditions such as IBD [123,124] with upregulation of T_H1/T_H17 cytokines contributing to the development of chronic barrier dysfunction and symptomatic IBD. The modest upregulation of T_H1/T_H17 cytokines observed in uninfected *Chrm3*$^{-/-}$ small intestine is likely secondary to immune activation in the setting of defective barrier function, rather than to an undemonstrated anti-inflammatory effect of M3R on GI epithelial cells. Whether basal expression of T_H1/T_H17 cytokines affects the ability of *Chrm3*$^{-/-}$ mice to mount a T_H2 response to enteric nematode is currently unclear, although it is known that increases in IFN-γ can suppress host defense against *N. brasiliensis* [109].

Overall, our studies indicate that M3R activity contributes to homeostasis in uninfected small intestine as well as the generation of a T_H2 response to *N. brasiliensis* infection. Similar observations have been made regarding the possible contribution of M3R to T_H2 immunity in pulmonary models. Our data suggest that in addition to its role in immune response to enteric nematode infection, M3R may serve a counter regulatory role in the generation of AAM, demonstrating that MR, specifically M3R, play a key and previously undefined role in mucosal homeostasis as well as immune regulation and response to enteric nematodes within the GI tract.

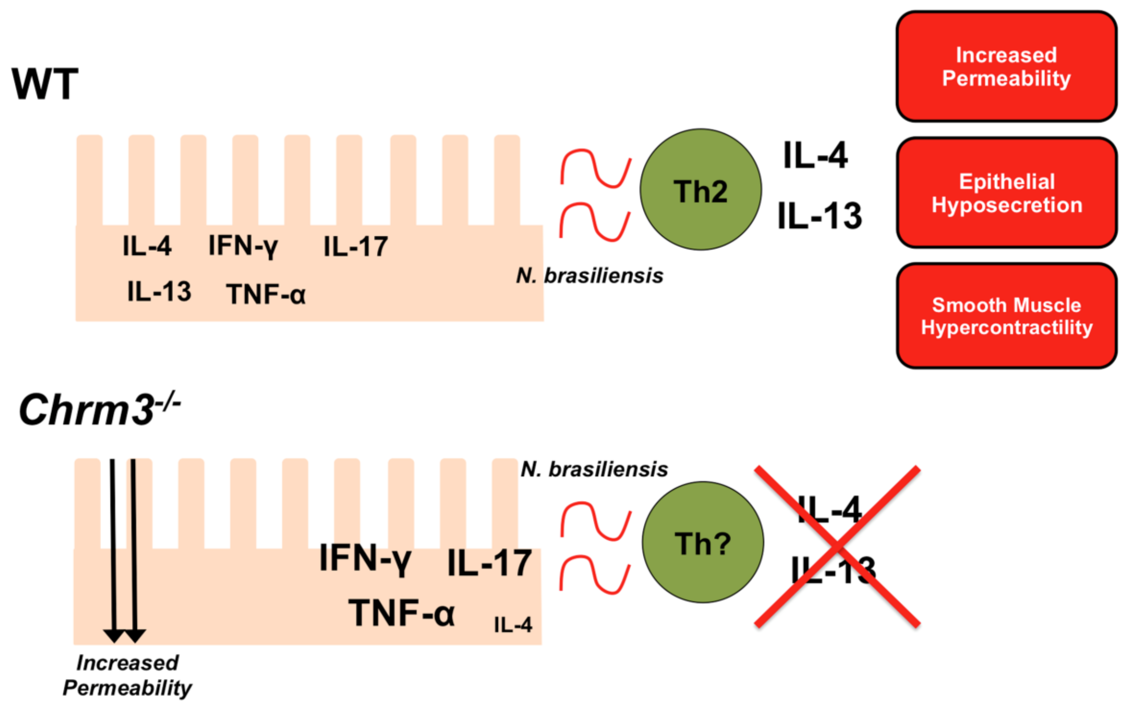

Figure 43: Proposed model of delayed nematode clearance in *Chrm3*$^{-/-}$ mice. A T_H2 response is mounted in WT intestine infected with *N. brasiliensis* resulting in downstream functional changes including increased permeability, epithelial hyposecretion, smooth muscle hypercontractility, and goblet cell expansion (not shown). In M3R intestine, a constitutive increase in permeability exists, as does increased expression of T_H1/T_H17 cytokines. In the setting of nematode infection T_H2 cytokines are not generated and resultant downstream physiologic changes in gut function are not observed, contributing to delayed nematode clearance.

Chapter 4: Discussion

We report herein a previously undescribed role for M3R in host defense within the small intestine and colon in response to both a T_H1/T_H17 inducing bacterium, *C. rodentium*, as well as a T_H2 inducing enteric nematode, *N. brasiliensis*. Of considerable interest is the different role of M3R in clearance of these two infections. In *C. rodentium* infection, M3R does not affect generation of the T_H1/T_H17 cytokines IFN-γ, TNF-α, or IL-17, but does contribute to innate host defense through its effects on mucin production and, consequently, the ability of *C. rodentium* to adhere to colonic mucosa. In *N. brasiliensis* infection, M3R contributes to generation of the T_H2 cytokines IL-4 and IL-13.

Infection with the A/E bacterium *C. rodentium* induces a marked upregulation of T_H1/T_H17 cytokines in both WT and *Chrm3*$^{-/-}$ mice, although clearance of *C. rodentium* from *Chrm3*$^{-/-}$ mice is delayed. Unlike *N. brasiliensis* infection, the host's ability to mount the appropriate cytokine response is not impaired. The more robust T_H1/T_H17 cytokine profile that is observed in *Chrm3*$^{-/-}$ mice is most likely due to persistent adherence of *C. rodentium* at 13 DPI whereas in WT mice *C. rodentium* has largely cleared. Although M3R is expressed by a variety of immune cells, the delay in clearing *C. rodentium* from *Chrm3*$^{-/-}$ mice is most likely due to decreased goblet cell numbers and reduced Mucin-2 in *Chrm3*$^{-/-}$ colon. Prior reports have demonstrated a critical role for mucins in preventing or minimizing contact of luminal microorganisms with the mucosal surface [37].

The abrogation of upregulation of IL-4 and IL-13 in *Chrm3*$^{-/-}$ small intestine despite *N. brasiliensis* infection prevents stereotypic downstream physiologic changes from occurring, including smooth muscle hypercontractility, increased epithelial permeability, decreased mucosal secretion and absorption, and goblet cell expansion, all of which contribute to nematode expulsion. An equine study examining cytokine production in neonates and foals demonstrated intact T_H1 cytokine production, but impaired T_H2 cytokine production in foals up to 3 months of age; however, neither MR, NR, or acetylcholine were discussed in the article nor was a potential mechanism that would explain these differences in cytokine production proffered [125]. It is possible that cholinergic tone acting at M3R expressed on T cells triggers a heretofore unidentified downstream pathway that contributes to production and/or release of T_H2 cytokines from T cells. Alternatively, M3R expressed on antigen presenting cells could affect the ability of these cells to phagocytose or present antigen, but if this were the case one would expect the T_H1/T_H17 response to be blunted as well.

In addition to its role in host defense, MR also influence the phenotype and function of BMDM. Our studies indicate the muscarinic signaling causes BMDM to attain a CAM phenotype, an effect mediated by M3R. In the setting of cholinergic stimulation, where both MR and NR are activated, one can imagine that signaling at M3R may serve a counter regulatory effect to counterbalance the anti-inflammatory effects on macrophage phenotype mediated through $\alpha7$. Other studies examining the role of M3R in mostly alveolar macrophages have also suggested a pro-inflammatory role for M3R [13,68] in that setting, a finding that our studies support. Treating rats with atropine, a non-specific MR antagonist, inhibited antibody and T cell proliferation; however, neither the effect of atropine on cytokine profiles, nor the effects of MR subtype blockade were reported [70]. Nonetheless, our studies indicate a pro-inflammatory role for M3R, consistent with prior reports examining the role of M3R in immune response within the lung. It is possible that pro-inflammatory M3R signaling serves as a check against anti-inflammatory signaling via α7.

Overall, our studies indicate a clear role for M3R in host defense, specifically in response to enteric nematode and enteric bacterial infections, as well as a role for M3R in modulation of macrophage phenotype and function. These findings support an expanding role for cholinergic receptors not only in the regulation of inflammatory conditions, as is extensively described with respect to α7, but also in clearance of enteric pathogens. Our findings provide the foundation for additional work examining the contribution of muscarinic tone to modulation of inflammation within the GI tract and have the potential to provide new insights that may indicate novel methods for manipulating chronic inflammatory conditions such as IBD.

REFERENCES

1. Shah N, Khurana S, Cheng K, Raufman JP. Muscarinic receptors and ligands in cancer. *American journal of physiology. Cell physiology*, 296(2), C221-232 (2009).
2. Beckmann J, Lips KS. The non-neuronal cholinergic system in health and disease. *Pharmacology*, 92(5-6), 286-302 (2013).
3. Wessler I, Kirkpatrick CJ. Acetylcholine beyond neurons: the non-neuronal cholinergic system in humans. *British journal of pharmacology*, 154(8), 1558-1571 (2008).
4. Rosas-Ballina M, Olofsson PS, Ochani M *et al.* Acetylcholine-synthesizing T cells relay neural signals in a vagus nerve circuit. *Science*, 334(6052), 98-101 (2011).
5. Kawashima K, Fujii T, Moriwaki Y, Misawa H. Critical roles of acetylcholine and the muscarinic and nicotinic acetylcholine receptors in the regulation of immune function. *Life sciences*, 91(21-22), 1027-1032 (2012).
6. Mazloom R, Eftekhari G, Rahimi M *et al.* The role of alpha7 nicotinic acetylcholine receptor in modulation of heart rate dynamics in endotoxemic rats. *PloS one*, 8(12), e82251 (2013).
7. Sato KZ, Fujii T, Watanabe Y *et al.* Diversity of mRNA expression for muscarinic acetylcholine receptor subtypes and neuronal nicotinic acetylcholine receptor subunits in human mononuclear leukocytes and leukemic cell lines. *Neuroscience letters*, 266(1), 17-20 (1999).
8. Snoek SA, Verstege MI, van der Zanden EP *et al.* Selective alpha7 nicotinic acetylcholine receptor agonists worsen disease in experimental colitis. *British journal of pharmacology*, 160(2), 322-333 (2010).
9. van Westerloo DJ, Giebelen IA, Florquin S *et al.* The vagus nerve and nicotinic receptors modulate experimental pancreatitis severity in mice. *Gastroenterology*, 130(6), 1822-1830 (2006).
10. Wang H, Yu M, Ochani M *et al.* Nicotinic acetylcholine receptor alpha7 subunit is an essential regulator of inflammation. *Nature*, 421(6921), 384-388 (2003).
11. Zhou H, Liang H, Li ZF, Xiang H, Liu W, Li JG. Vagus nerve stimulation attenuates intestinal epithelial tight junctions disruption in endotoxemic mice through alpha7 nicotinic acetylcholine receptors. *Shock*, 40(2), 144-151 (2013).
12. Wess J. Molecular biology of muscarinic acetylcholine receptors. *Critical reviews in neurobiology*, 10(1), 69-99 (1996).
13. Kistemaker LE, Bos IS, Hylkema MN *et al.* Muscarinic receptor subtype-specific effects on cigarette smoke-induced inflammation in mice. *The European respiratory journal*, 42(6), 1677-1688 (2013).
14. Wu J, Lukas RJ. Naturally-expressed nicotinic acetylcholine receptor subtypes. *Biochemical pharmacology*, 82(8), 800-807 (2011).
15. Papke RL. Merging old and new perspectives on nicotinic acetylcholine receptors. *Biochemical pharmacology*, 89(1), 1-11 (2014).
16. Albuquerque EX, Pereira EF, Alkondon M, Rogers SW. Mammalian nicotinic acetylcholine receptors: from structure to function. *Physiological reviews*, 89(1), 73-120 (2009).
17. Bourin M, Ripoll N, Dailly E. Nicotinic receptors and Alzheimer's disease. *Current medical research and opinion*, 19(3), 169-177 (2003).

18. Dhawan S, Cailotto C, Harthoorn LF, de Jonge WJ. Cholinergic signalling in gut immunity. *Life sciences*, 91(21-22), 1038-1042 (2012).
19. Blalock JE, Smith EM. Conceptual development of the immune system as a sixth sense. *Brain, behavior, and immunity*, 21(1), 23-33 (2007).
20. Dinarello CA, Cannon JG, Wolff SM *et al.* Tumor necrosis factor (cachectin) is an endogenous pyrogen and induces production of interleukin 1. *The Journal of experimental medicine*, 163(6), 1433-1450 (1986).
21. Tracey KJ, Morgello S, Koplin B *et al.* Metabolic effects of cachectin/tumor necrosis factor are modified by site of production. Cachectin/tumor necrosis factor-secreting tumor in skeletal muscle induces chronic cachexia, while implantation in brain induces predominantly acute anorexia. *The Journal of clinical investigation*, 86(6), 2014-2024 (1990).
22. Watkins LR, Goehler LE, Relton JK *et al.* Blockade of interleukin-1 induced hyperthermia by subdiaphragmatic vagotomy: evidence for vagal mediation of immune-brain communication. *Neuroscience letters*, 183(1-2), 27-31 (1995).
23. Goehler LE, Relton JK, Dripps D *et al.* Vagal paraganglia bind biotinylated interleukin-1 receptor antagonist: a possible mechanism for immune-to-brain communication. *Brain research bulletin*, 43(3), 357-364 (1997).
24. Tracey KJ. Reflex control of immunity. *Nature reviews. Immunology*, 9(6), 418-428 (2009).
25. Rosas-Ballina M, Ochani M, Parrish WR *et al.* Splenic nerve is required for cholinergic antiinflammatory pathway control of TNF in endotoxemia. *Proceedings of the National Academy of Sciences of the United States of America*, 105(31), 11008-11013 (2008).
26. Matteoli G, Boeckxstaens GE. The vagal innervation of the gut and immune homeostasis. *Gut*, 62(8), 1214-1222 (2013).
27. Matteoli G, Gomez-Pinilla PJ, Nemethova A *et al.* A distinct vagal anti-inflammatory pathway modulates intestinal muscularis resident macrophages independent of the spleen. *Gut*, (2013).
28. Ghia JE, Blennerhassett P, Kumar-Ondiveeran H, Verdu EF, Collins SM. The vagus nerve: a tonic inhibitory influence associated with inflammatory bowel disease in a murine model. *Gastroenterology*, 131(4), 1122-1130 (2006).
29. Ghia JE, Blennerhassett P, Collins SM. Impaired parasympathetic function increases susceptibility to inflammatory bowel disease in a mouse model of depression. *The Journal of clinical investigation*, 118(6), 2209-2218 (2008).
30. Ghia JE, Blennerhassett P, Deng Y, Verdu EF, Khan WI, Collins SM. Reactivation of inflammatory bowel disease in a mouse model of depression. *Gastroenterology*, 136(7), 2280-2288 e2281-2284 (2009).
31. Ghia JE, Park AJ, Blennerhassett P, Khan WI, Collins SM. Adoptive transfer of macrophage from mice with depression-like behavior enhances susceptibility to colitis. *Inflammatory bowel diseases*, 17(7), 1474-1489 (2011).
32. Choi KM, Kashyap PC, Dutta N *et al.* CD206-positive M2 macrophages that express heme oxygenase-1 protect against diabetic gastroparesis in mice. *Gastroenterology*, 138(7), 2399-2409, 2409 e2391 (2010).

33. Wehner S, Behrendt FF, Lyutenski BN *et al.* Inhibition of macrophage function prevents intestinal inflammation and postoperative ileus in rodents. *Gut*, 56(2), 176-185 (2007).
34. Eskandari MK, Kalff JC, Billiar TR, Lee KK, Bauer AJ. LPS-induced muscularis macrophage nitric oxide suppresses rat jejunal circular muscle activity. *The American journal of physiology*, 277(2 Pt 1), G478-486 (1999).
35. Costa L, Roth M, Miglino N *et al.* Tiotropium sustains the anti-inflammatory action of olodaterol via the cyclic AMP pathway. *Pulmonary pharmacology & therapeutics*, 27(1), 29-37 (2014).
36. Xu ZP, Yang K, Xu GN *et al.* Role of M3 mAChR in in vivo and in vitro models of LPS-induced inflammatory response. *International immunopharmacology*, 14(3), 320-327 (2012).
37. Sonnenberg GF, Artis D. Innate lymphoid cell interactions with microbiota: implications for intestinal health and disease. *Immunity*, 37(4), 601-610 (2012).
38. Fanning AS, Jameson BJ, Jesaitis LA, Anderson JM. The tight junction protein ZO-1 establishes a link between the transmembrane protein occludin and the actin cytoskeleton. *The Journal of biological chemistry*, 273(45), 29745-29753 (1998).
39. Cunningham KE, Turner JR. Myosin light chain kinase: pulling the strings of epithelial tight junction function. *Annals of the New York Academy of Sciences*, 1258, 34-42 (2012).
40. Clayburgh DR, Shen L, Turner JR. A porous defense: the leaky epithelial barrier in intestinal disease. *Laboratory investigation; a journal of technical methods and pathology*, 84(3), 282-291 (2004).
41. Wang F, Schwarz BT, Graham WV *et al.* IFN-gamma-induced TNFR2 expression is required for TNF-dependent intestinal epithelial barrier dysfunction. *Gastroenterology*, 131(4), 1153-1163 (2006).
42. Fasano A, Shea-Donohue T. Mechanisms of disease: the role of intestinal barrier function in the pathogenesis of gastrointestinal autoimmune diseases. *Nature clinical practice. Gastroenterology & hepatology*, 2(9), 416-422 (2005).
43. Camilleri M, Madsen K, Spiller R, Greenwood-Van Meerveld B, Verne GN. Intestinal barrier function in health and gastrointestinal disease. *Neurogastroenterology and motility : the official journal of the European Gastrointestinal Motility Society*, 24(6), 503-512 (2012).
44. Turner JR. Intestinal mucosal barrier function in health and disease. *Nature reviews. Immunology*, 9(11), 799-809 (2009).
45. Keita AV, Soderholm JD. The intestinal barrier and its regulation by neuroimmune factors. *Neurogastroenterology and motility : the official journal of the European Gastrointestinal Motility Society*, 22(7), 718-733 (2010).
46. Hirota CL, McKay DM. M3 muscarinic receptor-deficient mice retain bethanechol-mediated intestinal ion transport and are more sensitive to colitis. *Canadian journal of physiology and pharmacology*, 84(11), 1153-1161 (2006).
47. Verkman AS. Mammalian aquaporins: diverse physiological roles and potential clinical significance. *Expert reviews in molecular medicine*, 10, e13 (2008).
48. Loo DD, Zeuthen T, Chandy G, Wright EM. Cotransport of water by the Na+/glucose cotransporter. *Proceedings of the National Academy of Sciences of the United States of America*, 93(23), 13367-13370 (1996).

49. Sleisenger MH, Feldman M, Friedman LS, Brandt LJ. *Sleisenger and Fordtran's gastrointestinal and liver disease : pathophysiology, diagnosis, management* (Saunders/Elsevier, Philadelphia , PA, 2010).
50. Johansson ME, Phillipson M, Petersson J, Velcich A, Holm L, Hansson GC. The inner of the two Muc2 mucin-dependent mucus layers in colon is devoid of bacteria. *Proceedings of the National Academy of Sciences of the United States of America*, 105(39), 15064-15069 (2008).
51. Kim YS, Ho SB. Intestinal goblet cells and mucins in health and disease: recent insights and progress. *Current gastroenterology reports*, 12(5), 319-330 (2010).
52. Peterson LW, Artis D. Intestinal epithelial cells: regulators of barrier function and immune homeostasis. *Nature reviews. Immunology*, 14(3), 141-153 (2014).
53. Bergstrom KS, Kissoon-Singh V, Gibson DL *et al.* Muc2 protects against lethal infectious colitis by disassociating pathogenic and commensal bacteria from the colonic mucosa. *PLoS pathogens*, 6(5), e1000902 (2010).
54. Denning TL, Wang YC, Patel SR, Williams IR, Pulendran B. Lamina propria macrophages and dendritic cells differentially induce regulatory and interleukin 17-producing T cell responses. *Nature immunology*, 8(10), 1086-1094 (2007).
55. Uronis JM, Muhlbauer M, Herfarth HH, Rubinas TC, Jones GS, Jobin C. Modulation of the intestinal microbiota alters colitis-associated colorectal cancer susceptibility. *PloS one*, 4(6), e6026 (2009).
56. Dupaul-Chicoine J, Dagenais M, Saleh M. Crosstalk between the intestinal microbiota and the innate immune system in intestinal homeostasis and inflammatory bowel disease. *Inflammatory bowel diseases*, 19(10), 2227-2237 (2013).
57. Tait Wojno ED, Artis D. Innate lymphoid cells: balancing immunity, inflammation, and tissue repair in the intestine. *Cell host & microbe*, 12(4), 445-457 (2012).
58. Molodecky NA, Soon IS, Rabi DM *et al.* Increasing incidence and prevalence of the inflammatory bowel diseases with time, based on systematic review. *Gastroenterology*, 142(1), 46-54 e42; quiz e30 (2012).
59. Xavier RJ, Podolsky DK. Unravelling the pathogenesis of inflammatory bowel disease. *Nature*, 448(7152), 427-434 (2007).
60. Cader MZ, Kaser A. Recent advances in inflammatory bowel disease: mucosal immune cells in intestinal inflammation. *Gut*, 62(11), 1653-1664 (2013).
61. Hunter MM, Wang A, Parhar KS *et al.* In vitro-derived alternatively activated macrophages reduce colonic inflammation in mice. *Gastroenterology*, 138(4), 1395-1405 (2010).
62. Rizzo A, Monteleone I, Fina D *et al.* Inhibition of colitis by IL-25 associates with induction of alternatively activated macrophages. *Inflammatory bowel diseases*, 18(3), 449-459 (2012).
63. Leung G, Wang A, Fernando M, Phan VC, McKay DM. Bone marrow-derived alternatively activated macrophages reduce colitis without promoting fibrosis: participation of IL-10. *American journal of physiology. Gastrointestinal and liver physiology*, 304(9), G781-792 (2013).
64. Bonaz B, Picq C, Sinniger V, Mayol JF, Clarencon D. Vagus nerve stimulation: from epilepsy to the cholinergic anti-inflammatory pathway. *Neurogastroenterology and motility : the official journal of the European Gastrointestinal Motility Society*, 25(3), 208-221 (2013).

65. de Jonge WJ. The Gut's Little Brain in Control of Intestinal Immunity. *ISRN gastroenterology*, 2013, 630159 (2013).
66. Cailotto C, Gomez-Pinilla PJ, Costes LM *et al.* Neuro-anatomical evidence indicating indirect modulation of macrophages by vagal efferents in the intestine but not in the spleen. *PloS one*, 9(1), e87785 (2014).
67. Pieper MP. The non-neuronal cholinergic system as novel drug target in the airways. *Life sciences*, 91(21-22), 1113-1118 (2012).
68. Cao R, Dong XW, Jiang JX *et al.* M(3) muscarinic receptor antagonist bencycloquidium bromide attenuates allergic airway inflammation, hyperresponsiveness and remodeling in mice. *European journal of pharmacology*, 655(1-3), 83-90 (2011).
69. Kistemaker LE, Bos IS, Hylkema MN *et al.* Muscarinic receptor subtype-specific effects on cigarette smoke-induced inflammation in mice. *The European respiratory journal : official journal of the European Society for Clinical Respiratory Physiology*, (2013).
70. Razani-Boroujerdi S, Behl M, Hahn FF, Pena-Philippides JC, Hutt J, Sopori ML. Role of muscarinic receptors in the regulation of immune and inflammatory responses. *Journal of neuroimmunology*, 194(1-2), 83-88 (2008).
71. Lundgren O, Jodal M, Jansson M, Ryberg AT, Svensson L. Intestinal epithelial stem/progenitor cells are controlled by mucosal afferent nerves. *PloS one*, 6(2), e16295 (2011).
72. Higgins LM, Frankel G, Douce G, Dougan G, MacDonald TT. Citrobacter rodentium infection in mice elicits a mucosal Th1 cytokine response and lesions similar to those in murine inflammatory bowel disease. *Infection and immunity*, 67(6), 3031-3039 (1999).
73. Zheng Y, Valdez PA, Danilenko DM *et al.* Interleukin-22 mediates early host defense against attaching and effacing bacterial pathogens. *Nature medicine*, 14(3), 282-289 (2008).
74. Symonds EL, Riedel CU, O'Mahony D, Lapthorne S, O'Mahony L, Shanahan F. Involvement of T helper type 17 and regulatory T cell activity in Citrobacter rodentium invasion and inflammatory damage. *Clinical and experimental immunology*, 157(1), 148-154 (2009).
75. Alipour M, Lou Y, Zimmerman D *et al.* A balanced IL-1beta activity is required for host response to Citrobacter rodentium infection. *PloS one*, 8(12), e80656 (2013).
76. Maaser C, Housley MP, Iimura M *et al.* Clearance of Citrobacter rodentium requires B cells but not secretory immunoglobulin A (IgA) or IgM antibodies. *Infection and immunity*, 72(6), 3315-3324 (2004).
77. Vallance BA, Deng W, Knodler LA, Finlay BB. Mice lacking T and B lymphocytes develop transient colitis and crypt hyperplasia yet suffer impaired bacterial clearance during Citrobacter rodentium infection. *Infection and immunity*, 70(4), 2070-2081 (2002).
78. Wlodarska M, Willing B, Keeney KM *et al.* Antibiotic treatment alters the colonic mucus layer and predisposes the host to exacerbated Citrobacter rodentium-induced colitis. *Infection and immunity*, 79(4), 1536-1545 (2011).

79. El Asmar R, Panigrahi P, Bamford P *et al.* Host-dependent zonulin secretion causes the impairment of the small intestine barrier function after bacterial exposure. *Gastroenterology*, 123(5), 1607-1615 (2002).
80. Yang Z, Grinchuk V, Ip SP *et al.* Anti-Inflammatory Activities of a Chinese Herbal Formula IBS-20 In Vitro and In Vivo. *Evidence-based complementary and alternative medicine : eCAM*, 2012, 491496 (2012).
81. Youakim A, Ahdieh M. Interferon-gamma decreases barrier function in T84 cells by reducing ZO-1 levels and disrupting apical actin. *The American journal of physiology*, 276(5 Pt 1), G1279-1288 (1999).
82. Madden KB, Yeung KA, Zhao A *et al.* Enteric nematodes induce stereotypic STAT6-dependent alterations in intestinal epithelial cell function. *Journal of immunology*, 172(9), 5616-5621 (2004).
83. Hue S, Ahern P, Buonocore S *et al.* Interleukin-23 drives innate and T cell-mediated intestinal inflammation. *The Journal of experimental medicine*, 203(11), 2473-2483 (2006).
84. Brown JB, Cheresh P, Goretsky T *et al.* Epithelial phosphatidylinositol-3-kinase signaling is required for beta-catenin activation and host defense against Citrobacter rodentium infection. *Infection and immunity*, 79(5), 1863-1872 (2011).
85. Hasnain SZ, Wang H, Ghia JE *et al.* Mucin gene deficiency in mice impairs host resistance to an enteric parasitic infection. *Gastroenterology*, 138(5), 1763-1771 (2010).
86. Li W, Yan F, Zhou H *et al.* P. aeruginosa lipopolysaccharide-induced MUC5AC and CLCA3 expression is partly through Duox1 in vitro and in vivo. *PloS one*, 8(5), e63945 (2013).
87. Tytgat KM, Buller HA, Opdam FJ, Kim YS, Einerhand AW, Dekker J. Biosynthesis of human colonic mucin: Muc2 is the prominent secretory mucin. *Gastroenterology*, 107(5), 1352-1363 (1994).
88. Atuma C, Strugala V, Allen A, Holm L. The adherent gastrointestinal mucus gel layer: thickness and physical state in vivo. *American journal of physiology. Gastrointestinal and liver physiology*, 280(5), G922-929 (2001).
89. Hasnain SZ, Evans CM, Roy M *et al.* Muc5ac: a critical component mediating the rejection of enteric nematodes. *The Journal of experimental medicine*, 208(5), 893-900 (2011).
90. de Jonge WJ, van der Zanden EP, The FO *et al.* Stimulation of the vagus nerve attenuates macrophage activation by activating the Jak2-STAT3 signaling pathway. *Nature immunology*, 6(8), 844-851 (2005).
91. Lorsbach RB, Murphy WJ, Lowenstein CJ, Snyder SH, Russell SW. Expression of the nitric oxide synthase gene in mouse macrophages activated for tumor cell killing. Molecular basis for the synergy between interferon-gamma and lipopolysaccharide. *The Journal of biological chemistry*, 268(3), 1908-1913 (1993).
92. Deplancke B, Gaskins HR. Microbial modulation of innate defense: goblet cells and the intestinal mucus layer. *The American journal of clinical nutrition*, 73(6), 1131S-1141S (2001).
93. Szentkuti L, Riedesel H, Enss ML, Gaertner K, Von Engelhardt W. Pre-epithelial mucus layer in the colon of conventional and germ-free rats. *The Histochemical journal*, 22(9), 491-497 (1990).

94. Specian RD, Neutra MR. Mechanism of rapid mucus secretion in goblet cells stimulated by acetylcholine. *The Journal of cell biology*, 85(3), 626-640 (1980).
95. Borovikova LV, Ivanova S, Zhang M *et al.* Vagus nerve stimulation attenuates the systemic inflammatory response to endotoxin. *Nature*, 405(6785), 458-462 (2000).
96. Huston JM, Tracey KJ. The pulse of inflammation: heart rate variability, the cholinergic anti-inflammatory pathway and implications for therapy. *Journal of internal medicine*, 269(1), 45-53 (2011).
97. Pavlov VA, Ochani M, Gallowitsch-Puerta M *et al.* Central muscarinic cholinergic regulation of the systemic inflammatory response during endotoxemia. *Proceedings of the National Academy of Sciences of the United States of America*, 103(13), 5219-5223 (2006).
98. Koarai A, Traves SL, Fenwick PS *et al.* Expression of muscarinic receptors by human macrophages. *The European respiratory journal*, 39(3), 698-704 (2012).
99. The FO, Boeckxstaens GE, Snoek SA *et al.* Activation of the cholinergic anti-inflammatory pathway ameliorates postoperative ileus in mice. *Gastroenterology*, 133(4), 1219-1228 (2007).
100. Guarini S, Altavilla D, Cainazzo MM *et al.* Efferent vagal fibre stimulation blunts nuclear factor-kappaB activation and protects against hypovolemic hemorrhagic shock. *Circulation*, 107(8), 1189-1194 (2003).
101. Chen C, Zhang Y, Du Z *et al.* Vagal efferent fiber stimulation ameliorates pulmonary microvascular endothelial cell injury by downregulating inflammatory responses. *Inflammation*, 36(6), 1567-1575 (2013).
102. Zhao M, He X, Bi XY, Yu XJ, Gil Wier W, Zang WJ. Vagal stimulation triggers peripheral vascular protection through the cholinergic anti-inflammatory pathway in a rat model of myocardial ischemia/reperfusion. *Basic research in cardiology*, 108(3), 345 (2013).
103. Artis D, Grencis RK. The intestinal epithelium: sensors to effectors in nematode infection. *Mucosal immunology*, 1(4), 252-264 (2008).
104. Hotez PJ, Brindley PJ, Bethony JM, King CH, Pearce EJ, Jacobson J. Helminth infections: the great neglected tropical diseases. *The Journal of clinical investigation*, 118(4), 1311-1321 (2008).
105. Zaccone P, Burton O, Miller N, Jones FM, Dunne DW, Cooke A. Schistosoma mansoni egg antigens induce Treg that participate in diabetes prevention in NOD mice. *European journal of immunology*, 39(4), 1098-1107 (2009).
106. Harnett W, Harnett MM. Immunomodulatory activity and therapeutic potential of the filarial nematode secreted product, ES-62. *Advances in experimental medicine and biology*, 666, 88-94 (2009).
107. Fleming JO. Helminth therapy and multiple sclerosis. *International journal for parasitology*, 43(3-4), 259-274 (2013).
108. Elliott DE, Urban JJ, Argo CK, Weinstock JV. Does the failure to acquire helminthic parasites predispose to Crohn's disease? *FASEB journal : official publication of the Federation of American Societies for Experimental Biology*, 14(12), 1848-1855 (2000).
109. Finkelman FD, Shea-Donohue T, Morris SC *et al.* Interleukin-4- and interleukin-13-mediated host protection against intestinal nematode parasites. *Immunological reviews*, 201, 139-155 (2004).

110. Shea-Donohue T, Sullivan C, Finkelman FD *et al.* The role of IL-4 in Heligmosomoides polygyrus-induced alterations in murine intestinal epithelial cell function. *Journal of immunology*, 167(4), 2234-2239 (2001).
111. Madden KB, Whitman L, Sullivan C *et al.* Role of STAT6 and mast cells in IL-4- and IL-13-induced alterations in murine intestinal epithelial cell function. *Journal of immunology*, 169(8), 4417-4422 (2002).
112. Zhao A, McDermott J, Urban JF, Jr. *et al.* Dependence of IL-4, IL-13, and nematode-induced alterations in murine small intestinal smooth muscle contractility on Stat6 and enteric nerves. *Journal of immunology*, 171(2), 948-954 (2003).
113. Ishiwata K, Nakao H, Nakamura-Uchiyama F, Nawa Y. Immune-mediated damage is not essential for the expulsion of Nippostrongylus brasiliensis adult worms from the small intestine of mice. *Parasite immunology*, 24(7), 381-386 (2002).
114. Zhao A, Bossone C, Pineiro-Carrero V, Shea-Donohue T. Colitis-induced alterations in adrenergic control of circular smooth muscle in vitro in rats. *The Journal of pharmacology and experimental therapeutics*, 299(2), 768-774 (2001).
115. Zhao A, Urban JF, Jr., Morimoto M *et al.* Contribution of 5-HT2A receptor in nematode infection-induced murine intestinal smooth muscle hypercontractility. *Gastroenterology*, 131(2), 568-578 (2006).
116. Urban JF, Jr., Noben-Trauth N, Donaldson DD *et al.* IL-13, IL-4Ralpha, and Stat6 are required for the expulsion of the gastrointestinal nematode parasite Nippostrongylus brasiliensis. *Immunity*, 8(2), 255-264 (1998).
117. Qian J, Galitovskiy V, Chernyavsky AI, Marchenko S, Grando SA. Plasticity of the murine spleen T-cell cholinergic receptors and their role in in vitro differentiation of naive CD4 T cells toward the Th1, Th2 and Th17 lineages. *Genes and immunity*, 12(3), 222-230 (2011).
118. Kistemaker LE, Bos ST, Mudde WM *et al.* Muscarinic M(3) receptors contribute to allergen-induced airway remodeling in mice. *American journal of respiratory cell and molecular biology*, 50(4), 690-698 (2014).
119. Khan WI, Blennerhasset PA, Varghese AK *et al.* Intestinal nematode infection ameliorates experimental colitis in mice. *Infection and immunity*, 70(11), 5931-5937 (2002).
120. Weinstock JV, Elliott DE. Helminths and the IBD hygiene hypothesis. *Inflammatory bowel diseases*, 15(1), 128-133 (2009).
121. Maizels RM, Balic A, Gomez-Escobar N, Nair M, Taylor MD, Allen JE. Helminth parasites--masters of regulation. *Immunological reviews*, 201, 89-116 (2004).
122. Cameron HL, Perdue MH. Muscarinic acetylcholine receptor activation increases transcellular transport of macromolecules across mouse and human intestinal epithelium in vitro. *Neurogastroenterology and motility : the official journal of the European Gastrointestinal Motility Society*, 19(1), 47-56 (2007).
123. D'Inca R, Di Leo V, Corrao G *et al.* Intestinal permeability test as a predictor of clinical course in Crohn's disease. *The American journal of gastroenterology*, 94(10), 2956-2960 (1999).
124. Wyatt J, Vogelsang H, Hubl W, Waldhoer T, Lochs H. Intestinal permeability and the prediction of relapse in Crohn's disease. *Lancet*, 341(8858), 1437-1439 (1993).

125. Wagner B, Burton A, Ainsworth D. Interferon-gamma, interleukin-4 and interleukin-10 production by T helper cells reveals intact Th1 and regulatory TR1 cell activation and a delay of the Th2 cell response in equine neonates and foals. *Veterinary research*, 41(4), 47 (2010).